NASA Contractor Report 3949

Advanced Fabrication Techniques for Hydrogen-Cooled Engine Structures

O. A. Buchmann, V. V. Arefian,
H. A. Warren, A. A. Vuigner,
and M. J. Pohlman

AiResearch Manufacturing Company
A Division of the Garrett Corporation
Torrance, California

NASA

National Aeronautics
and Space Administration

Scientific and Technical
Information Branch

1985

CONTENTS

CONTENTS (Continued)

LIST OF ILLUSTRATIONS

LIST OF ILLUSTRATIONS (Continued)

LIST OF ILLUSTRATIONS (Continued)

vii

LIST OF ILLUSTRATIONS (Continued)

LIST OF TABLES

LIST OF TABLES (Continued)

INTRODUCTION

The NASA Hypersonic Research Engine (HRE) program (ref. 1), a major contributor to Scramjet technology development, led to the use of rectangular offset-fin, plate-fin coolant passages in hydrogen-cooled engine structures. This program culminated in the successful design, fabrication and test of the first lightweight, hydrogen-cooled engine structure. The design life for the HRE cooled structures was 100 cycles and 10 hours, limited by creep and low-cycle fatigue.

Subsequent research at NASA-Langley led to a lightweight, fixed-geometry, modular, airframe integrated Scramjet concept promising high installed performance (net thrust) over a wide Mach number range. The Scramjet design study program (ref. 2), also sponsored by NASA, is an extension of the preliminary thermal-structural design of an airframe-integrated Scramjet study conducted by NASA (ref. 3) and has defined a practical engine concept that has sound basis in materials and manufacturing technology with emphasis placed on the engine thermal-structural design.

The advanced fabrication techniques program for hydrogen-cooled engine structures described in this report was undertaken in support of the Scramjet design study. The objective was to develop coolant passage geometries, material systems, and joining processes that would produce long-life hydrogen cooled structures. The program goal was to produce structures with a fatigue life two orders of magnitude greater than those produced on the HRE program. The selected panel structure had to yield adequate heat transfer with an acceptable pressure drop and suitable structural properties with reasonable weight and fabrication complexity.

The program consisted of two phases. During the first phase, studies were conducted to define the configuration design, material selection, and fabrication process. Tensile, creep, and fatigue tests were performed to establish basic material properties. Small samples were constructed to substantiate the fabrication process and inspection techniques. Development tests, including burst and creep rupture, were performed to validate structural performance. During the second phase of the program, fatigue characteristics of three candidate material systems were investigated and additional low cycle fatigue (LCF) tests were run on the most promising material.

The NASA Project Manager was Mr. H. N. Kelly, Aerothermal Loads Branch, Loads and Aerelasticity Division, NASA Langley Research Center. The AiResearch Program Manager was Mr. O. A. Buchmann. The principal contributors to the program were Messrs. J. J. Killackey and V. V. Arefian (Program Engineers); H. A. Warren (Structural Analysis); A. A. Vuigner (Thermal Analysis); and M. J. Pohlman (Materials Engineering).

Commercial products are identified in this report to adequately describe materials; this does not constitute official endorsement, expressed or implied, of such products, or manufacturers, by the National Aeronautics and Space Administration.

SYMBOLS

C	intercept of cycle life line at $N_F = 1$, (constant coefficient)
D.P.	ductility parameter,
E	Young's modulus, psi
F_{pc}	creep strain fraction of total strain, dimensionless
F_{pp}	plastic strain fraction of total strain, dimensionless
HRB	hardness on Rockwell "B" scale
HRC	hardness on Rockwell "C" scale
K	stress concentration factor, dimensionless
K_E	effective stress concentration factor in fatigue, dimensionless
K_T	theoretical stress concentration factor, dimensionless
n	slope of cycle life line (constant exponent), dimensionless
N_F	cycles to failure
N_{pc}	cycles to failure due to creep relaxation strain, dimensionless
N_{pp}	number of cycles to failure due to plastic strain only (no creep), dimensionless
P	pressure, psi
R	stress ratio, minimum stress divided by maximum stress, dimensionless
RA	percent reduction in area, dimensionless
t	time, hrs
T	temperature, °R or °F as indicated
ΔT	temperature difference, °R or °F as indicated
$\Delta\varepsilon_{pc}$	applied creep strain range
$\Delta\varepsilon_{peak}$	peak strain range (in extreme fiber) caused by wrap of specimen on mandrel
$\Delta\varepsilon_{pp}$	applied plastic strain range
σ	stress, psi

2

DEVELOPMENT PLAN

Past studies of hydrogen-cooled hypersonic propulsion systems used cooled structures having very limited thermal fatigue life. Reduced life of fabricated specimens is attributed to (1) reductions in material properties due to brazing processes, (2) strain concentration in the face plate resulting from the reinforcing effect of the fin material, and (3) concurrent creep damage (references 4 and 5). All of these are closely tied to the material system, configuration geometry, and processes used in the manufacture of the cooled structure.

To attain an operational life of 1,000 hrs. and 10,000 cycles in a hydrogen-cooled engine, it is essential that: the as-brazed material ductility be improved; temperature differences across the coolant passages be minimized; local strain due to configuration geometry be minimized; and the relatively weaker braze joint and braze affected material be placed away from the hot face sheet in lower temperature, non-critical areas.

Effort was undertaken to develop coolant passage geometries, material systems, fabrication technologies and joining processes that will provide longer-life, hydrogen-cooled structures. Selection was based on existing materials and development of known manufacturing technology. However, special consideration was given to scaling these techniques to full-scale engines.

Configuration

Three categories of passage configurations were investigated: (1) rectangular plate-fin, (2) machined or cast rectangular grooves, and (3) machined or cast pin-fins. The latter two configurations provide for locating the braze joint away from the hot face sheet, resulting in lower stress concentrations in the face sheet. The channel and pin-fin heat exchange surfaces provide better LCF and creep rupture lives than the plate-fin passages. These face plate patterns were selected for further evaluation.

Material System

Material screening considered three classes of materials based on thermal conductivity. Selection of the candidate materials was based on the combination of desirable properties including LCF performance, creep-strength, oxidation resistance, metallurgical stability and fabricability. Nickel 201 and Inconel 617 were selected for further evaluation.

Fabrication

Mechanical machining, electrical discharge machining (EDM), and photo-chemical machining (PCM) processes were evaluated for generation of the candidate cooling jacket face plate configuration. The PCM process produces the desired surface features with the least stress concentration in the face sheet. The process is also scalable to full-size panels.

Several filler alloys were considered and evaluated for joining the candidate materials, Nickel 201 and Inconel 617. Selection of the candidate alloys was based on the properties of the alloys to provide high-strength at operating temperature, high ductility, resistance to oxidation, acceptable wetting and flow, and minimum alloying with the parent metal. Palniro 1 and boronized nickel chrome filler alloys were ultimately selected for brazing Nickel 201 and Inconel 617, respectively.

Testing

Tests were formulated to evaluate the candidate selections, verify analytical predictions, and to define additional test requirements to arrive at a basic design capable of fulfilling the program goals.

Tensile tests were conducted to determine the combined effects of brazing and aging on the properties of the candidate materials, Nickel 201 and Inconel 617. Results indicated reduced ductility for both materials. The LCF tests performed on Inconel 617 hollow bar specimens subjected to pseudobraze and age cycles substantiated the reduced ductility findings from the tensile tests. Consequently, additional LCF tests, for both Nickel 201 and Inconel 617 materials in candidate passage configurations, were conducted to experimentally determine the LCF lives of the candidate designs and to provide basis for correlating analytical predictions with test results.

Creep-rupture tests were specified on pressurized channel and pin-fin Nickel 201 and Inconel 617 panels to determine the creep life of Nickel 201 panels and to verify the creep life of Inconel 617.

Elevated temperature fatigue tests were conducted on brazed Nickel 201/Inconel 718 panels using fluidized bed temperature cycling to determine the ability of the braze joint to accommodate the stresses generated by the difference between the thermal expansion coefficients of the Nickel 201 face sheet and the Inconel 718 support plate.

LCF tests were conducted on brazed Nickel 201/Hastelloy X and brazed Inconel 617 panels, using reverse bending machines to evaluate the fatigue characteristics of the candidate material systems. The tests were conducted in two phases. During the initial phase, reverse bending fatigue tests were conducted on channel specimens of both Nickel 201/Hastelloy X and Inconel 617 specimens and both lateral and longitudinal channel orientations. Based on the initial phase test results, Nickel 201 was selected for further evaluation using both pin-fin and lateral channel face plates to experimentally establish LCF life at design heat fluxes.

CONCEPT SELECTION AND EVALUATION

Thermal Loading Definition

The cooled structure for this study was defined as a 2-ft-long panel that is exposed to an average heat flux of 300 Btu/sec-ft^2, with a maximum heat flux of 500 Btu/sec-ft^2 at the outlet end, resulting in a heat load of 600 Btu/sec per foot of panel width. The coolant is hydrogen, with a minimum outlet temperature of 1600°R and an outlet pressure of 750 psi. The coolant inlet temperature is 100° to 500°R, depending on coolant demand, availability, and usage upstream of the panel. This inlet temperature range results in a flow rate range of interest of approximately 0.10 to 0.15 lbm/sec per foot of panel width. The average coolant temperature will vary from about 700° to 900°R with 800°R a nominal value.

Design results of the HRE project (ref. 1) resulted in selection of a cooling jacket pressure drop range of 150 to 250 psid, exclusive of manifolding, control valves, and associated line losses. Combined with the core outlet pressure of 750 psia, this was used to establish the coolant average pressure drop per unit of panel length at 6 to 10 psi/in. at average panel coolant conditions of 800°R and 850 psia.

In summary, the panel configuration screening was based on the following nominal operating conditions:

Coolant flow rate	0.10 to 0.15 lbm/sec-ft
Coolant pressure drop	6 to 10 psi/in.
Average coolant conditions for pressure drop performance	800°R, 850 psia
Conditions for panel thermal performance evaluation	1600°R, 750 psia, 500 Btu/sec-ft^2

Candidate Configuration and Material

Candidate cooling jacket configurations were devised with the objective of extending fatigue life of the engine structural panels and utilizing desirable materials and fabrication techniques (fig. 1). The candidates are grouped into three categories: (1) rectangular plate-fin, (2) milled or cast fin (grooved) passages, and (3) milled or cast pin fins or spines. Typical dimensions are shown.

Concept 1 is the rectangular plate-fin surface. For this surface, the plain, perforated (or slotted), and offset variations were considered. The perforated fin is similar to the plain fin except that the sheet stock is perforated in a regular pattern prior to forming. Concept 2A is a plain rectangular channel configuration; in concept 2B, the webs are set into the prime structure to increase joining contact area; concept 2C has trapezoidal webs for increased strength; and concept 2D features circular passages joined
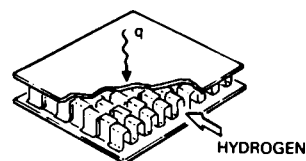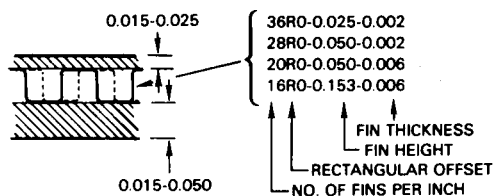
5
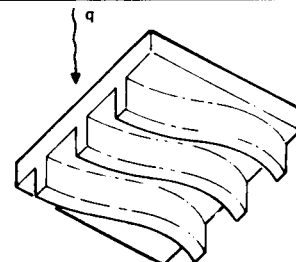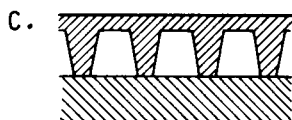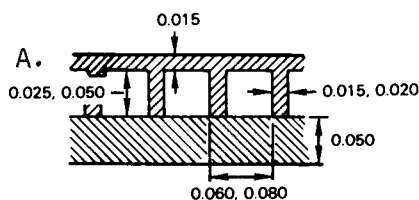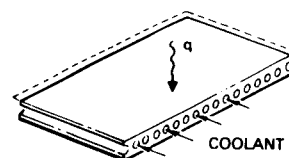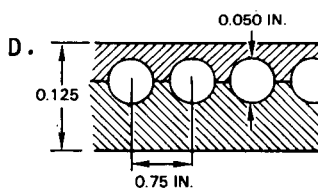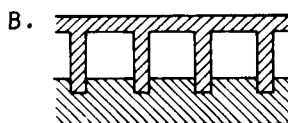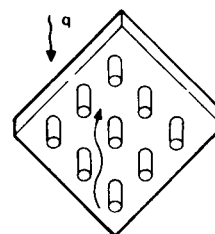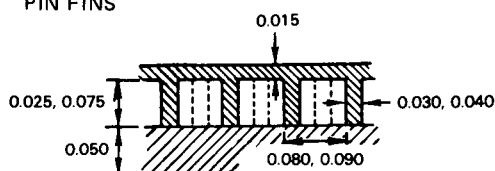
Figure 1.-Candidate cooling jacket configurations.

along the circle centers. In all concept 2 configurations, the webs can be straight or wavy in the flow direction. The wavy concept increases both heat transfer and lateral stiffness over the straight channel. All concept 2 joint bonds are placed away from the hot surface. Concept 3 is the cast or milled pin-fin configuration. The pins can be oriented either in-line or staggered with respect to the coolant flow.

Both concepts 2 and 3 provide an opportunity to taper the coolant passages either in height or width. In this way, variations in heat flux along the length of the flow route can be accommodated with a resulting conservation of pressure drop. Variation in channel width accommodates converging/diverging

6

flow passages as designed into the 3D Scramjet. The rectangular offset fin also provides this capability. Variation in flow passage height with concept 1, however, requires stepping of the flow passage in discrete increments, resulting in difficult tolerance control.

Screening considered three classes of materials based on thermal conductivity. The superalloy class (Hastelloy X, Haynes 188, X-40, etc.) is characterized by a nominal thermal conductivity of 10 Btu/hr-ft-°F at the average engine operating temperature (850°F). A second class includes such materials as pure nickel and TD nickel with a conductivity of 30 Btu/hr-ft-°F. The third class comprises the refractory metals molybdenum, TZM, and tungsten, with a conductivity of 60 Btu/hr-ft-°F at temperature.

The conductivity at local operating conditions will vary substantially from these nominal values. For example, the conductivity of Hastelloy X varies from 5 to 15 Btu/hr-ft-°F over the temperature range of 70° to 1600°F; however, the average values are adequate for configuration screening. In the majority of results to be presented, the superalloy conductivity (10 Btu-hr-ft-°F) will be emphasized.

Thermal Performance

Thermal performance results for the candidate configurations are presented in Table 1. The results include the in-depth temperature difference (ΔT) across the cooling jacket passages and the pressure drop per unit of flow length at the panel outlet and average conditions. The ΔT is a measure of low cycle fatigue life (established from the structural analysis); the unit pressure drop is a measure of the capability to operate within typical pressure limits. The unit pressure drop for the 2-ft panel length should be 6 to 10 psi/in, either on an average or length-weighted basis. Thus, if a lower pressure drop configuration is used in the panel inlet section, the unit pressure drop in the 500 Btu/sec-ft^2 outlet section can be increased.

All configurations were analyzed for 0.12 lb/sec flow per foot of panel width, at 1600°R and 750 psia outlet coolant conditions, with 500 Btu/sec-ft^2 maximum heat flux. Average panel unit pressure drop was evaluated at 800°R, 850 psia.

Three types of plate-fin surfaces were analyzed (plain, perforated and offset). As expected, the heat transfer/pressure drop characteristic of the perforated plate-fin is between the plain and offset fins of equivalent size. The effect of fin offset length was considered by using correlations from ref. 6.

Machined channel passages were divided into two groups--straight (rectangular, trapezoidal, and circular passages) and wavy (rectangular passages). The trapezoidal passage is basically a tapered fin with a thickness of 0.30 in. adjacent to the hot gas face, tapering to 0.015 in. The wavy passage considered was sinusoidal in shape and had an amplitude of about 2 passage widths (2 x 0.08 in.) and a wave length of 10 passage widths (10 x 0.08 in.)

7

TABLE 1.—THERMAL PERFORMANCE RESULTS OF CANDIDATE COOLING JACKET CONFIGURATIONS

Configuration	Type	Dimensions or Designation	Cooling Jacket In-Depth Temperature Difference, °R — Material Thermal Conductivity, Btu/hr-ft-°R			Coolant Unit Pressure Drop, psi/in.		Comments
			10	30	60	Panel Outlet Conditions	Panel Average Conditions	
Plate-fin	Plain	20R-.020-.002	600	370	280	13.3	4.6	
Plate-fin	Perforated	20R-.020-.002	520	320	240	18.6	6.4	
Plate-fin	Perforated	20R-.050-.006	740	450	310	2.4	0.8	
Plate-fin	Offset	36R-.025-.050(0)-.002	490	280	210	36.1	12.5	
Plate-fin	Offset	36R-.025-.025(0)-.002	440	260	190	62.0	21.5	
Plate-fin	Offset	28R-.050-.100(0)-.006	620	350	240	9.0	3.1	
Plate-fin	Offset	28R-.050-.050(0)-.006	535	310	215	11.9	4.1	Same designation as plate fin used.
Machined grooved channels (straight)	Rectangular	12.5R-.025-.020	550	250	140	7.1	2.5	
Machined grooved channels (straight)	Rectangular	12.5R-.050-.020	830	410	240	1.2	0.4	
Machined grooved channels (straight)	Trapezoidal	16.6R-.025-(0.15-.030)	465	195	106	9.2	3.3	Fin tapers from 0.030 in. near hot sheet to 0.015 in.
Machined grooved channels (straight)	Trapezoidal	16.6R-.050-(0.15-.030)	660	305	175	1.7	0.6	
Machined grooved channels (straight)	Circular	13.3 passages per inch, 0.050-in. passage dia.	570	240	130	1.9	0.7	1/13.3 = 0.075-in passage
Machined grooved channels (wavy)	Rectangular	12.5R-.050-.020	680	355	220	3.6	1.3	
Pin-fin	Staggered	S_p=.080, L_p=.025, D_p=.040	420	210	130	173.2	61.2	S_p = center-to-center-pin spacing, in.
Pin-fin	Staggered	S_p=.080, L_p=.050, D_p=.040	530	290	195	49.7	17.6	L_p = pin (or passage) height, in.
Pin-fin	Staggered	S_p=.080, L_p=.075, D_p=.040	620	370	250	19.8	7.0	D_p = pin dia, in.
Pin-fin	Staggered	S_p=.080, L_p=.050, D_p=.030	560	350	250	23.7	8.4	
Pin-fin	In-line	S_p=.080, L_p=.050, D_p=.040	510	290	200	38.3	13.6	

Two types of pin-fin arrangements (as shown in Table 1) were considered--staggered and in-line. For dimensionally similar pin-fins (S_p = 0.80 in., D_p = 0.040 in., L_p = 0.050 in.), in-depth T's for staggered and in-line configuration are approximately the same, but the pressure drop is lower for the in-line configuration.

For the thermal performance results of candidate configurations presented in Table 1, the following conclusions were reached:

(1) Plate-fin--Perforated fins do not yield any significant advantages. For about the same ΔT, the 28R-.050-.050 offset fin pressure drop is 35 percent less. Decreasing the offset length reduces the ΔT by 50 to 70°R with a corresponding increase of 25 percent in pressure drop.

(2) Machined channels--Best performance is obtained with 0.025-in. groove depth, which is believed to be feasible for brazing. The trapezoidal shape gives good results. Compared to 28R-.050-.100 offset plate-fin surface, the trapezoid ΔT is 155°R less for about the same pressure drop. Additional reductions in ΔT could possibly be obtained by using a wavy pattern, which would maintain the panel average ΔP at less than 10 psi/in.

(3) Pin-fin--This configuration yields the lowest ΔT, but the pressure drop for the 0.025-in.-high staggered pattern is higher than allowable; the entire allowable pressure drop would be consumed in less than 2.0 in. of flow length. For the same ΔT, the pin-fin pressure drop is three times greater than for the rectangular groove passages; for the same pressure drop, the rectangular channel thermal conductance is greater.

Candidate Alloy Properties

A consistent set of material properties was required to permit comparisons of LCF life. Since the LCF predictive techniques use reduction of area to account for the material ductility, this parameter was fundamental. Since the cooling jackets use thin gage material, the properties of sheet materials rather than bar or plate were desired. Properties of the candidate alloys are listed in Table 2.

Wrought Superalloys

Hastelloy X is included in Table 2 because it is the baseline material. Haynes Alloy 188, a new alloy since initiation of the HRE program, has better strength and ductility than Hastelloy X. Predicted reduction in area at 1450°F is 31 percent for Haynes Alloy 188 (references 7 and 8). Weldability, formability, brazeability, and oxidation resistance are all good. Rene 41 has better strength but lower ductility than Haynes 188. Fatigue life of Rene 41 may not be better than for Hastelloy X or HA 188, and it is difficult to braze and must be heat treated.

TABLE 2.-ESTIMATED MATERIAL PROPERTIES FOR LCF LIFE PREDICTION[1]
(APPROXIMATELY 100 HRS IN AIR AT TEMPERATURE SHOWN)

	Temp, °F	Hastelloy X	Narloy-Z	X-40	TZM (Bare)	René 41	TD Nichrome	Haynes 188	Inconel 617	Nickel 200
Yield stress, ksi	1450	31	9[4]	41	61 (55)[2]	85	30	32	27	6
(before exposure)	1600	27		37	58 (48)[2]	72	23	27	27	3
Yield stress, ksi	1450	23		40	55	80	27	42	32	5
(after exposure)[3]	1600	20		35	50	68	20	33	30	2
1000-hr rupture	1450	12	2[4]	25	44	30	13	18	18	2
stress, ksi	1600	6		17	42	14	10	10	10	1
100-hr rupture	1450	16	3[4]	32	45	45	15	24	25	3
stress, ksi	1600	9		20	43	23	12	13	14	1
Young's modulus,	1450	20	8[4]	21	31	20	20	24	20	20
10^6 psi (tension)	1600	19		19	29	17	17	23	17	17
Young's modulus,	1450	21	8[4]	22	39	23	26	24	20	20
10^6 psi (dynamic)	1600	20		20	39	22	25	23	17	17
Thermal expansion	1450	9.0	9.5[5]	8.9	3.1	8.3	9.1	9.1	8.5	9.0
coefficient, 10^{-6} in./in./°F	1600	9.1		9.0	3.1	8.7	9.3	9.4	8.7	9.1
Reduction in area,	1450	27	← Brazed properties unknown →							
brazed, percent	1600	29								
Reduction in area,	1450	36	75[4]	16	5	11	5	43	60	97
parent metal, percent	1600	40		19	5	22	2	80	75	99

(1) Value shown is most likely average value expected for 0.015-in.-thick sections
(2) Coated properties shown in parentheses
(3) Approximately 100 hr in air at temperature shown
(4) At 1200°F
(5) To 1200°F (mean)

TD nickel-chromium (TD Ni-Cr) was considered because of its high strength. good oxidation resistance, and thermal conductivity. A similar material, DS nickel-chromium (DS Ni-Cr) was also considered but its properties are not as well characterized as for TD Ni-Cr. Because of an uncertain supply situation, and low ductility, TD Ni-Cr or DS Ni-Cr were not retained as candidates.

Inconel alloy 617 is a nickel-chromium-cobalt-molybdenum alloy with good higher temperature strength. Rotating beam fatigue tests show excellent high cycle fatigue strength at 1600°F. The alloy exhibits good metallurgical stability in the critical intermediate temperature range and retains its ductility after 1000 hr of exposure to temperatures of 1200° to 1600°F.

Cast Superalloys

The cast superalloys contain larger amounts of hardening elements (Al, Ti) than the wrought alloys and therefore are stronger, but ductility generally is lower. For example, the cobalt-base alloy X-40 contains 25 percent chromium and has excellent oxidation resistance; however, reduction in area at 1600°F is only 19 percent; hence the fatigue life would be limited. In view of the fabrication difficulties inherent in a cast alloy (especially when scaling to full-size engine structures), and poor LCF life, X-40 was discarded as a candidate alloy.

Refractory Metals

Both tungsten and molybdenum have exceptional creep and tensile strength at high temperatures when compared with superalloys, and, in addition, have high thermal conductivities and low expansion coefficients, both of which serve to keep thermal stresses low. These desirable attributes, however, are offset by poor oxidation resistance and the occurrence of embrittlement at low temperatures. Tantalum and columbium were not considered in the analysis because they absorb large atomic percentages of hydrogen, leading to lattice distortion, swelling, and embrittlement.

Tungsten has the lowest expansion coefficient of all the candidates. The major disadvantage of tungsten is its high ductile-to-brittle transition temperature (DBTT). The DBTT normally ranges from 0° to 300° or 400°F, making fabrication difficult. Coatings for tungsten are not as well developed as those for molybdenum, nor is there as much experimental data. The best coatings are the disilicides, applied by pack cementation.

Molybdenum and the TZM molydenum alloys have several attractive features, i.e., high thermal conductivity, low expansion, and fair fabricability. The DBTT for TZM alloy is less than 0°F, which permits ordinary fabrication processes; exposure to cryogenic hydrogen should be prevented.

Molybdenum and TZM have no oxidation resistance above 1300°F. There are coatings and claddings available that may afford adequate protection at 1600°F for extended periods, but applicable design data is lacking or inadequate. The only metallic coating likely to endure the expected thermal and chemical environment is platinum. But only small laboratory samples of TZM have been successfully clad with platinum (ref. 9). Furthermore, no data could be found to verify that platinum would provide reliable protection from oxidation at the temperatures of interest, and it is expected that the tolerance to damage (self-healing ability) would be poor.

Other electroplated and clad metal coatings have been investigated--notably nickel, chromium, and combinations thereof. However, differential expansion and contraction during thermal cycling are likely to cause failure by spalling due to the brittleness of the intermetallic compounds and the thermal stresses generated at the coating/substrate interface.

Most of the efforts to protect molybdenum alloys from oxidation since 1960 have involved silicide or aluminide coatings that are designed to be self-healing at use temperatures that are several hundred degrees higher than those of interest for this program. The glassy film will not be nearly as self-healing at 1600°F as it will at the original design temperatures for the coatings. The silicide coatings also exhibit a "pest" reaction at these intermediate temperatures (900° to 1700°F), causing premature failure. The aluminide coatings available include a liquid phase (Sn-Al) above 475°F, which may pose erosion problems. Lastly, there is likely to be a compatibility problem between the coating and braze alloy, which requires basic development to establish compatible materials and thermal process cycles. Because of these considerations molybdenum alloys were rejected for further consideration.

Molybdenum-50 Rhenium (Mo-50 Re) alloy has strength similar to molybdenum and a low ductile-brittle transition temperature (-425°F) compared with +70°F for pure molybdenum. The oxidation resistance of Mo-50 Re, however, is expected to be similar to that of pure molybdenum, necessitating the need for a protective coating. In addition, the cost of the material and the limitations on size availability eliminate the Mo-50 Re alloy from serious consideration for large size panels.

Alternative Materials

High conductivity materials based on copper and nickel also were considered. The high thermal conductivity minimizes the temperature gradients across the structure and result in lower operating temperatures when compared to superalloys.

In the copper family, Narloy Z and dispersion-strengthened copper are available. The former has been developed and used for actively cooled rocket nozzle liners, but appears to have insufficient oxidation resistance, strength, or creep resistance at the expected service temperatures (1260°F). Dispersion-strengthened copper may have sufficient strength but has poor ductility and is not expected to have adequate low-cycle fatigue life.

The nickel alloy offering the best combination of thermal conductivity and mechanical properties at 1335°F is Nickel 201, a low-carbon, commercially pure nickel. Available oxidation data (ref. 10) indicate consumption of only 0.0006 in. of metal by oxidation for 1000 hrs at 1335°F. If necessary, coatings could be applied to further reduce oxidation. In particular, an insulating coating developed by NASA (ref. 11) could be used to further reduce the metal service temperature as well as improve oxidation resistance.

Structural Analysis

Stress concentration Factors.--Finite element models were made to determine the stress concentration factors for pin-fin panel construction. Two types of pin geometry were analyzed. The first type is the configuration produced by photo chemical milling (PCM) the pins as an integral part of the hot face sheet. These pins have a tapered profile with a smooth transition to the back side of the face sheet. The second pin geometry analyzed consisted of a straight pin brazed to the back side of the face sheet, with a braze fillet transition to the face sheet. Both configurations consisted of 0.030-in. dia. staggered pins at 0.090-in. spacing with a 0.015-in. face sheet. The computer model for the PCM pin is shown in fig. 2. The results of the analysis are presented in Table 3.

The stress concentration factors are very close. For a given thermal strain, the lower concentration effect of the smooth transition for the PCM pins is partially offset by the higher face sheet stiffness between PCM pins as compared to straight, brazed pins. This higher face sheet stiffness results in a higher average strain rate between pins.

12
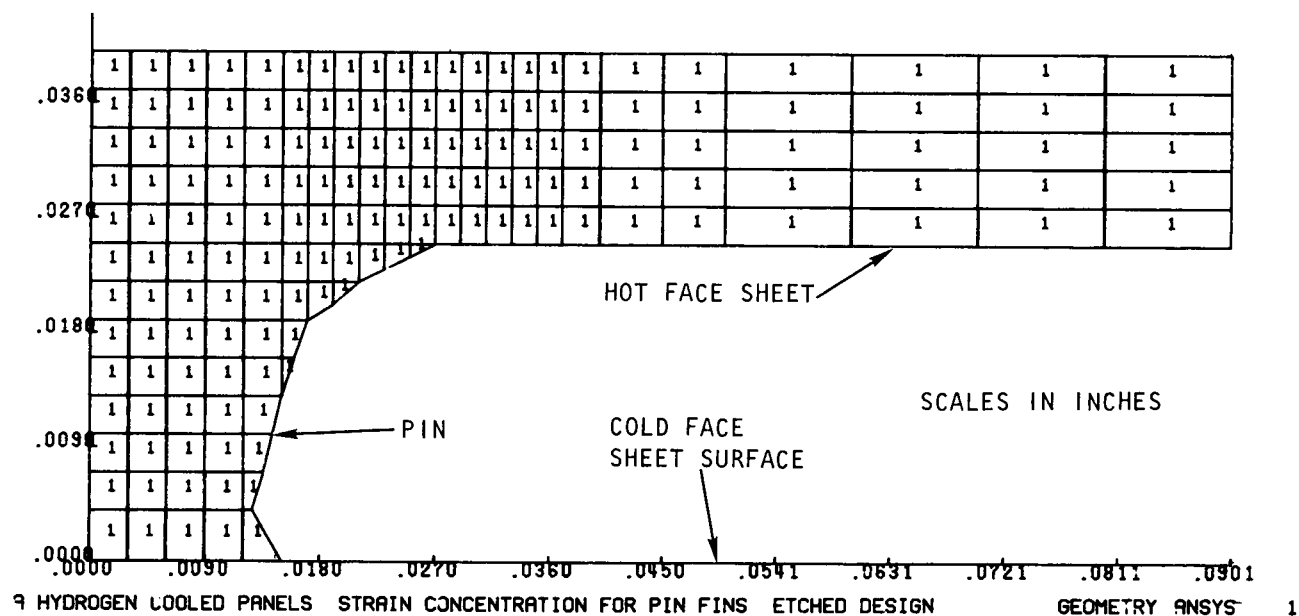
Figure 2.-Computer model of PCM pins.

A-18695

TABLE 3.-STRESS CONCENTRATION FACTORS, K, FOR PIN-FINS

Pin Type	K
PCM (integral)	1.65
Straight (brazed)	1.70

Pressure deflections and stresses.--Another finite element model was con-structed to determine the pillowing effect and face sheet stresses resulting from applying 750 psi pressure to a section of pin-fin panel. The properties of Hastelloy X at 1600°F were used for the analysis. The model consisted of a 0.015-in. face sheet supported by 0.030-in. dia staggered pins on 0.090-in. centers. Results of the analysis indicate that the face sheet will bow 6.7 μin. between pins, and the maximum stress in the face sheet between pins is 3070 psi. The creep rate for 3070 psi stress at 1600°F is 0.001 percent/hr or 1 percent in 1000 hrs. This creep rate is low, and no appreciable permanent pillowing is anticipated in the 1000-hr design life of the panel. A contour plot of the face sheet is shown in fig. 3.

LCF life estimates.--Comparative LCF life estimates were made for nine candidate materials based on the properties presented in Table 2. Where the reduction-in-area values for brazed specimens were lacking, a percent reduction similar to the known value for Hastelloy X was assumed.

X .0000107

D .0000000
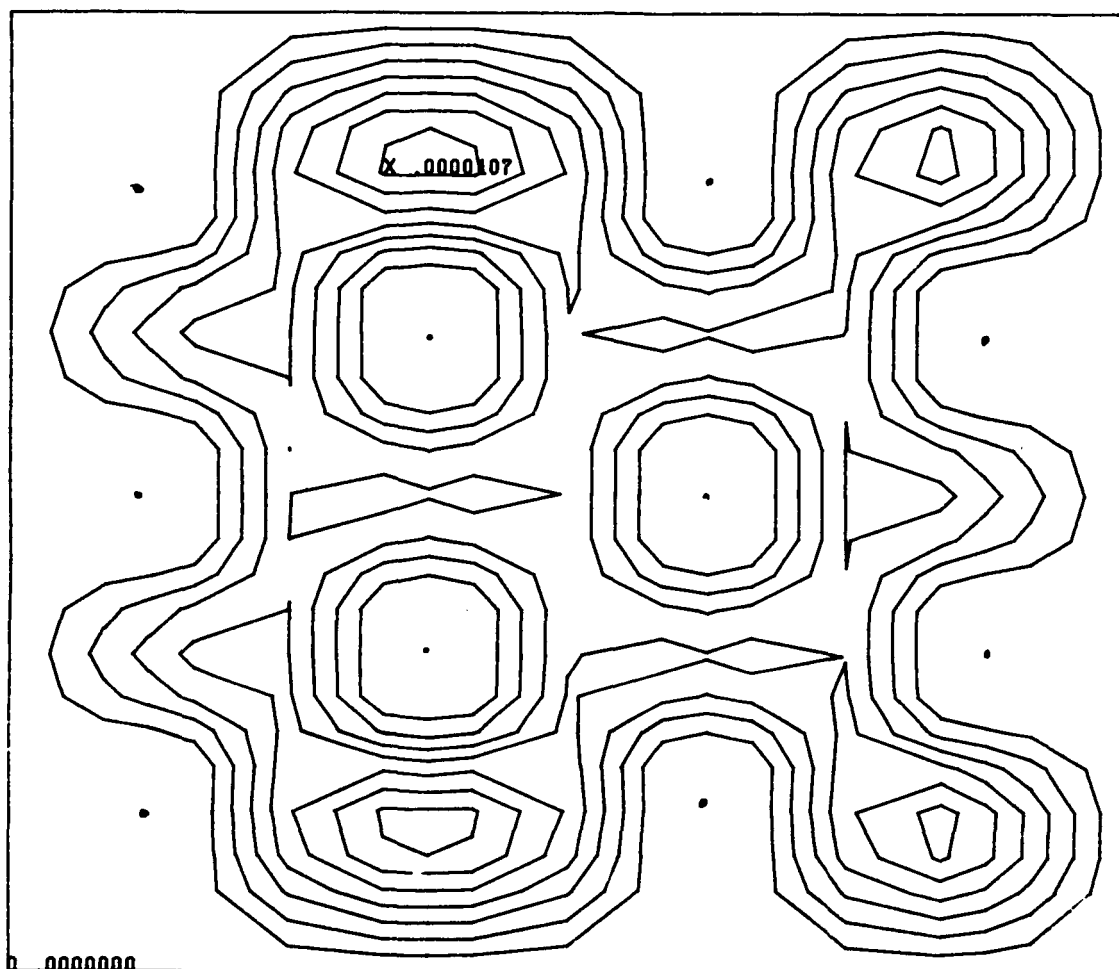
A-18582

Figure 3.-Face sheet deflection for pin-fin design under pressure load.

The strain range partitioning method of estimating fatigue life was used in the analysis, for the two cycles illustrated in fig. 4. Case 1 assumes that the structure is heated and then immediately cooled with no hold time. Case 2 assumes a hold time of 6 minutes, which permits creep to take place. The creep is illustrated by the reduction in stress from point A to point B in fig. 4. For the analysis it was assumed that the face sheet would creep-relieve to a stress level (point B), which if sustained, would produce rupture in 1000 hrs.

Use of the stress to produce rupture in 1000 hrs for the relaxed stress value at point B assures being on the flat portion of the stress-relaxation curve of stress versus time. The actual stress level at the end of a 6-min. hold time may be somewhat higher than the assumed level. Since the amount of plastic strain in each cycle due to creep is proportional to yield stress minus the final stress after creep, use of the lower value for the final stress is conservative.

14
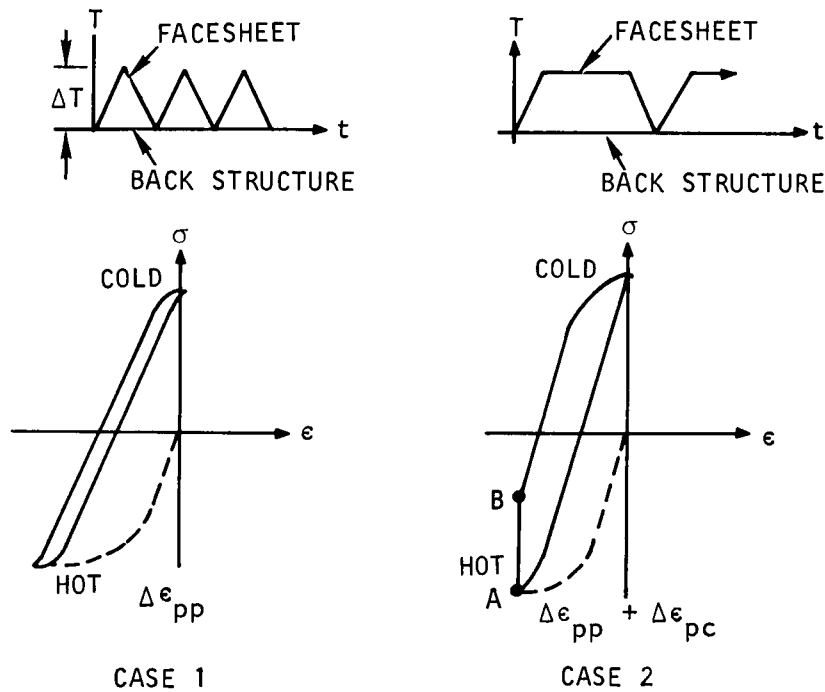
Figure 4.-Strain range components produced in face sheet with
and without hold time in the thermal histories.

The strain range partitioning technique is presented in the following
equations:

(a) For cycling with no hold time

$$N_{pp} = \left[\frac{0.75 \ D.P.}{\Delta\epsilon_{pp}}\right]^{1.67}$$

where N_{pp} = number of cycles to failure

$D.P.$ = ductility parameter = $\ln \dfrac{100}{100-RA}$

RA = percent reduction in area

$\Delta\epsilon_{pp}$ = applied plastic strain

$= \dfrac{\text{applied stress} - 2 \times \text{yield stress}}{\text{Young's Modulus}}$

0.75 and 1.67 are constants found to give good agreement
between predictions and test results for a number of materials.

15

(b) <u>For cycling with hold time</u>

$$N_{pp} = \left[\frac{0.75 \; D.P.}{\Delta\varepsilon_{pp} + \Delta\varepsilon_{pc}} \right]^{1.67} \qquad N_{pc} = \left[\frac{1.25 \; D.P.}{\Delta\varepsilon_{pp} + \Delta\varepsilon_{pc}} \right]^{1.25}$$

where N_{pp} = cycles to failure if the entire plastic strain was applied with

no hold time.

N_{pc} = cycles to failure if the entire plastic strain was applied by

creep relaxation.

$\Delta\varepsilon_{pc}$ = applied creep strain

$= \dfrac{\text{yield stress} - \text{relaxed stress}}{\text{Young's Modulus}}$

1.25 is a constant found to give good agreement between
predictions and test results for a number of materials.

$$N_F = \frac{1}{\dfrac{F_{pp}}{N_{pp}} + \dfrac{F_{pc}}{N_{pc}}} \qquad = \text{cycles to failure}$$

where
$$F_{pp} = \frac{\Delta\varepsilon_{pp}}{\Delta\varepsilon_{pp} + \Delta\varepsilon_{pc}}$$

$$F_{pc} = \frac{\Delta\varepsilon_{pc}}{\Delta\varepsilon_{pp} + \Delta\varepsilon_{pc}}$$

The results of the analysis are summarized in Table 4 for the cycle with a 6-min. hold time. The ΔT values used in Table 4 were taken from thermal analyses results.

Conclusions reached regarding the suitability of each of the candidate alloys are summarized in the following paragraphs.

Hastelloy X: This material, which serves as the program baseline, will exhibit a fatigue life of about 1000 cycles for a passage geometry close to optimum.

René 41: The LCF life for this material is inferior to Hastelloy X except for the circular passage design (configuration 4, Table 4), for which the life is about 10,000 cycles. René 41 is difficult to braze and weld, and is sensitive to strain concentration. These considerations led to rejection of René 41 as a candidate.

TABLE 4.—ESTIMATED LCF LIFE FOR COOLING JACKET CONFIGURATIONS(2) WITH HOLD TIME

Material (1)	No. 1 Plate-fin		No. 2 Machined Fin		No. 3 Machined Trap. Fin		No. 4 Circular Passages		No. 5 Machined Wavy Fin		No. 6 Pin Fins (Staggered)		No. 7 Pin Fins (Staggered)		No. 8 Pin Fins (In-line)	
	ΔT	LCF Life	ΔT	LCF Life	ΔT	LCF Life	ΔT	LCF Life	ΔT	LCF Life	ΔT	LCF Life	ΔT	LCF Life	ΔT	LCF Life
Hastelloy X	490	320	550	700	465	940	570	1,500	680	490	620	520	560	620	510	720
René 41	490	180	550	380	465	680	570	10,000	680	230	620	250	560	300	510	360
Haynes 188	490	400	550	860	465	1,100	570	1,700	680	590	620	640	560	760	510	890
Inconel 617	490	1,020	550	2,420	465	3,100	570	4,450	680	1,800	620	1,950	560	2,150	510	2,450
X-40 (Cast)	-	-	550	230	465	320	570	540	680	150	620	170	560	200	510	240
TD-NiCr	490	2	550	4	465	6	570	11	680	2	620	3	560	4	510	4
TZM	210	8	140	8	106	8	130	8	220	8	250	8	250	8	200	8
Nickel (3) 200	280	2,300	250	82,000	195	110,000	240	170,000	355	48,000	370	40,000	350	44,000	290	58,000
Narloy-Z	100	18,000	70	130,000	70	130,000	80	8	110	49,000	130	21,000	130	21,000	100	130,000

(1) Temperature difference obtained from Table 1.

(2) Dimensions or designation of the surface configuration are as follows (see also fig. 1 and Table 1):

Config. No.		Config. No.	
1	36R- 0.025-0.050-0.002 fins	5	12.5-0.050-0.020 wavy fins
2	12.5 R-0.025-0.020 rectangular fin	6	S_p 0.08, L_p 0.075, D_p = 0.040
3	16.6 R-0.025=(0.015 to 0.030), trapezoidal fin	7	S_p 0.08, L_p 0.05, D_p = 0.030
4	13.3 circular passages/in., 0.05 dia	8	S_p 0.08, L_p 0.05, D_p = 0.040

(3) Reduction in area of 70% assumed for LCF calculation

Haynes 188: This alloy offers only a modest increase in cycle life compared with Hastelloy X. The small difference does not warrant the use of Haynes 188, considering the extensive data base that presently exists for Hastelloy X.

Inconel 617: This alloy yields the best results of all the superalloys evaluated. The high cycle life is attributable to the ductility of the material, which reaches a maximum near the 1600°F operating temperature. The 10,000-cycles design life is not achieved. The relatively good performance, however, combined with the generally attractive overall characteristics led to selection of this alloy as a candidate.

X-40 (cast superalloy): LCF life with the optimum circular passage configuration is less than 1000 cycles and less than that obtained with Hastelloy X. In view of the fabrication difficulties with a cast alloy, and the low cycle life, X-40 was dropped as a candidate alloy.

TD nickel chrominum: The low ductility of this material results in an unacceptable cycle life; the material was dropped from further consideration.

TZM: Cycle life is infinite; the material remains within the elastic limit throughout the operating cycle. Oxidation protective coatings are required with TZM material. No satisfactory coating was found and TZM was dropped as a candidate alloy.

Nickel 200 and 201: Nickel 200 is commercially pure nickel. The increased thermal conductivity (compared with the superalloys) and superior ductility combine to yield a predicted cycle life considerably above the required 10,000 cycles. The low creep-rupture strength limits the applicability of plate-fin geometries. Oxidation resistance appears adequate without protective coatings at the operating conditions. Nickel 201, a low carbon version of Nickel 200, has better creep strength compared with Nickel 200. Nickel 201 is also reported to be less subject to embrittlement by intergranularly precipitated carbon or graphite when held at temperatures of 600° to 1400°F for extended periods. Nickel 201 was therefore, selected as a candidate.

Narloy-Z: The LCF life is predicted to be more than adequate; however, like other precipitation-hardened copper alloys, Narloy-Z will over age with a resultant decrease in strength at minimum acceptable operating temperatures for this application. After 100 hrs the alloy would soften and become unusable.

Selected Materials and Passage Geometries

The materials selected for evaluation were Inconel 617 and Nickel 201. These materials were selected based on the combination of desirable properties, including the predicted low-cycle-fatigue performance, creep strength, oxidation resistance, metallurgical stability (no aging effects), and fabricability.

18

Candidate cooled passage configurations were:

(a) Plate fin

(b) Machined fin

(c) Photochemically milled (PCM) circular or trapozoidal shaped channels

(d) Photochemically milled (PCM) pin fins

Low-cycle-fatigue life and creep analyses show that the longest cycle life can
be obtained using the PCM process to form channel-type passages. This geometry
was selected as the primary panel configuration; PCM pin-fins were selected as
a second configuration. Pin fins have application to situations involving
locally high heat fluxes, in which the relatively high unit pressure drop can
be accommodated.

MATERIAL PROPERTY TESTS

General

Additional basic material properties were needed to further evaluate the
selected candidate materials. Data on the combined effects of brazing and
aging cycles on the ductility of Nickel 201 and Inconel 617 were not available.
In addition, the available tensile data is reported on bar specimens whereas
the panels employ sheet materials. Consequently, tests were conducted to
obtain the required material properties.

Nickel 201 Tensile Properties

Specimen design.--The two types of specimens used for the tensile testing
of the Nickel 201 sheet materials are shown in fig. 5. The first set of tensile
tests were performed on 0.50-in. wide strips of Nickel 201 sheet material with
the thickness of the central portion reduced to 0.015 in. Subsequent tests were
conducted with the dog-bone specimen design with a 0.50-in. wide and 0.030-in.
thick central test section. The reduction in thickness of both types of speci-
mens was accomplished by a chemical etching process to simulate the process used
in fabrication of the panels.

Test results.--Results of room-temperature and elevated temperature
tensile tests on Nickel 201 sheet material are summarized in Tables 5 and 6,
respectively.

The room temperature tests on the as-received material indicated that the
material was somewhat work hardened.

19
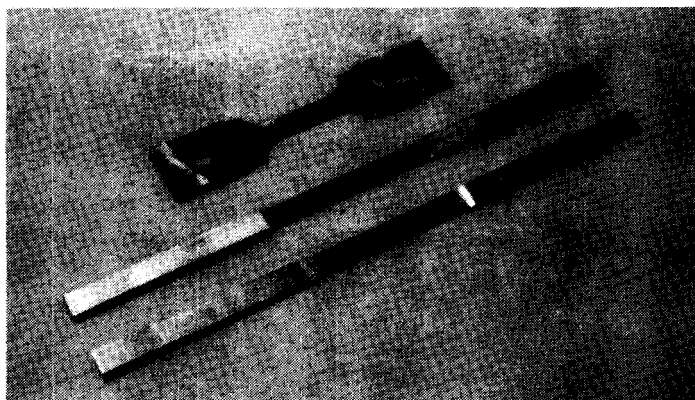
F-34902

Figure 5.-Tensile test specimen.

The elevated-temperature tensile tests were run at 1400°F, which is the average of the pin-fin and channel panels hot face sheet operating temperatures. This also is the specified temperature level for the panel creep-rupture tests and for the LCF tests.

One of the dog-bone specimens was sectioned (prior to aging) to establish the edge form to be used in computing the cross-sectional area. The form of the chemically milled section is shown in fig. 6.

For the room temperature results, the following conclusions can be made:

(a)   For the annealed material, the yield strength is at the low limit for the material, although the ultimate is close to nominal. The ductility, as measured by reduction in area (RA), also is low. Both the reduced yield strength and ductility can be attributed to the effect of material thinness; it is doubtful that the chemical machining process is a contributing factor.

(b)   Brazing degrades yield strength about 30 percent; subsequent aging does not result in further degradation.

(c)   Brazing degrades ductility, and subsequent aging results in further loss of ductility.

(d)   Aging causes most of the damage, i.e., loss of ultimate tensile strength and ductility. Nickel 201, a low carbon version of Nickel 200, is not susceptible to embrittlement by intergranularly precipitated carbon or graphite when held at temperatures of 600° to 1400°F for extended periods of time. Therefore, the oxidation that occurs during the air aging cycle is probably the main cause of degradation.

20

TABLE 5.-TENSILE TEST DATA FOR NICKEL 201 AT ROOM TEMPERATURE

Test Specimen Type	Processing	Test Item No.	Ultimate Strength, ksi	Yield Strength, ksi	Percent Elongation (2)	Percent Reduction in Area (RA) (2)	Modulus, E 10⁻⁶ psi	Hardness Rockwell B
"Strip" 0.015-in. thick test section	As-received Test data	1	65.3	53.3	21.0	32.4	30.0	74.5
		1A	73.2	60.2	23.0	28.5	31.3	66.0
		1B	73.4	60.8	23.0	20.8	29.9	74.8
		1C	72.6	63.5	14.0	30.0	28.4	74.5
		1D	71.8	57.8	16.0	20.1	30.0	74.5
	Average		71.3	59.1	19.4	26.4	29.9	72.8
	Supplier Hard sheet		90 to 115	70 to 105	15 to 20	-	-	90 min.
	data (1) Annealed sheet		55 to 75	15 to 30	55 to 40	-	-	70 max.
"Dog-bone" 0.030-in. thick test section	Annealed (1400°F for 15 min.)	3	61.6	11.6	45	39.3		
		3A	60.8	11.5	45	39.3		
		3B	60.7	12.1	40	37.7		
	Average		61.0	11.7	43	38.8		
	Pseudo brazed (2070°F for 10 min.)	4	52.3	8.3	29	19.2		
		4A	52.3	8.0	29	24.8		
		4B	52.3	7.6	30	25.4		
		4C	53.4	7.9	32	22.9		
	Average		52.6	8.0	30	23.1		
	Pseudo brazed and aged in air for 1000 hrs at 1450°F	5	34.0	8.2	25	13.5		
		5A	33.0	8.3	22	16.3		
		5B	33.2	8.5	22	16.6		
		5C	36.4	8.4	26	17.0		
		5D	32.2	9.1	21	15.6		
	Average		33.8	8.5	23	15.8		
	Aged in air only, 1000 hrs at 1450°F	6	39.1	10.0	25	13.1		
		6A	39.4	10.2	26	17.6		
		6B	34.2	10.4	21	20.4		
		6C	40.6	9.8	23	14.7		
		6D	40.6	9.9	26	13.0		
	Average		28.8	10.1	24	15.8	Note (4)	Note (4)
	Brazed at 2070°F for 5 min. and aged in argon at 1450°F for 100 hrs	7	50.8	6.8	33	39		
		7A	46.4	5.3	30	43		
		7B	52.4	12.0	28	39		
	Average		49.9	8.0 (3)	30.3	40.3		
	Brazed at 2070°F for 5 min. and aged in argon at 1450°F for 300 hrs	8	54.5	6.8	30	38		
		8A	53.6	6.6	27	41		
		8B	54.0	6.9	30	40		
	Average		54.0	6.8 (3)	29	39.7		
	Brazed at 2070°F for 5 min. and aged in argon at 1450°F for 1000 hrs	9	46.9	8.1	47	38		
		9A	47.4	7.4	52	29		
		9B	46.3	4.5	46	32		
	Average		46.9	6.7 (3)	48.3	33		
	Aged in argon only for 100 hrs at 1450°F	10	56.8	9.0	44	54		
		10A	56.7	8.3	42	52		
		10B	57.4	8.5	43	53		
	Average		57.0	8.6 (3)	43	53		
	Aged in argon only for 300 hrs at 1450°F	11	55.2	7.6	33	53		
		11A	56.3	9.9	34	52		
		11B	54.1	9.4	32	42		
	Average		55.2	9.0 (3)	33	49		
	Aged in argon only for 1000 hrs at 1450°F	12	47.5	6.0	43	30		
		12A	60.2	8.7	39	7		
		12B	49.1	6.4	48	37		
	Average		52.3	7.0 (3)	43.3	24.7		

(1) Huntington alloys, "Nickel Alloys", 15M2-72T-15, 1972.

(2) Elongation and reduction of area data for each sheet specimen may vary approximately ±50 percent due to uncertainties inherent in measuring technqiues.

(3) Yield strength values are approximate.

(4) Not evaluated for these specimens.

21

TABLE 6.-TENSILE TEST DATA FOR NICKEL 201 AT 1400°F
("Dog-Bone" 0.030-in Thick Test Section)

Processing	Test Item No.	Ultimate Strength, ksi	Yield Strength, ksi	Percent Elongation (1)	Percent Reduction in Area (RA) (1)
Annealed (1400°F for 15 min.)	2	17.4	5.1	51	53.6
	2A	17.8	5.5	41	41.3
	2B	17.3	5.3	52	43.8
Average		17.5	5.3	48	46.2
Pseudo brazed (2070°F for 10 min.)	3	15.9	5.0	43	39.5
	3A	14.4	5.2	43	40.0
	3B	15.2	4.7	42	37.5
	3C	15.1	4.3	36	38.5
	3D	14.2	4.3	34	37.4
Average		15.0	4.7	40	38.6
Pseudo brazed and aged in air for 1000 hrs at 1450°F	4	9.2	5.8	11	20.8
	4A	10.2	5.9	13	19.8
	4B	9.3	5.7	12	21.0
	4C	9.4	5.2	10	16.3
	4D	9.8	6.1	9	19.2
Average		9.6	5.7	11	19.4
Aged in air only, 1000 hrs at 1450°F	5	11.2	5.5	16	17.8
	5A	12.2	5.5	15	17.0
	5B	11.3	5.4	15	23.0
	5C	9.9	5.4	15	17.0
	5D	12.2	5.9	19	20.2
Average		11.4	5.5	16	19.0
Brazed at 2070° for 5 min. Aged in Argon at 1450°F for 100 hrs	6	12.9	3.4	29	34
	6A	15.3	4.9	44	33
	6B	11.7	4.3	23	17
Average (4)		13.3	4.2 (2)	32	28
Brazed at 2070°F for 5 min. Aged in Argon at 1450°F for 300 hrs	7	6.4	4.4	7	8
	7A	12.7	3.4	30	23
	7B	12.4	3.2	18	20
Average (4)		10.5	3.7 (2)	18.3	17
Brazed at 2070°F for 5 min. Aged in Argon at 1450°F for 1000 hrs	8	11.9	3.8	27	21
	8A	10.9	4.1	16	19
	8B	11.0	3.4	16	-(3)
Average (4)		11.3	3.8 (2)	19.7	20
Aged in Argon only for 100 hrs at 1450°F	9	13.3	5.9	19	18
	9A	13.7	4.9	24	36
	9B	15.2	6.2	43	28
Average (4)		14.1	5.7 (2)	28.7	27.3
Aged in Argon only for 300 hrs at 1450°F	10	6.2	4.8	5	2
	10A	9.1	5.2	9	9
	10B	9.1	3.6	11	-(3)
Average (4)		8.1	4.5 (2)	8.3	5.5
Aged in Argon only for 1000 hrs at 1450°F	11	12.5	4.9	29	24
	11A	6.4	4.8	7	8
	11B	11.2	2.9	21	-(3)
Average (4)		10.0	4.2 (2)	19	16

(1) Elongation and reduction of area data for each sheet specimen may vary approximately +50 percent due to uncertainties inherent in measurement technique.

(2) Yield strength values are approximate.

(3) Specimen failed in transition radius.

(4) Data is questionable. Refer to explanation in text.

22
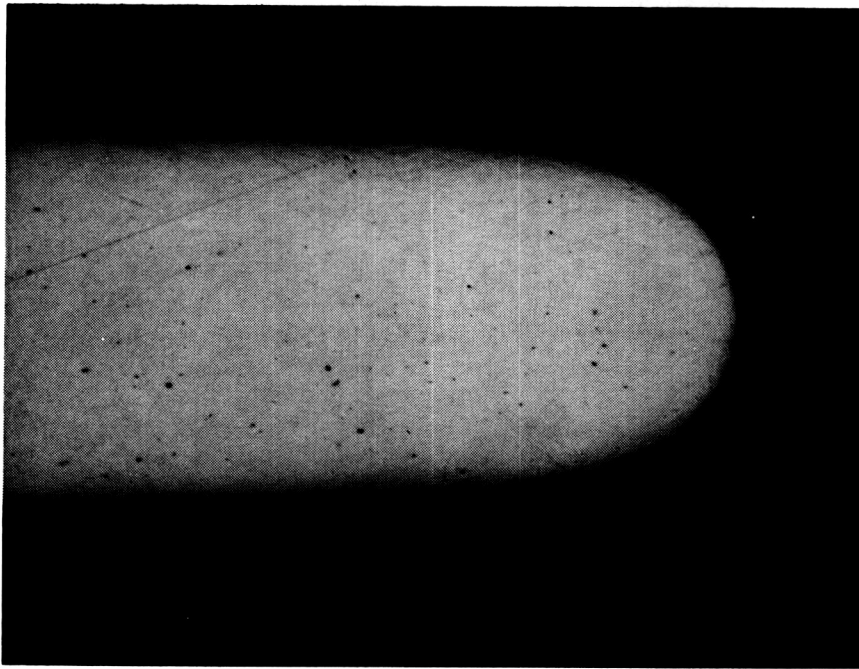
F-34932

Figure 6.-Edge form on Nickel 201 tensile test specimens.

The elevated temperature test results with the dog-bone specimens aged in air (Table 6) substantially agree with room temperature trends. There is substantial reduction in ductility due to brazing and aging, although the yield strength slightly improves after aging.

To separate the effects of braze cycle and aging from those of oxidation a series of tests were conducted on dog-bone-type tensile test specimens which had been aged in an inert argon atmosphere. Half of the specimens were subjected to a 2070°F pseudo-braze cycle prior to aging. Specimens were aged for 100, 300 and 1000 hrs. The room temperature and elevated temperature test results are presented in Tables 5 and 6, respectively.

Both room temperature and elevated temperature load vs. deflection curves exhibited a section of indicated load increase with no deflection; a short section where the deflection varied linearly with load; and a section where deflection increased at an increasing rate relative to loading. Because of shortness of the linear portion of the curve, accurate determination of the slope was impossible. As a result, the yield strength values shown in Tables 5 and 6 for argon-aged specimens are only approximate.

Clip-on type extensometers were used for all tests to determine the load-deflection plot. No problems were encountered during the room temperature tests. However, during the 1400°F tests, the clips produced noticeable indentations into the test specimens. There also appeared to be some preferential localized oxidation at the clip attach points. The combined effect of the

localized oxidation and the introduction of the stress concentration produced by the indentations, resulted in fracture of all except four of the high temperature specimens at the clip attach points. Due to the possibility of premature fracture caused by these effects, the ultimate strength, elongation, and reduction of area values for test item nos. 6 through 11 in Table 6 are questionable.

Comparison of the ultimate strength, elongation, and reduction in area results for the argon-aged specimens with those aged in air indicates that oxidation reduces the ductility of the Nickel 201 material by a factor of two and the ultimate strength by about 30 percent. The aging process appears to be the governing factor in lowering the ductility, and the change produced by the braze cycle is minimal.

Although a marked improvement in reduction in area (RA) is realized for the brazed and argon-aged Nickel 201 material (33 percent) over those brazed and aged in air (16 percent), the argon-aged RA is still well below the 97 percent figure listed in Table 2 for Nickel 200 parent material and the 70 percent value assumed for Nickel 201 in the LCF life calculations in Table 4. This may indicate a reduced LCF life for Nickel 201 in the planned application.

The engine panels are exposed to hydrogen atmosphere during operation and are, therefore, more closely represented by conditions encountered during the argon aging cycle. Hydrogen embrittlement of the parent metal is a further consideration in this application. Tests to ascertain the effects of hydrogen exposure on the material ductility are most meaningful using specimens representing the selected cooling jacket configurations, at design temperature and pressure. No embrittlement testing was done on this program.

Inconel 617 Tensile Properties

Specimen design.--Three types of specimens were used in the tensile tests. The strip type specimen was shown earlier in fig. 5. The central portion of the specimen was reduced to 0.015-in. The solid bar specimen is shown in fig. 7.
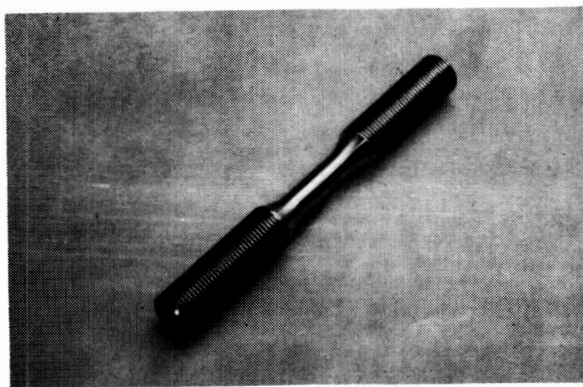
F-34922

Figure 7.-Inconel 617 bar tensile test specimen.

24

The test section on these specimens measured 0.44-in. To obtain additional data on Inconel 617 material with a thickness between the 0.015-in. thick sheet material and the 0.44-in. bar specimens, tubular low-cycle-fatigue test specimens of the design shown in fig. 8 were subjected to tensile testing. The thickness of the gage section on these specimens was 0.060-in.
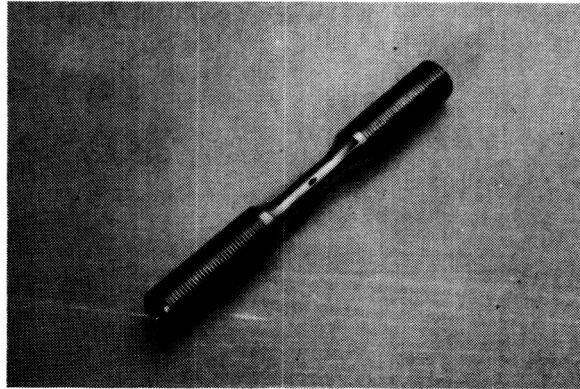
F-34923

Figure 8.-Inconel 617 low-cycle fatigue and tensile test specimen.

Test results.--The results of the room temperature and elevated temperature tensile tests on Inconel 617 are summarized in Tables 7 and 8, respectively.

The room-temperature tests on the as-received material indicate that the material was cold worked, probably because of the mechanical machining process used to obtain the desired 0.015-in. test section thickness.

Room temperature and elevated temperature tests were performed to determine the effects of brazing and elevated temperatures on material properties.

The ductility of the sheet specimens as indicated by elongation and reduction in area measurements (data item 2, Table 7 and data item 1, Table 8), appears to have been substantially reduced by the brazing and aging process.

The room temperature tensile test results for the bar specimens closely match the typical data provided by the supplier, Hungtington Alloys, for the as-received material. The yield strength slightly exceeds the typical data; the ductility, as measured by reduction in area (RA), is about equal to the typical data. The measured properties of the brazed and aged material confirm the supplier's data for aged material only. There is distinct reduction in ductility (RA) accompanied by increases in both the ultimate and yield strengths due to aging (see Inconel 617 creep rupture panel test results).

The reduction in area of the hollow-bar specimens tested at 1600°F (22.6 percent) falls between the reduction in area of the 0.44-in. dia. solid bar (54.7 percent) and that of the 0.015-in. thick sheet (11.4 percent). The decrease in properties from bar to sheet is due to the combined effect of oxidation/braze penetration and the normal thickness effect.

TABLE 7.-TENSILE TEST DATA FOR INCONEL 617 AT ROOM TEMPERATURE

Test Specimen Type	Processing	Test Item No.	Ultimate Strength, ksi	Yield Strength, ksi	Percent Elongation (1)	Percent Reduction in Area (RA) (1)	Modulus, E 10^{-6} psi
"Strip" 0.015-in. thick test section	As-received	1	136.4	88.3	37.0	35.4	31.0
		1A	132.2	75.1	43.0	40.1	33.1
		1B	136.4	75.2	43.0	36.0	33.0
		1C	144.8	84.3	37.0	31.3	34.5
		1D	144.0	88.5	39.0	28.7	35.0
	Average		138.8	82.3	39.8	34.3	33.3
	Supplier data for solution-treated, cold rolled sheet (2)		110.0	47.0	54	-	-
	Brazed with Palniro I and exposed 1000 hrs at 1600°F in air	2	123.4	68.6	18	21.1	
		2A	120.6	54.3	34	26.8	
	Average		122.0	61.5	26	24.0	
"Solid bar" 0.44-in. dia. test section	As-received	3	112.5	46.6	64	55.2	29.0
		3A	112.8	47.9	64	55.2	29.7
	Average		112.6	47.2	64	55.2	29.4
	Supplier data for solution-treated, hot rolled rod (3)		106.6	42.9	70	57	-
	Pseudo brazed and aged 1000 hrs at 1600°F in air	4	115.1	46.3	40	32.3	28.5
		4A	117.1	46.9	40	34.8	29.0
	Average		116.1	46.6	40	34.0	28.8
	Supplier data for hot rolled rod, aged 1000 hrs at 1600°F (3)		119	48	46	43	-

(1) Elongation and reduction of area test data for each sheet specimen may vary approximately
    ± 50 percent due to uncertainties inherent in measuring techniques.

(2) Huntington Alloys, "Inconel Alloy 617" 20M9-72T-46, 1972.

(3) Data sheet, International Nickel Company.

TABLE 8.-TENSILE TEST DATA FOR INCONEL 617 AT 1600°F

Test Specimen Type	Processing	Test Item No.	Ultimate Strength, ksi	Yield Strength, ksi	Percent Elongation (1)	Percent Reduction in Area (RA) (1)	Modulus, E 10^{-6} psi
"Strip" 0.015-in. thick test	Brazed with Palniro I and exposed 1000 hrs at 1600°F in air	1	41.2	25.8	10.2	10.9	15.9
		1A	47.1	29.5	7.8	3.0	19.5
		1B	45.9	28.2	12.5	15.6	15.0
		1C	39.2	25.4	8.7	16.2	13.8
	Average		43.4	27.2	9.8	11.4	16.1
	Supplier data for solution annealed, cold rolled sheet (2)		45	24	76	-	-
"Solid bar" 0.44-in. dia test section	Pseudobrazed and aged 1000 hrs at 1600°F in air	2	36.4	26.0	83.0	60.1	19.3
		2A	43.4	23.5	65.0	52.6	19.3
		2C	45.1	21.8	63.0	51.4	19.3
	Average		41.6	23.8	70.3	54.7	19.3
	Supplier data for solution annealed, hot rolled rod (2)		47	37	43	-	-
"Hollow-bar" 0.060-in. thick test section	Pseudobrazed and aged 1000 hrs at 1600°F in air	3	63.5	30.6	-	22.2	-
		3A	58.5	31.0	-	22.9	-
	Average		61.0	30.8	-	22.6	-

(1) Elongation and reduction of area test data for each sheet specimen may vary approximately
    ± 50 percent due to uncertainties inherent in measurment techniques.

(2) Huntington alloys, "Inconel Alloy 617" 20M8-79-T-46, 1979.

Low Cycle Fatigue Properties

Nickel 201 LCF predictions.--Fatigue test data obtained on Nickel 200 material as part of the Hypersonic-Research Engine program were reviewed (ref. 12). Nickel 201, the material being investigated in this program, is identical in composition to Nickel 200 except for the carbon content, which is limited to 0.02 percent maximum compared with 0.15 percent maximum for Nickel 200. The LCF data for Nickel 200 and 201 should therefore be comparable.

A comparison between the data from the HRE program and a prediction using an RA of 70 percent to account for braze effects, and an outer fiber temperature of 1450°F is shown in fig. 9. The predicted life is based on a 6-minute hold-time; and thus includes a factor for creep damage. The plastic strain range for plate-fin and machined-fin specimens is indicated in fig. 9.

Also included in fig. 9 is a life prediction based on the 33 percent RA value obtained from specimens subjected to a pseudo-braze cycle, aged in Argon for 1000 hrs, and tested at room temperature. For the channel specimens, which are close to the machined fin configuration, the cycle life is as follows:

Prediction with RA = 70 percent: 13,000 cycles

HRE panel test data (average):   3,000 cycles

Prediction with RA = 33 percent: 2,200 cycles

Inconel 617 LCF tests.--The test plan for the low cycle fatigue testing of Inconel 617 material was based on plastic-plastic (P-P) strain cycle (refer to Table 9) in conjunction with the expected test times. It was judged that the data available from the P-P cycle testing would be adequate to determine the compatibility of Inconel 617 with the design requirements.

California State University at Long Beach (CSULB) was selected to perform the LCF testing on their Materials Test System (MTS) equipment.

In selecting the MTS facilities, various methods of strain measurement and control were considered. The most accurate of these involves the use of high-temperature extensometers. The selected approach at CSULB uses a calibrated cross head. This is the method customarily used in this facility, and it has been evaluated as consistent with the objectives of the program, that is, the data available would be of sufficient accuracy to provide the desired evaluation of basic properties.

Test specimen design.--The LCF test specimen is shown in figs. 8 and 10. The specimens were subjected to a pseudo-braze cycle (braze temperature and time conditions but no braze alloy) and then aged in air for 1000 hrs at 1600°F prior to testing. The unprocessed bars were used to establish the as-received properties.
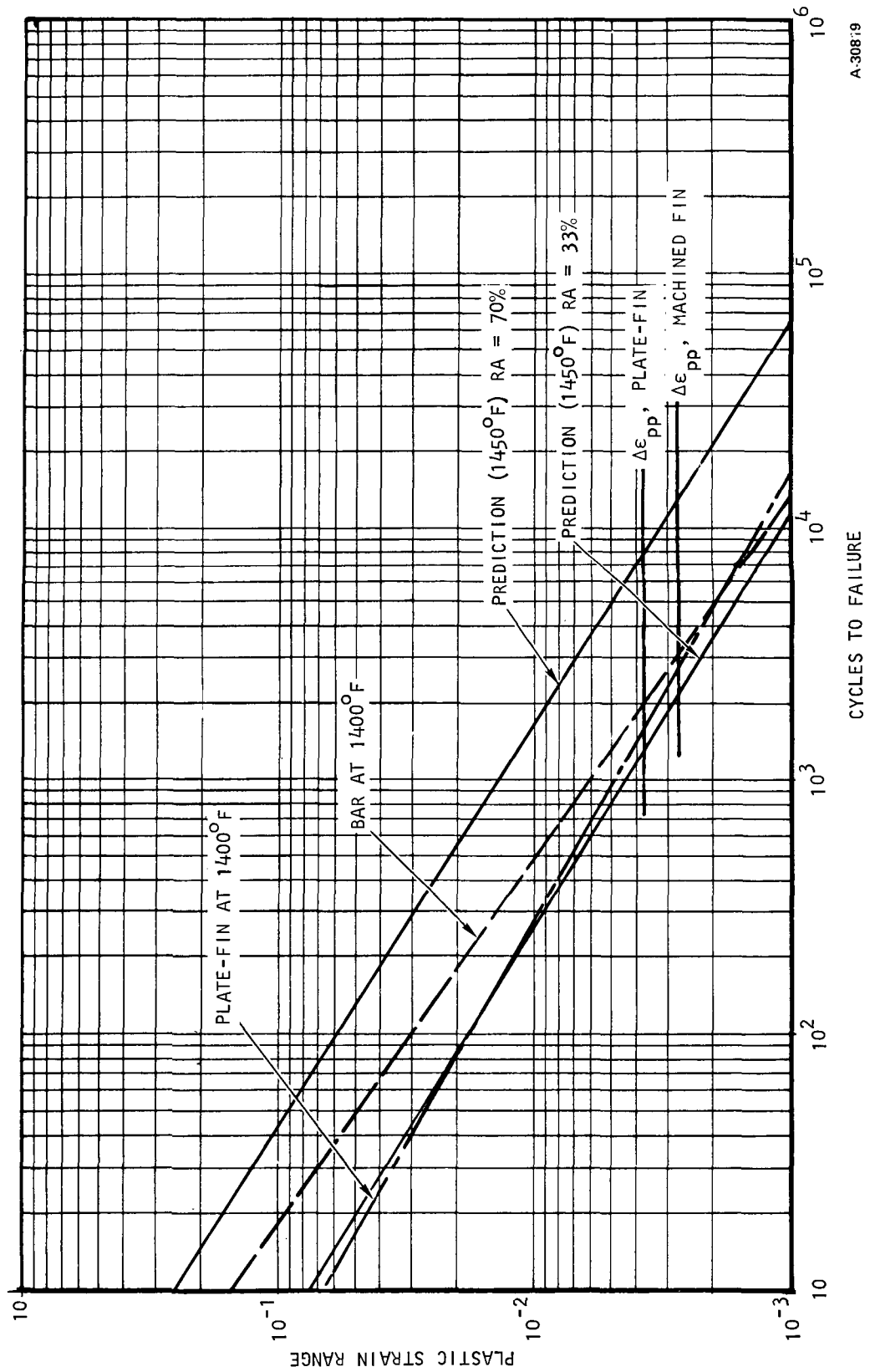
Figure 9.-Fatigue life comparison. Nickel 201.

TABLE 9.-INCONEL 617 LCF TESTING - P-P CYCLE

Test Temp, °F	Number of Specimens	Applied Strain Range, in./in.	Equivalent ΔT °F	Estimated[1] Cycles to First Crack	Estimated Test Times, hr
	3	0.0287	2000	310	0.2
1600	3	0.0144	1000	1,280	0.7
	3	0.0067	466	10,000	5.6

STRAIN - TIME HISTORY
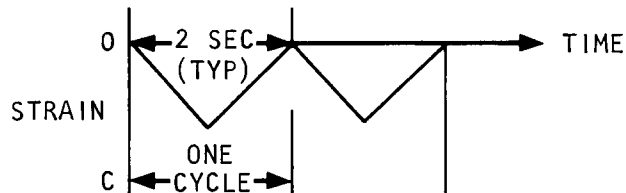
[1]Based on a RA of 65 percent and a K_E of 1.78
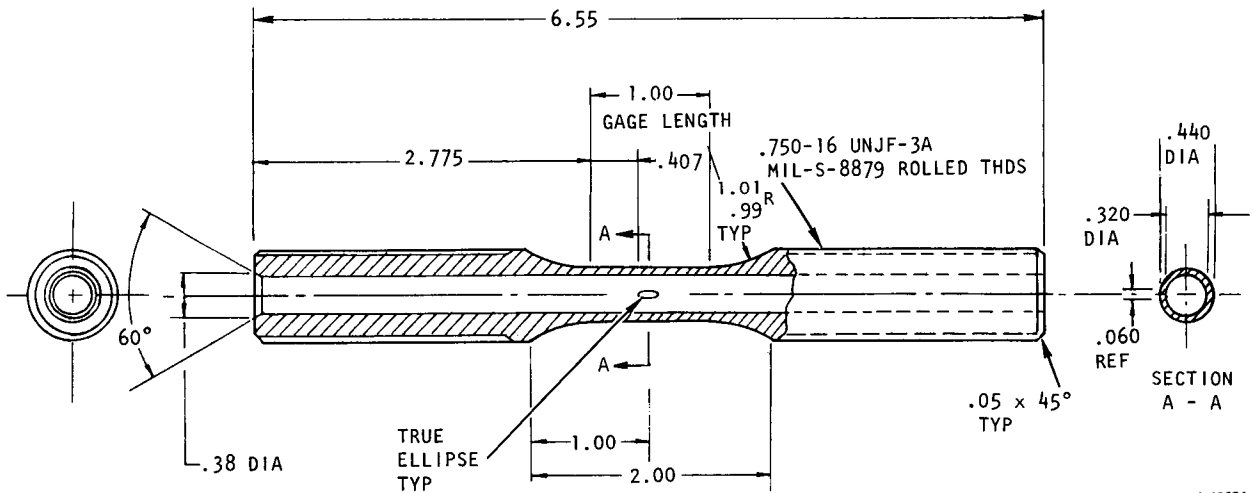
Figure 10.-Inconel 617 low-cycle fatigue test specimen.

Test results.--Results of the Inconel 617 low cycle fatigue test using a P-P cycle are shown in fig. 11. The predicted curve based on typical proper- ties as published by Huntington Alloys is shown for reference. The design strain
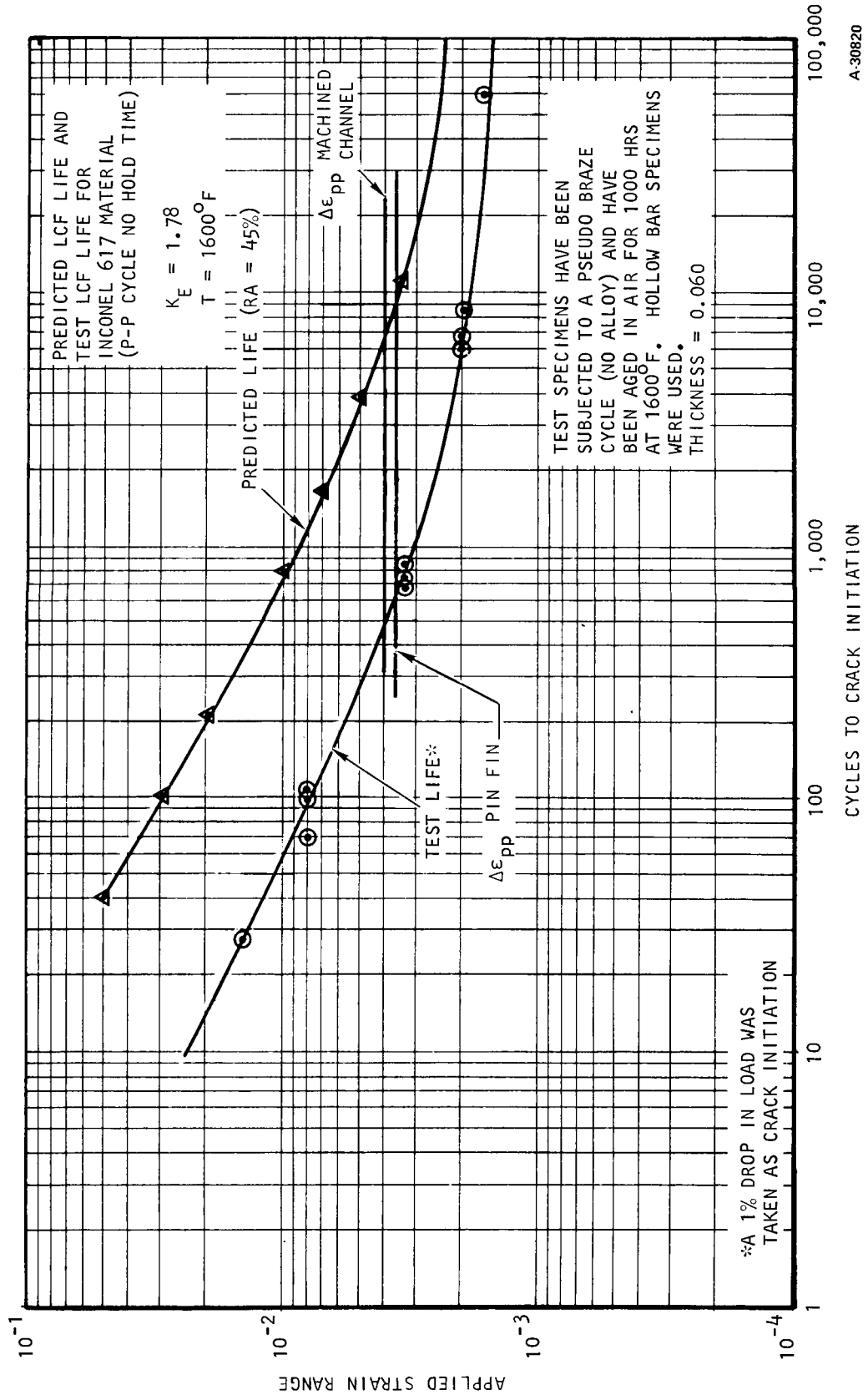
Figure 11.-Low cycle fatigue test of Inconel 617

ranges for the machined channel and pin fin configurations are also included for reference. Specimen behavior was as expected and no anomalies were observed. Specimen fracture occurred along a line normal to the specimen centerline and in the center of the elliptical cutout, as predicted.

The results show that for the same total strain range, the test specimen cycle life is about one order of magnitude less than predicted. The reduced life is attributed to the deleterious effects of exposure to high temperature braze cycle and aging in air for 1000 hrs at 1600°F.

The predicted P-P cycle life was recomputed using the yield strength and reduction in area (RA) values obtained from the solid and tubular bar tensile tests and are presented in Table 10. The formula used to predict P-P LCF life is as follows:

$$N_{pp} = \left[\frac{0.75 \ D.P}{\Delta \varepsilon_{pp}} \right]^{1.67}$$

where:

$$D.P. = \ln \frac{100}{100-RA}$$

$\Delta \varepsilon_{pp}$ = Local plastic strain range

The constants 0.75 and 1.67 are universal factors that have been found to agree well with the LCF test results for a number of materials.

Good correlation is obtained between the analytically predicted fatigue life, using the RA values from tensile tests, and the LCF test results for the hollow bar specimens. The close agreement between the predicted LCF lives obtained analytically and from experimental data substantiates the use of analytical techniques to evaluate the life expectancy of engine panels at conditions that may differ from the specific and limited test conditions.

The low cycle fatigue testing on the Inconel 617 specimens was limited to the P-P cycle illustrated in Table 9. In the actual panel application the cycle will be a combination of the P-P and P-C cycles whereby the thermally induced stresses are maintained for an appreciable length of time causing creep relaxation strain to occur. A combined P-P/P-C was assumed and the LCF life predictions were re-calculated for several applied strain ranges using the RA and yield values obtained from bar and sheet tensile tests. The results are also presented in Table 10. A strain concentration factor of 1.78 was used so that all predicted LCF life values would be compatible with the test results from the hollow bar specimens. The creep strain results in a lower predicted life in all cases with the effect being greater for the lower applied strain ranges.

TABLE 10.—COMPARISON OF FATIGUE LIFE PREDICTIONS — INCONEL 617 AT 1600°F

Applied strain range[1]		0.00366[2] ($\Delta T = 420$)	0.00405[3] ($\Delta T = 465$)	0.00483 ($\Delta T = 555$)	0.00522 ($\Delta T = 600$)	0.00609 ($\Delta T = 700$)	0.00 ($\Delta T = 800$)
Localized strain range[4]		0.00651	0.00721	0.00860	0.00929	0.01084	0.01239
Predicted life cycles							
Published data (RA = 65%)	P-P Cycle only	9491	6865	4158	3397	2321	1702
	Combined P-P & P-C	3179	2717	2097	1836	1442	1160
0.44 solid bar (RA = 54.6%)[5]	P-P Cycle only	4164	3188	2075	1737	1234	928
	Combined P-P & P-C	2182	1848	1359	1193	923	730
0.06 hollow bar (RA = 22.6%)[5]	P-P Cycle only	632	484	315	264	187	141
	Combined P-P & P-C	393	325	233	202	152	118
0.015 sheet (RA = 11.4%)[5]	P-P Cycle only	210	157	99	82	57	43
	Combined P-P & P-C	126	103	72	62	46	36
Test curve — hollow bar specimens, P-P		620	475	290	240	170	125

[1] Values in brackets represent ΔT between face sheet and support

[2] Design point for pin fin configuration; refer to Table 1

[3] Design point for machined channel configuration; refer to Table 1

[4] Based on 1.78 stress concentration factor for hollow bar test specimen

[5] Hollow bar, exposed to pseudo-braze cycle and aged 1000 hrs at 1600°F in air; refer to Table 8

32

Fatigue test data obtained with the Inconel 617 specimens were also compared to data previously obtained with Hastelloy X material. The results are shown in fig. 12.
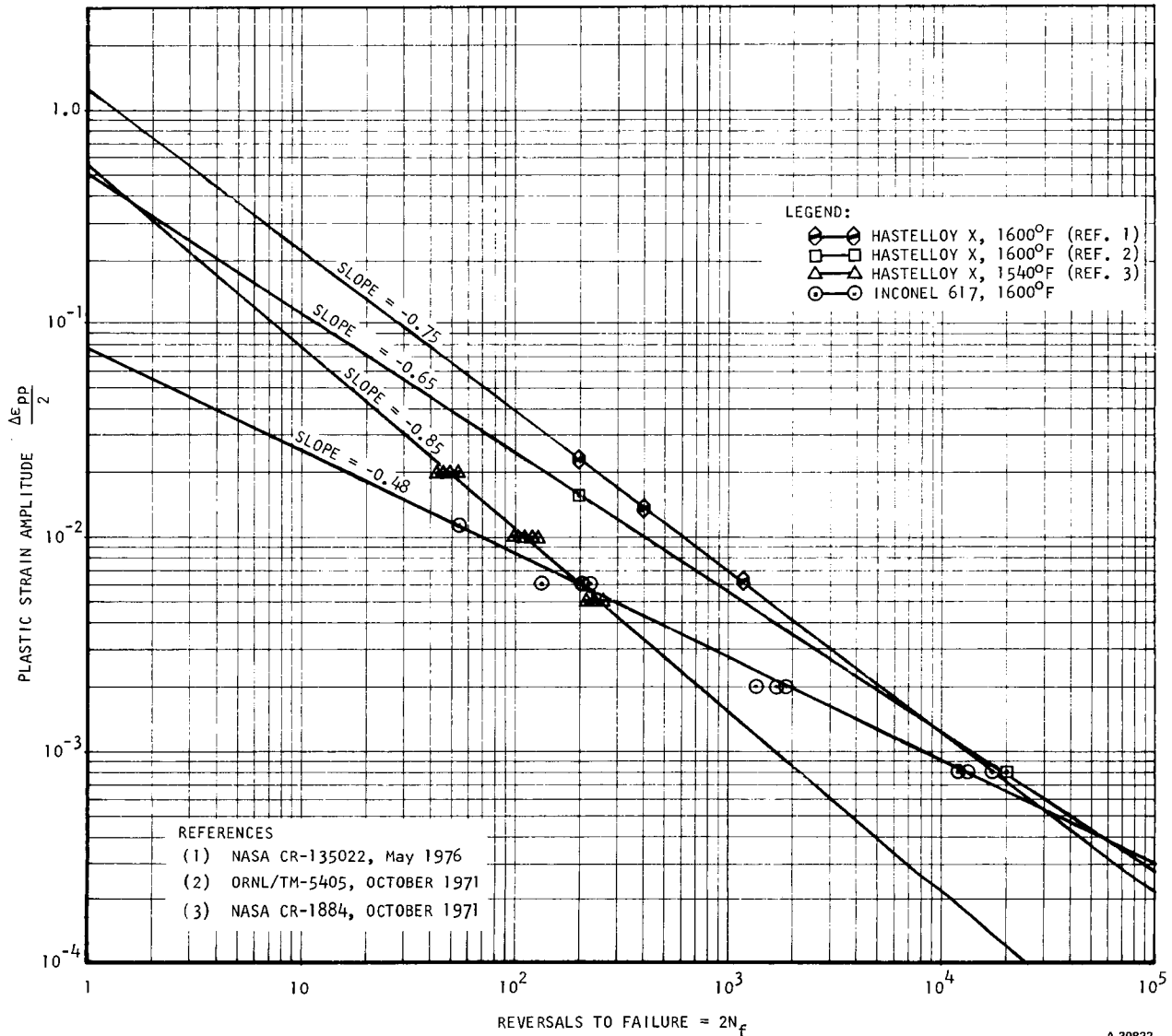

Figure 12.—Comparison of Inconel 617 test data with
Hastelloy X test data.

The Inconel 617 test specimen was designed to simulate the panel application including the thickness (0.060-in. wall) and the stress concentration (K_t, $_{max}$ = 1.78), while the Hastelloy X tests employed a bar specimen with K_t = 1.0. To be

consistent, the Inconel 617 data shown on fig. 12 were corrected for the strain concentration effect by multiplying the total applied strain by the strain concentration factor. At the 10,000 cycle design life (20,000 reversals), the two materials are equivalent in terms of allowable plastic strain. The low plastic strain for Hastelloy X reported in ref. 13 is attributed to the low cycle rate used in testing. According to ref. 13: "Creep damage apparently dominated at 1540°F (1110°K)."

The predicted LCF life was calculated for the pin fin and machined channel panel configurations using both the published material properties for non-aged material and the reduced material properties obtained from tensile tests performed on the hollow bar tensile specimens which had been subjected to a pseudo-braze cycle and aged in air for 1000 hrs at 1600°F. The calculations were made for both Inconel 617 and Hastelloy X materials. Due to the similarity in composition between Hastelloy X and Inconel 617, the same aging factors were applied to both. The results are presented in Table 11.

TABLE 11.—PREDICTED LCF LIFE[1] FOR INCONEL 617 AND HASTELLOY X

Configuration	Basis for Material Properties	Inconel 617		Hastelloy X	
		P–P Cycle	Combined Cycle	P–P Cycle	Combined Cycle
Pin fin (ΔT = 420°F) T = 1600°F	Published Data	9638	3591	2962	1091
	Tensile & LCF Tests[2]	778	449	320	178
Channel (ΔT = 465°F) T = 1600°F	Published Data	7132	3105	2143	935
	Tensile & LCF Tests[2]	590	372	239	147

[1]Peak strain was based on the calculated 1.65 stress concentration factor for the pin fins and channels.

[2]Material exposed to pseudo-braze cycle and aged 1000 hrs at 1600°F. The reduction in properties found in tests with Inconel 617 at 1600°F were applied to Hastelloy X in the absence of actual data and due to the similar composition of Hastelloy X and Inconel 617.

The effect of aging on predicted LCF life is quite apparent. The predicted LCF life for the combined cycle based on aged material properties is only 14 percent to 19 percent of the LCF life using published material data. Inconel 617 has larger calculated LCF lives for both configurations than Hastelloy X and is believed to be the better of the two materials for the scramjet application.

Conclusions and Recommendations

The results of the tensile tests performed on Nickel 201 and Inconel 617 indicate that the ductility of both materials is substantially reduced due to combined effects of brazing and aging cycles. The results of the low-cycle fatigue tests conducted on Inconel 617 specimens also indicate a lower attained LCF life in comparison with the analytical predictions using published data. The lower test LCF life is in keeping with the lower ductility found during the tensile tests.

Both Nickel 201 and Inconel 617, however, provide an improvement in LCF life over Hastelloy X. It is anticipated that the LCF life of an actual panel would be greater than the predicted life. The full aging effect would not be realized until toward the end of its life and the average ductility would be greater than the 1000-hr values used in the prediction calculations.

FABRICATION PROCESS DEVELOPMENT

Panel Design

Creep-rupture test specimen design (2- by 3-in. panels) is shown in figs. 13, 14, 15, and 16. The assembly with the spaced channel pattern face plate, shown in fig. 15, was designed to be tested at the hot face temperature. In this configuration, every other channel has been eliminated to provide a larger brazing area. The increased braze joint area was expected to compensate for the reduced braze joint strength at the hot face temperature, and rupture was expected to occur in the channel arch.

Coolant Passage Generation

Photochemical milling (PCM) was specified for coolant passage generation as the best method with regard to LCF life. Additionally, chemical machining is attractive because of the relatively lower cost and shorter turn-around time associated with this process in comparison to other available options such as mechanical machining and EDM (electrical discharge machining).

Hastelloy X specimens were used for initial evaluation of the photochemical milling process and indicated feasibility. Typical PCM Nickel 201 channel and pin-fine pattern face plates are shown in fig. 17. An Inconel 617 channel specimen is shown in fig. 18.
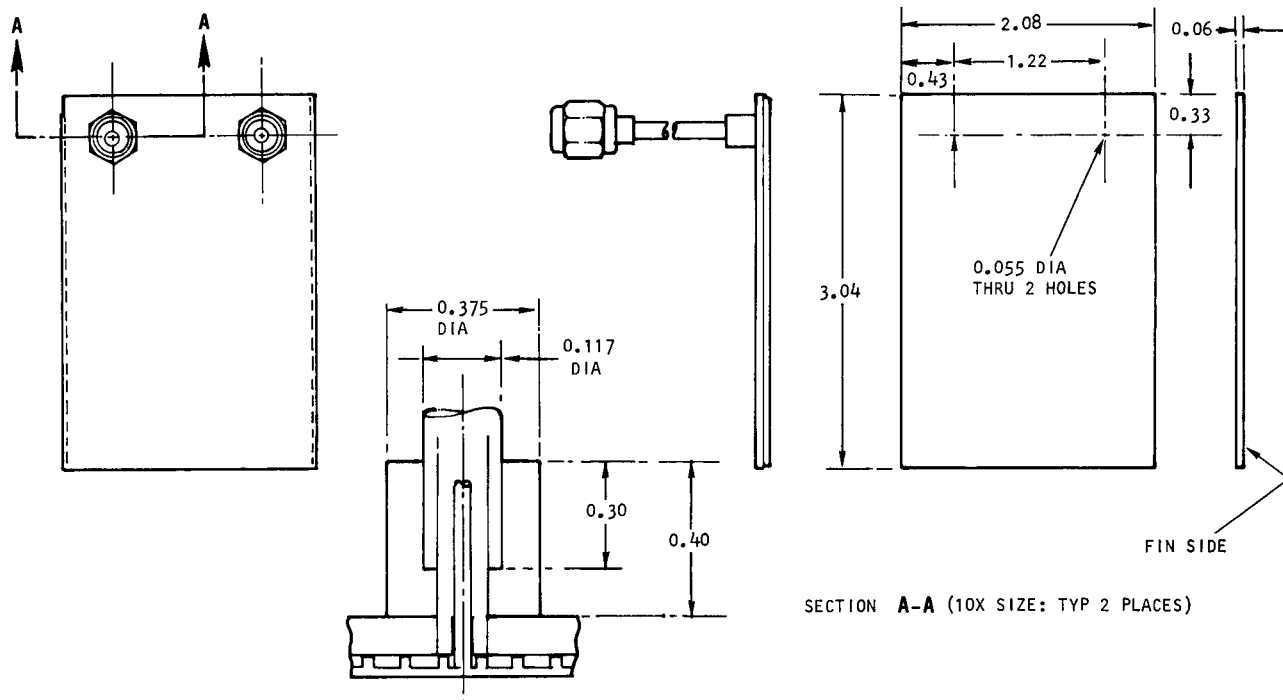
Figure 13.-Test panel assembly.
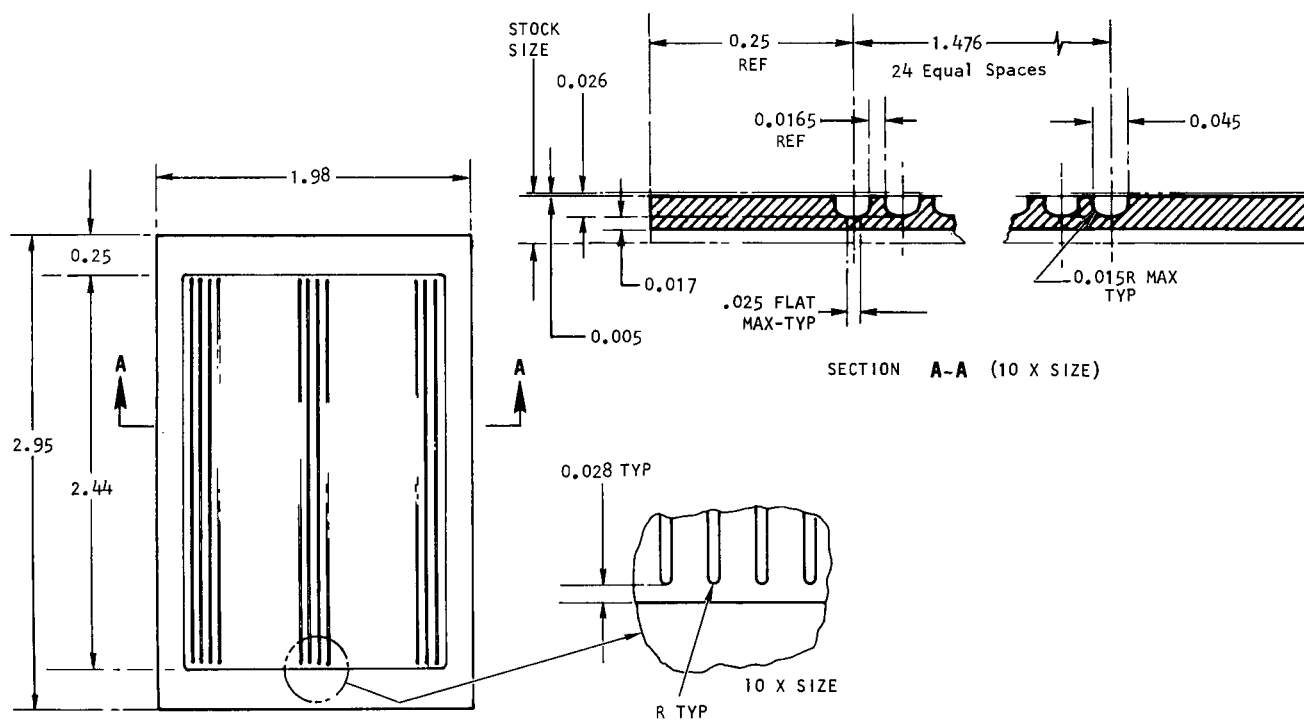
Figure 14.-Face plate with channel pattern.

A-31239

SECTION **A-A** (10X SIZE)
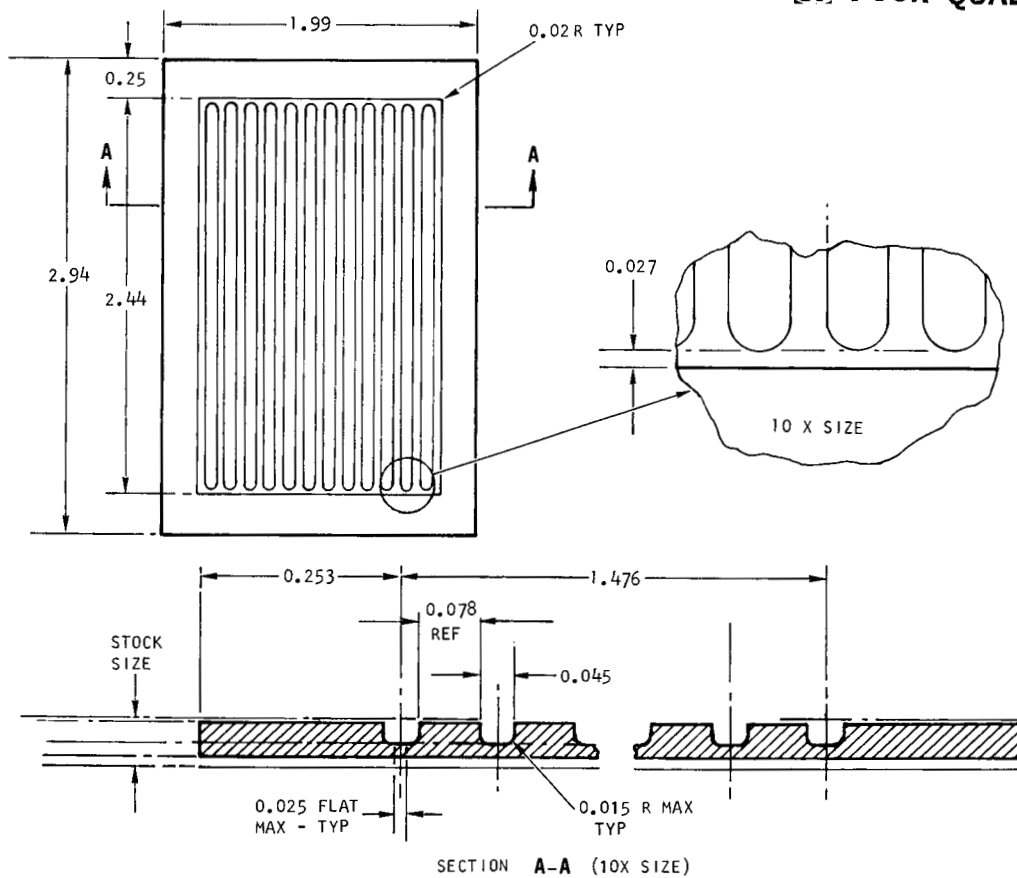
Figure 15.-Face plate with spaced-channel pattern.

SECTION **D-D**
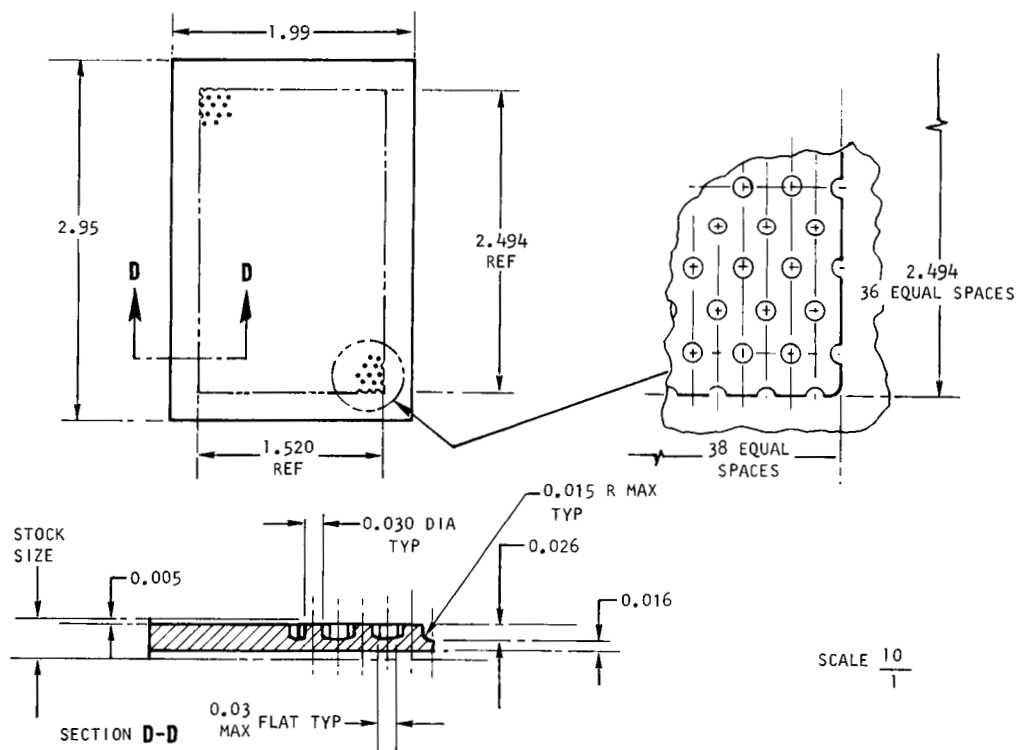
Figure 16.-Face plate with pin-fin pattern.

A-31240
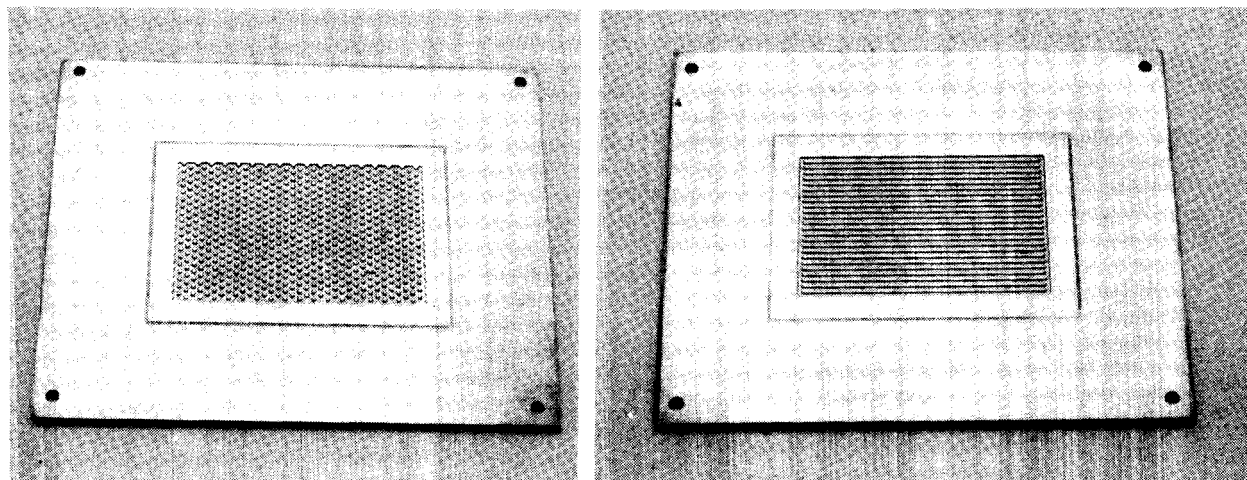
F-34921

Figure 17.-PCM Nickel-201 face plates.
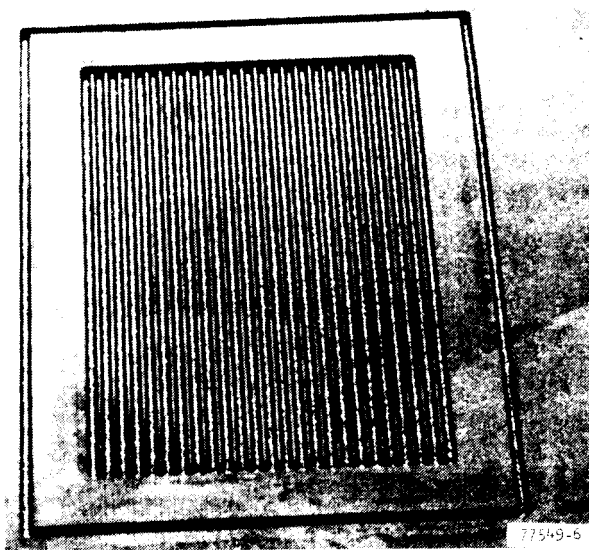
Figure 18.-Inconel 617 channel specimen.

Joining Development

Palniro 1 (50 Au-25 Pd-25 Ni), was selected for panel brazing for the following reasons:

(a) High strength at operating temperature (1200°F)

(b) High ductility with corresponding resistance to low cycle fatigue

(c) Oxidation resistance (important for exposed edges)

F-34921

Figure 17.-PCM Nickel-201 face plates.
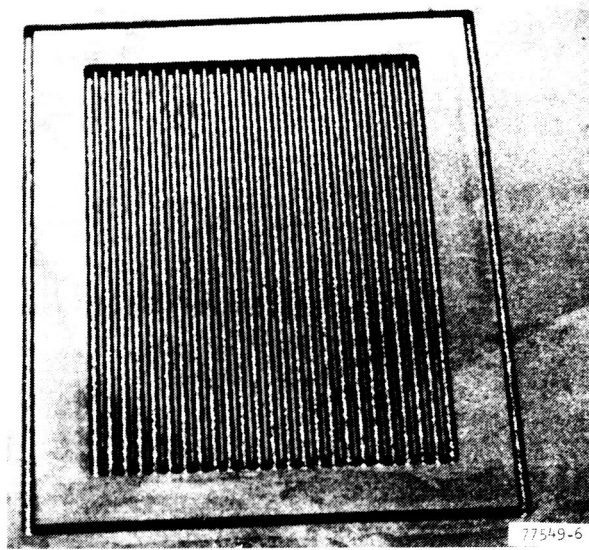
Figure 18.-Inconel 617 channel specimen.

Joining Development

Palniro 1 (50 Au-25 Pd-25 Ni), was selected for panel brazing for the following reasons:

    (a) High strength at operating temperature (1200°F)

    (b) High ductility with corresponding resistance to low cycle fatigue

    (c) Oxidation resistance (important for exposed edges)

(d) Excellent wetting and flow characteristics

(e) Minimal alloying with parent metal

(f) Other gold-base alloys are available to enable step brazing

(g) Available in foil form to permit accurate control of braze alloy
quantity (especially important in this application because of the
small coolant passage dimensions)

Tests were performed to verify the effectiveness of the selected alloy to
join the test panel materials, Inconel 617 and Nickel 201. T-section specimens
were brazed using a single layer of 0.001-in. Palniro 1 foil. Two Inconel 617
specimens were nickel plated, 0.0001 to 0.0002 in. thick, to promote alloy flow
and wetting.

A typical photomicrograph of an as-brazed section of each material is
shown in fig. 19. The braze alloy shows good gap filling, flow, and wetting,
no significant penetration, and no porosity on all specimens. Inconel 617
brazing was satisfactory with and without plating. However, as a precautionary
measure the plating was retained in subsequent brazing operations.

| 28X | 5021 | 28X | 5025 |

NICKEL 201   INCONEL 617-PLATED
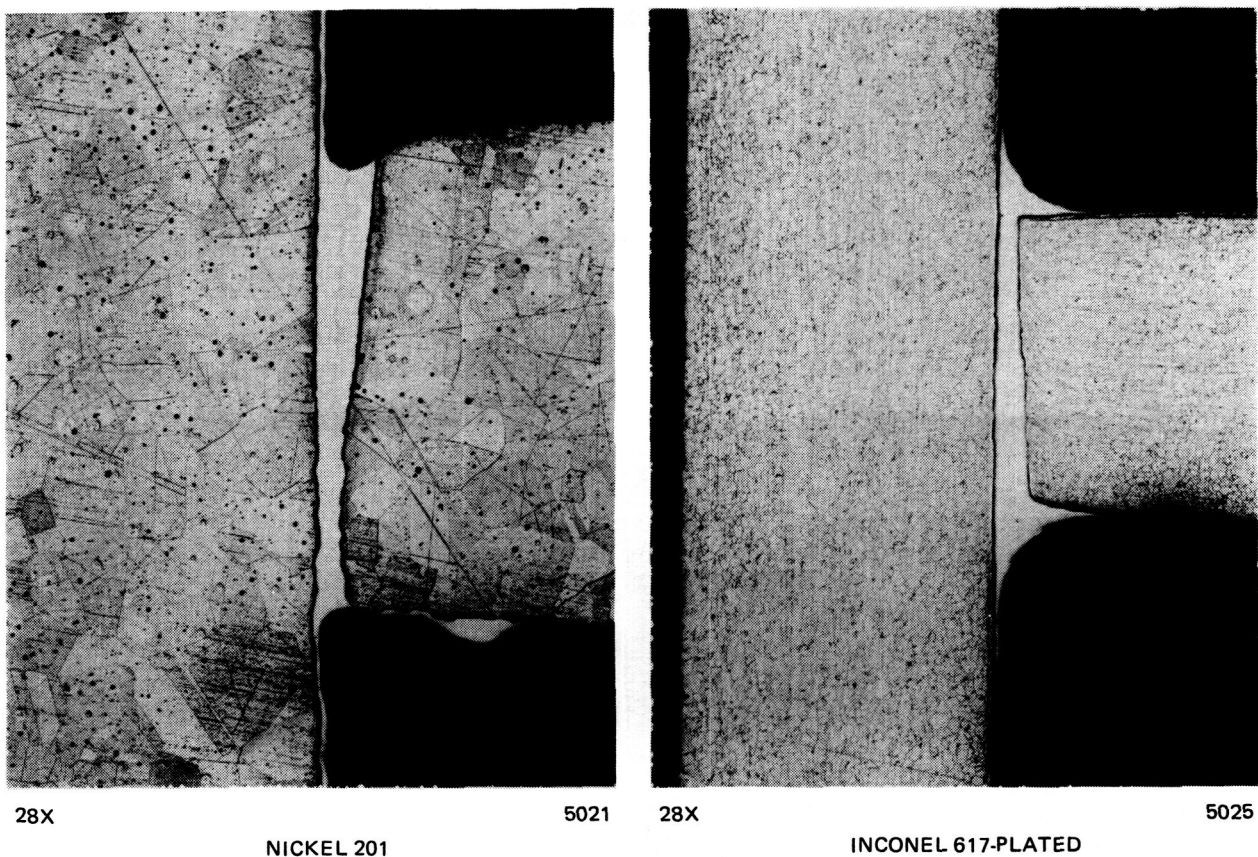
F-37140

Figure 19.-Palniro 1 brazing evaluation.

Nickel 201 panels.--Creep-rupture test panels were brazed using 0.001-in. thick Palniro 1 foil. Typical results of the holographic inspection preformed on a series of Nickel 201 panels are presented in fig. 20. Rework of panels that displayed holographic indications of voids, and that were judged repairable, was accomplished by inserting pins through face and back plates or by using a doubler brazed over the potentially weak areas. The remaining active panel area was adequate to obtain a valid measurement of the creep-rupture strength.

Braze joint evaluation.--Following creep-rupture testing, several of the Nickel 201 panels were sectioned for metallurgical evaluation of the Palniro 1 braze joints. Results showed indications of braze joint porosity (fig. 21). Creep-rupture test results have indicated that panel life for Nickel 201 is not limited by the braze joint properties (see Nickel 201 panel creep-rupture testing). Braze joint porosity, however, is of concern because it reduces the low cycle fatigue life of the panels by providing stress concentrations which serve as crack starters or crack joiners. Although a relatively minor effect, the joint strength is also reduced due to loss of load-bearing area, which is directly proportional to the percentage of voids in the cross-section. Consequently, a series of screening tests were conducted to identify the causes of this condition. The test series is specified in Table 12. The screening tests were selected to further evaluate the effects of panel flatness, amount of filler alloy, loading, and time-at-braze temperature.

Metallurgical examination of the brazed specimens showed that consistently sound braze joints could be obtained, free of porosity with no coolant passage plugging, as typified by fig. 22. Results further showed that fit-up is the most likely cause of voids. Local high spots or curvature prevent intimate contact. Fit-up is especially critical when the braze foil thickness is 0.001-in. or less. Hence, the selected procedure was to grind the test plates flat within 0.0005-in. and then hand lap to promote good contact.

Inconel 617 panels.--One pin-fin (SN 10) and one channel (SN 11) configuration creep-rupture test specimen were brazed using 0.0006-in. thick Palniro 1 filler alloy foil. The panels were nickel plated, 0.00005 to 0.0001-in. thick to enhance alloy flow and wetting. Typical results of holographic inspection performed on Inconel 617 panels are presented in fig. 23.

Creep-rupture test results are summarized in Table 13 and shown in fig. 24. Braze joint strength compared to parent metal properties and required strength is as follows:

Configuration	Ratio of Joint Strength to Base Metal Strength	Ratio of Joint Strength to Required Strength
Channel	0.31	6.3
Pin-Fin	0.35	3.0
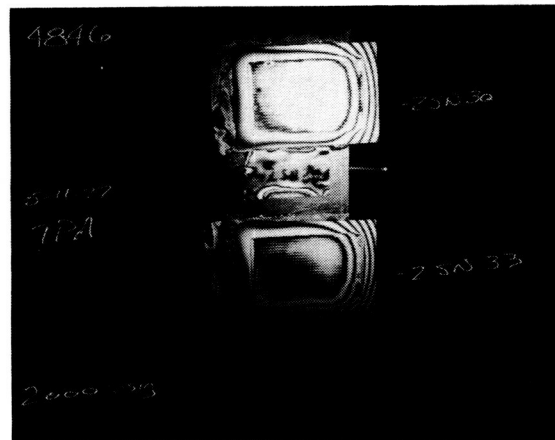
a. CHANNEL SPECIMEN AT 2000 PSIG
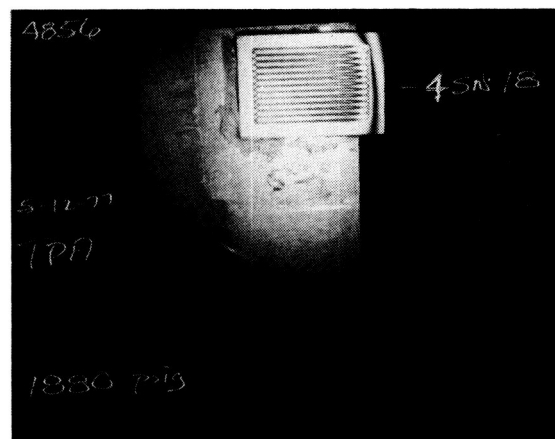
b. SPACED CHANNEL SPECIMEN AT 1880 PSIG
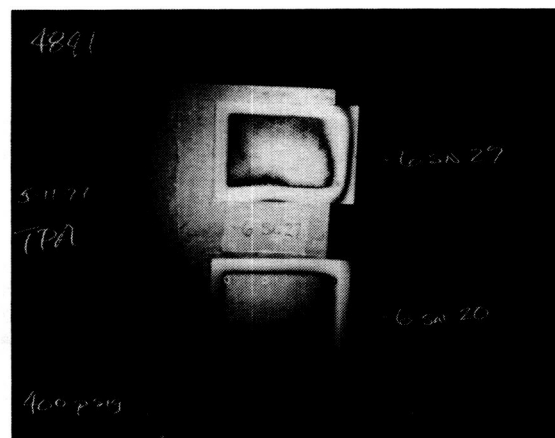
c. PIN-FIN SPECIMEN AT 400 PSIG

F-34951

Figure 20.—Nickel 201 panel holographic inspection.
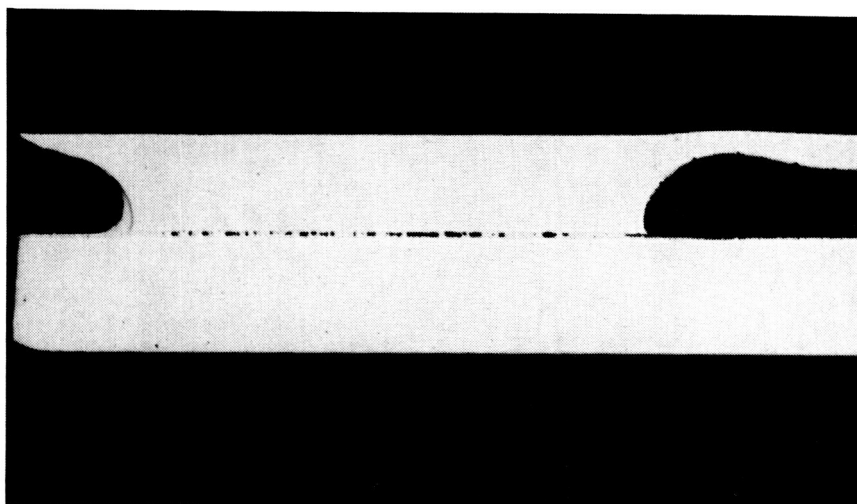
MICRO 9896   10X   F-34953

Figure 21.–Section through spaced-channel specimen after test.

TABLE 12.–SCREENING TESTS FOR
BRAZE JOINT VOIDS IN NICKEL

Specimen number	1	2	3	4	5
Braze alloy	Palniro 1	Palniro 1	Palniro 1	Palniro 1	NB 30
Thickness, in.	0.0006	0.0012	0.0012	0.0012	**
Load, psi	14	14	14	14*	14
Plating	Au	Au	Au	Au	Ni
Time at braze temperature, min.	10	10	1	1	1
Flatness, in.	0.0005	0.0005	0.0005	0.0005	0.0005

*Load applied at braze temperature
**Applied as powder, 0.2 g/sq. in.

The Palniro 1 braze joint strength is approximately a third of the parent metal strength, but the creep-rupture design margin is adequate for the intended application.

In both panels, separation occurred along the braze joint (fig. 25). Three layers are visible in the ruptured panel: (1) a white, gold-rich zone in the center, (2) a black area formed by a reaction between the braze and the base metal, and (3) a light grey diffusion zone.

42
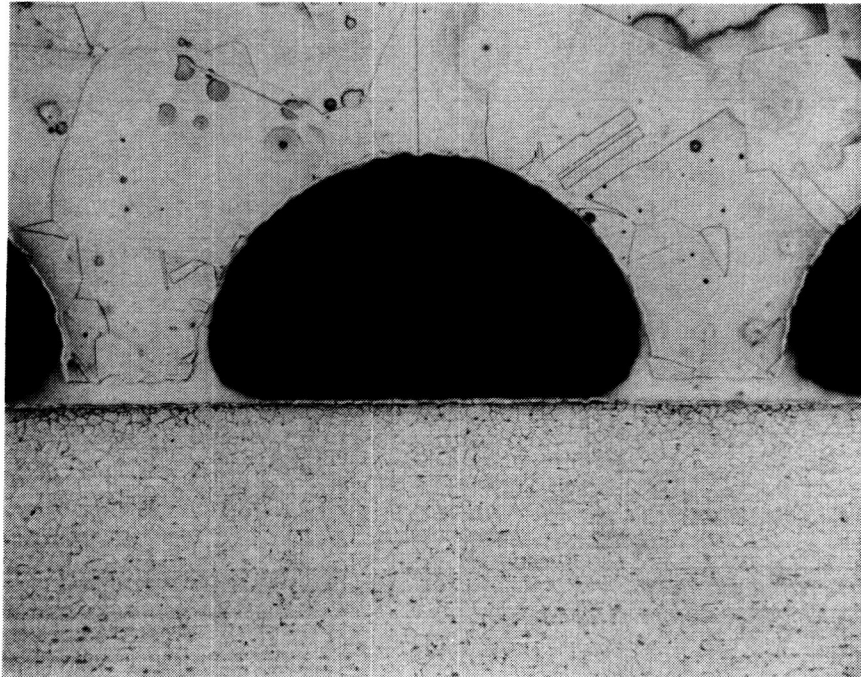
Figure 22.-Nickel 201 braze joint
evaluation, specimen no. 1.
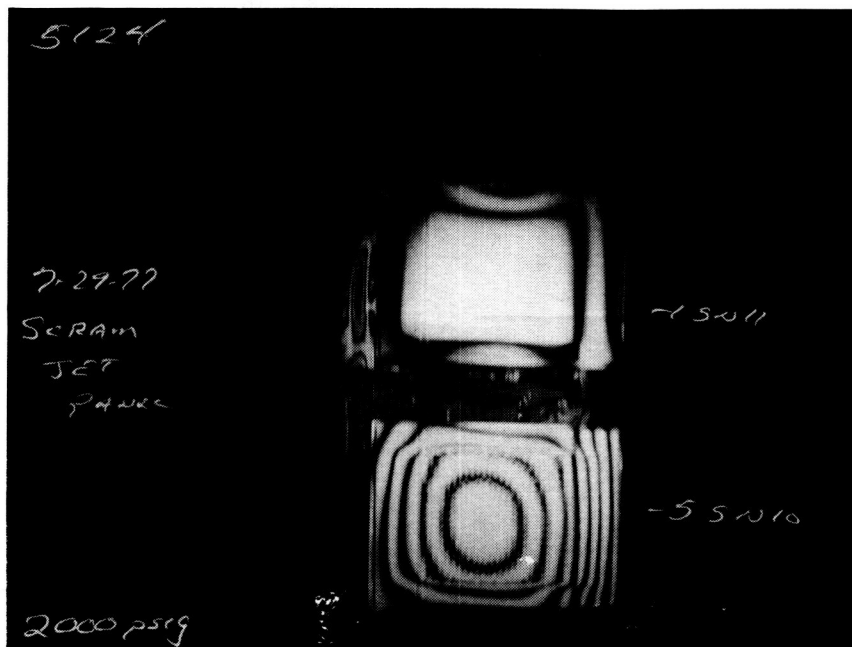
F-34946

The top of the photograph shows channel specimen at
2000 psig; The bottom is pin-fin specimen at 2000 psig.

Figure 23.-Inconel 617 panel holographic inspection.

43

TABLE 13.—INCONEL 617 PANEL CREEP-RUPTURE TEST DATA

Configuration	SN	Ambient Temp, °F	Applied Pressure, psig	Time-to-Rupture, hrs	LMP*	Location
Inconel 617 Channel	11	1250	6000	26.9	36.64	Braze joint
Inconel 617 Pin-Fin	10	1250	2950	19.6	36.41	Braze joint

*Larson-Miller parameter

A series of screening tests were conducted using Palniro 1, Palniro 7, Palniro RE, and Nicrobraz 30 (NB 30) filler alloys to evaluate the effects of foil thickness, brazing temperature, load and the plating type (gold or nickel) in formation of the multiregional braze joint structure. The brazing test parameters are presented in Table 14. The braze joint porosity was estimated from a visual examination of the photomicrographs of the unetched specimens and is related to joint fitup. Alloy characteristics are presented in Table 15.

Metallographic examination of the specimens listed in Table 14 indicated that all the joints, except NB 30, display the multiregional characteristics first observed in the separated creep-rupture test specimen.

To determine if these formations were unique with Inconel 617, an additional test was run using Hastelloy X base material and identical brazing conditions as listed below:

Braze alloy	Palniro 1
Foil thickness	0.0006 in.
Surface treatment (where used)	Nickel plated, 50 to 100 millionths of an inch thick
Brazing load	30 psi

The braze joint, as shown in fig. 26, indicates a multi-region structure similar to that observed with Inconel 617. It was concluded that a multi-region braze joint is not unique with Inconel 617 and would probably occur with other, similar nickel-based superalloys.
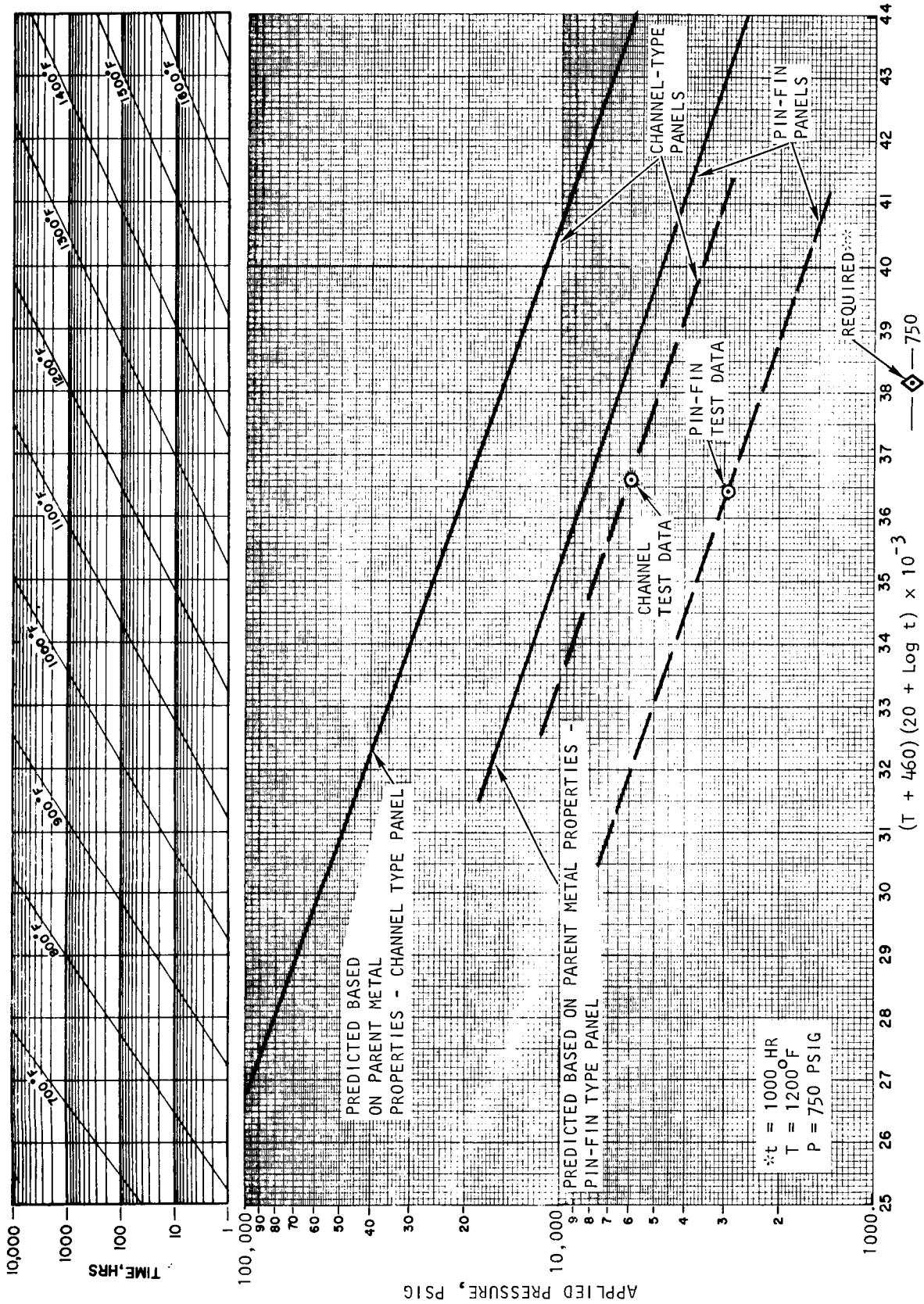
Figure 24.—Creep-rupture test results of Inconel 617 pin-fin and channel-type panels.

45

MICRO 9365   150X

a.   SEPARATED BRAZE JOINT
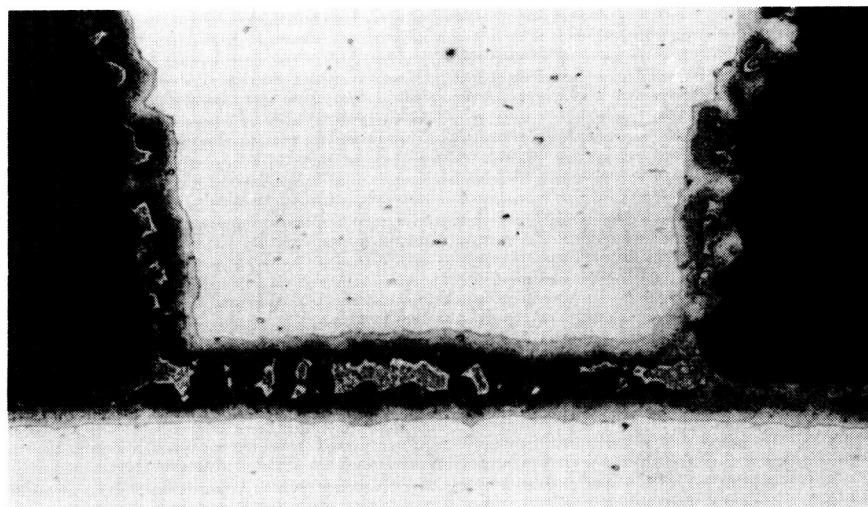
MICRO 9365   150X

b.   CONTINUOUS BRAZE JOINT

F-37712

Figure 25.-Section from SN 11 Inconel 617 channel test panel.

TABLE 14.-BRAZING PARAMETER INVESTIGATION

Specimen Number	Braze Alloy	Plating Material	Thickness, in.	Braze Load, psi	Estimated Braze Joint Porosity, Percent	Other Observations
1	Palniro 1	Ni	0.0006	30	60	
2	Palniro 1	Ni	0.0006	0	90	
3	Palniro 1	Ni	0.0006	5	60	Similar to 30-psi loading
4	Palniro 1	Ni	0.0018	5	10	
5	Palniro 1	Au	0.0006	30	5	
6	Palniro 7	Ni	0.001	30	1	
7	Palniro 7	Au	0.001	30	10	
8	NB 30	Ni	0.001*	30	70	
9	NB 30	Ni	0.001*	5	98	0.004 in. gap
10	Palniro RE	Ni	0.001	30	20	
11	Nioro	Ni	0.001	30	60	

*Applied in powder form (-325 mesh); amount estimated to be equivalent to 0.001 in. foil

TABLE 15.-BRAZE ALLOY COMPOSITION AND USUAL BRAZING TEMPERATURE

Alloy Designation	Composition	Usual Brazing Temperature, °F
NB 30	66Ni - 19Cr - 1Mn - 10Si - 4Fe	2130
Palniro 1	50Au - 25Pd - 25Ni	2070
Palniro RE	55Au - 37Ni - 8Pd	2025
Palniro 7	70Au - 22Ni - 8Pd	1925
Nioro	82Au - 18Ni	1800

Alternate braze alloy for Inconel 617.--Braze joint creep-rupture strength with Palniro 1 is a third of parent metal strength and appears adequate for the intended application, notwithstanding the multi-region braze joint structure. The braze joint structure could, however, degrade the panel low-cycle fatigue life. Effort was, therefore, undertaken to assess the relative merits of several alternates to the gold-nickel-palladium braze alloys. The alloys selected for evaluation possessed as many as possible of the desirable attributes of the gold-containing alloys, including the following:

- Good flow and filleting action

- Minimum perntration and alloying with parent metal

- Reasonable ductility (resistance to low-cycle fatigue)

- Braze temperature greater than 2000°F to provide for step brazing

- Available in foil form (uniform application, no binder contamination)

The following alloys were selected for screening:

(a). Nicrobraz 30--NB 30 has shown excellent high-temperature strength and resistance to fatigue. Control of the alloy application is a potential problem; sufficient powder must be used to minimize voids without plugging the coolant passages. In common with all powders, there is the contaminating influence of the organic binder.

(b) Nickel Boride--Electroless nickel and boron are plated on the parent metal. The parts are then joined by a liquid-activated diffusion bonding cycle--typically at 2150°F for 2 hrs at 100 psi. A post-bond diffusion cycle is used to diffuse the boron away from the joint leaving a strong, ductile joint.
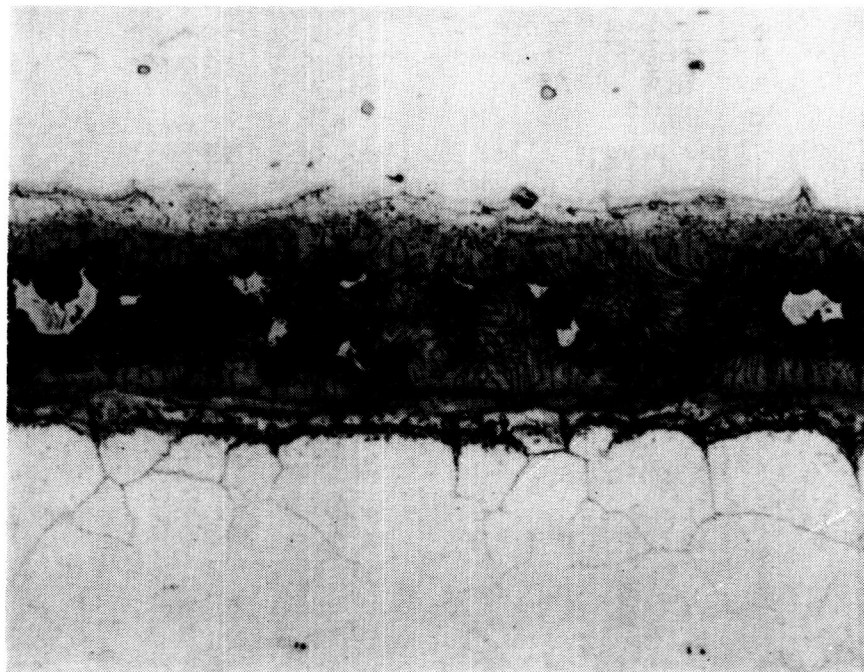
450X

a. NICKEL PLATED

450X
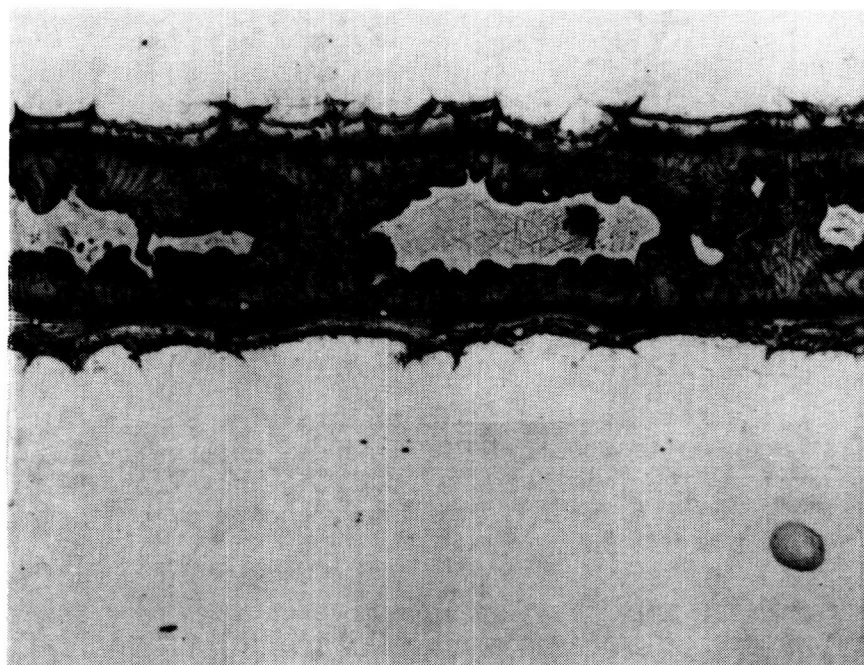
b. UNPLATED

F-34956

Figure 26.—Hastelloy X-Palniro 1 braze joint structure
(Ferric chloride/HCL etch).

49

(c) <u>Boronized Nickel-Chrome</u>—Ductile nickel-chrome foil is boronized using a vapor diffusion process developed by Materials Development Company. The outer foil covering is brittle, but the ductile central core permits handling of the foil. The alloy behaves much like a conventional nickel base powder alloy such as AMS 4778. By using a post-bond diffusion cycle, the joint embrittlement that usually results from boron-containing alloys can be eliminated.

Test specimens (1-in. wide sections of PCM panels) were fabricated and brazed in accordance with parameters specified in Table 16. After brazing, the panels were examined metallurgically to determine the following:

Joint uniformity

Extent of diffusion zone

Grain growth in parent metal

Porosity and joint continuity

Microhardness (related to ductility)

Plugging tendency

The results of the screening tests are summarized in the following paragraphs.

Nicrobraze 30 braze alloy (NB 30) evaluation.—NB 30 braze alloy powder was applied to the test pieces as specified in Table 16. Voids are present in all braze joints. At a 2130°F braze temperature, the alloy appears lumpy, suggesting too low a braze temperature. At a 2175°F braze temperature, the alloy flowed better but is still lumpy. Increased grain growth in Inconel 617 at 2175°F is observed with NB 30. Typical test results are shown in fig. 27.

Boronized nickel chrome evaluation.—Tests were performed using 0.001 in.-thick boronized nickel chrome foil as the filler alloy. Brazing parameters were as specified in Table 16.

The 1-hr cycle test results indicated that the base metal adjacent to the braze was hardened to the low HRC 30 range, apparently due to boron. The base metal away from the joint area was HRB 95. No excessive grain growth is observed in the Inconel 617 base metal and there is almost no errosion of the base metal by the braze alloy.

The longer 5-hr cycle resulted in a more uniform hardness and a homogeneous bond. Some evidence of grain growth across the joint, which is a step towards homogenization, is observed. No excessive grain growth in the base metal, however, is evident.

Results of the higher braze temperature (2250°F) and time (10 hrs) indicated an accelerated rate of boron diffusion and homogenization. The hardness measurements across the joint are uniform and are equal to the base metal,

50

TABLE 16.–SCREENING TESTS FOR INCONEL 617 ALTERNATE BRAZE ALLOY

Braze Alloy	Thickness in.		Load Psi	Plating	Braze Temperature °F	Time at Braze Temperature	Flatness in.
NB 30		Note 1	14	Ni	2130	10 min	0.0005
		Note 2	14	Ni	2130	10 min	0.0005
		Note 3	14	Ni	2130	10 min	0.0005
		Note 2	14	Ni	2175	10 min	0.0005
		Note 2	14	Ni	2175	10 min	0.0005
Bronized Nickel Chrome (BNiCr)		0.001	14	--	2100	1 hr	0.0005
		0.001	14	--	2100	5 hrs	0.0005
		0.001	14	--	2250	10 hrs	0.0005
		0.001	14	--	2100	10 hrs	0.0005
Nickel Boride (NiB)		0.001	14	--	2100	5 hrs	0.0005
		0.001	14	--	2100	10 hrs	0.0005

NOTES:

1. Applied as powder, 0.10 g/sq in.

2. Applied as powder, 0.15 g/sq in.

3. Applied as powder, 0.20 g/sq in.

about HRB 94, indicating that the boron has been diffused away. However, extensive grain growth is observed throughout the specimen which tends to degrade the base metal properties.

The 10-hr cycle at 2100°F resulted in a uniform hardness and a homogeneous bond without excessive grain growth in the base metal. A typical photomicrograph of this test specimen is presented in fig. 28. The braze joint appears to be free of voids. Hardness readings across the braze joint indicate that the braze alloy was HRB 97. The base metal adjacent to the braze was HRC 24, and the base metal away from the joint was HRC 20.
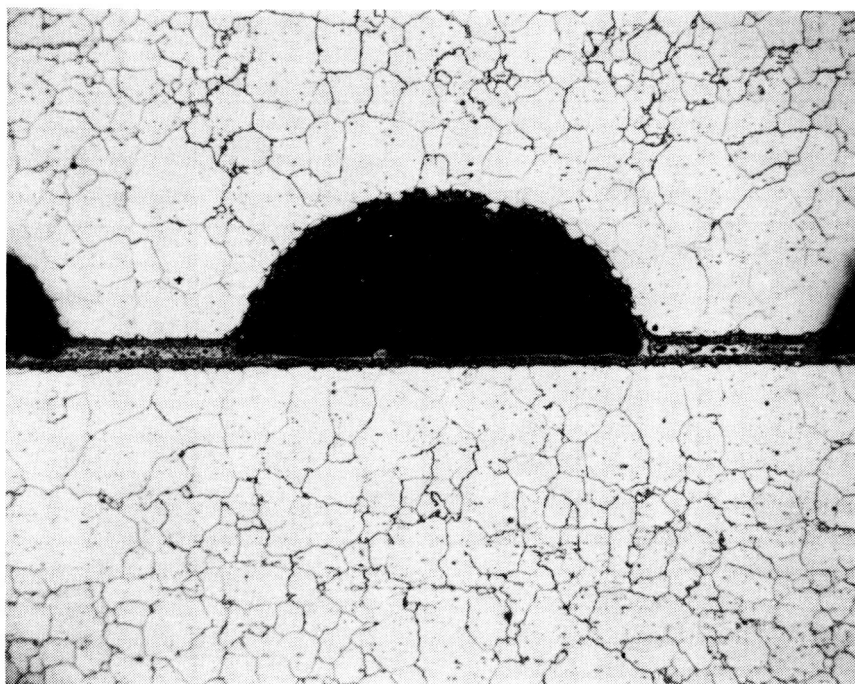
MR 11275 50X

F-34933

Figure 27.-Inconel 617 braze alloy evaluation,
NB 30, 0.15 g/sq in., 2175°F.
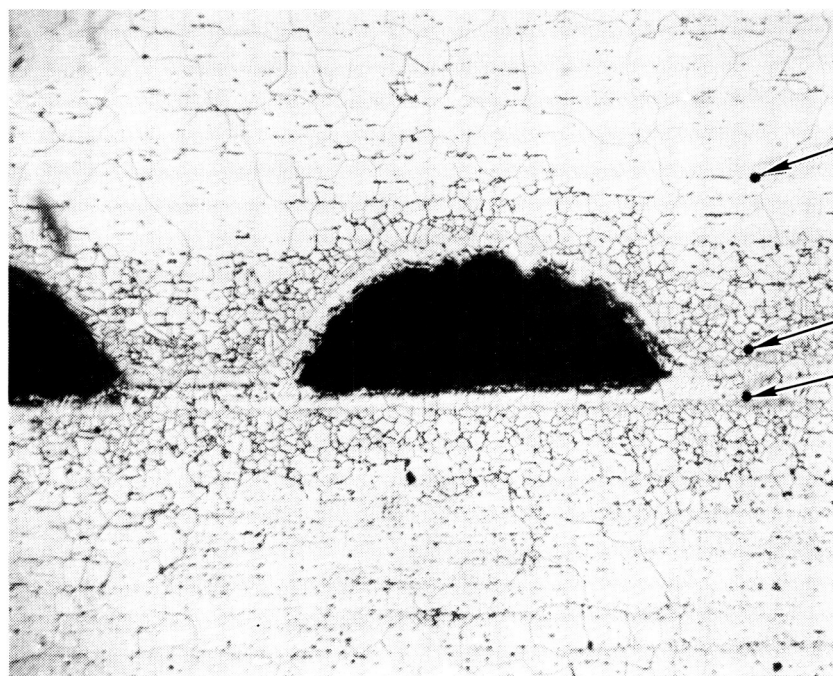
MR11268 50X

F-34935

Figure 28.-Isothermally solidified bond, boronized NiCr
foil, 10-hr cycle time at 2100°F.

These limited tests tend to indicate that results similar to the 10-hr cycle at 2100°F may be possible using a number of higher braze temperature and shorter heat treat time conditions. For the work reported here, the 10-hr, 2100°F cycle was selected.

Nickel boride plating evaluation.--Two samples plated with 0.001-in. thick nickel boride were brazed at 2100°F and heat treated for 5 and 10 hrs, respectively. The results for the 10-hr heat treat cycle are presented in fig. 29. The braze quality appears to be excellent. The hardness readings on this sample were HRB 97 at the center of the joint, HRC 20 in an area adjacent to the joint, and HRB 96 at the base metal away from the joint. The longer heat treat cycle results in a more uniform hardness across the joint and a more homogeneous bond, as evidenced by the reduced definition of the braze joint.
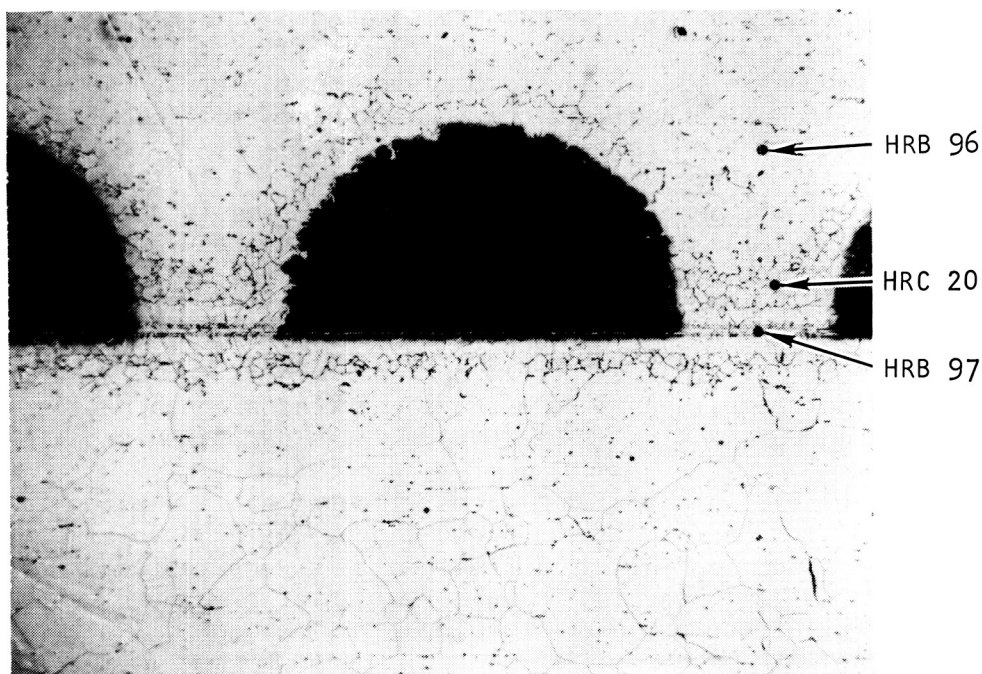
F-34940

Figure 29.-Isothermally solidified bond, NiB plated sample,
10-hr cycle time at 2100°F.

Discussion and recommendations.--The creep-rupture strength of the Inconel 617 panel brazed with Palniro 1 filler alloy is adequate for the intended application notwithstanding the multi-region braze joint structure.

Results of screening tests with Nicrobraz 30 suggest that the alloy contributes to increased grain growth in Inconel 617 at 2175°F. Futhermore, the alloy flow on Inconel 617 is sluggish and the joints appear to be lumpy with voids present.

The boronized nickel chrome (BNiCr) braze test specimen brazed at 2100°F and heat treated for 10 hrs has the most uniform hardness measurements of all the BNiCr brazed specimens. The 10-hr sample also demonstrates a more homogeneous bond when compared to the other BNiCr specimens, and the joint should provide excellent fatigue properties and a rupture strength approaching that of the base metal.

Of the nickel boride plated specimens tested, the sample brazed and heat treated for 10 hrs at 2100°F is the more preferable. The resulting braze is excellent; the hardness readings are uniform and the bond is homogeneous.

Either the boronized nickel chrome or the nickel boride braze alloys, brazed and heat treated at 2100°F for 10 hrs, seem to be very promising for brazing of Inconel 617. For the current application, the boronized nickel chrome is better suited because the foil is readily available and large areas can be alloyed with relative ease. The nickel boride braze alloy must be plated onto the desired surfaces. Plating of larger pieces would require a significant amount of development to ensure uniformity. Therefore, BNiCr foil was selected for all subsequent brazing efforts with Inconel 617.

Braze joint tensile tests.--To determine the test temperature for conducting the Inconel 617 panel creep rupture tests, tensile data on the strength of the BNiCr braze joint at elevated temperature was required. The braze joint operating at 1200°F could be more critical than the face sheet outer fiber which operates at 1600°F.

The Inconel 617 brazed tensile bar specimen is shown in fig. 30. After two cylindrical detail parts were brazed, a finishing operation was conducted to obtain the gage section dimensions, and the parts surface finished.

Six specimens were brazed and heat-treated at 2100°F for 10 hrs. Visual inspection of the bars indicated a sound braze with no voiding. The specimens were then machined to finish. Three specimens were tested at 1250°F and three at 1600°F. The test results presented in Table 17, compare very well with published values for typical unbrazed Inconel 617 material (Reference: Huntington alloys Inconel 617 Brochure; 1972).

The samples tested at 1250°F all broke through the boride precipitates in the grain boundaries adjacent to the braze. The reduction in area obtained from this test series is that of the braze joint.

The samples tested at 1600°F all broke in the parent metal about halfway between the braze joint and the end of the reduced section. The reduction in area results obtained indicate less ductility in the parent metal than given in the manufacturers data. This is probably caused by the thermal treatment of the bar rather than diffusion of boron.

Tensile tests at both temperatures produced uniform elongation with no abrupt changes at the braze joint, fig 31.

54
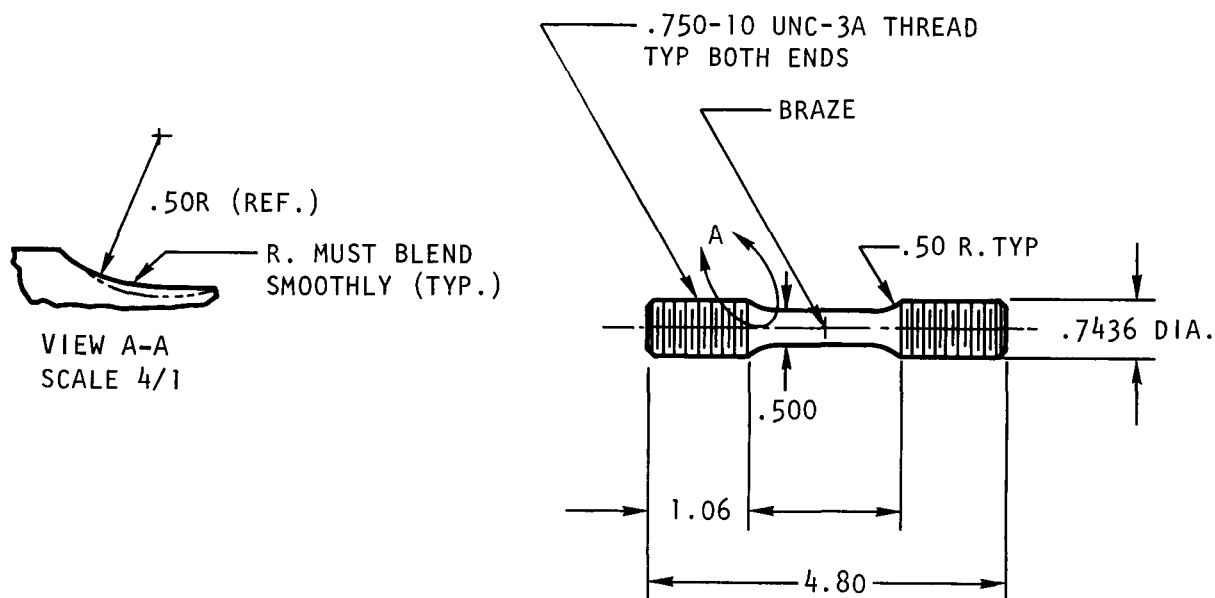
Figure 30.-Inconel 617 butt-brazed tensile bar.

Results of braze joint tensile tests indicate that the braze joint is weaker than the base metal at 1250°F and room temperature. At 1600°F, however, the parent metal strength drops off rapidly and is less than the braze joint. Fracture occurs away from the joint probably because the base metal is locally hardened due to boron penetration. At 1250°F the ultimate strength of the braze is probably very close to the base metal strength as indicated by the literature data. The reason for consistent rupture in the braze is likely due to a stress concentration effect from the large boride particles.

Results obtained from these tests should be applicable to the channel specimens. The strength at the location of the braze filler metal should be the same for both sample configurations. The differences that occur are due to the concentration of boron in the parent metal near the braze joint.

55

TABLE 17.—INCONEL 617 ELEVATED TEMPERATURE BRAZE TENSILE TESTS

Specimen No.	Test Temperature °F	Ultimate, KSI		Yield, KSI		Elogation Percent		Reduction in area, percent	
		Published**	Test	Published**	Test	Published**	Test	Published **	Test
1	1250	81	82.7	25	29.5	64	36.8	53	27.0
2	1250		83.6		28.7		36.0		27.5
3	1250		82.2		29.6		35.5		27.2
4	1600	42	52.8	28	27.4	99	57.0	86	66.5
5	1600		55.6		27.6		48.7		63.2
6	1600		77.9		26.5		50.0		46.0

**Solution treated hot-rolled rod.

56

F-34944

Figure 31.-Inconel 617 braze tensile test at 1600°F
(arrow points at braze joint).

PANEL CREEP-RUPTURE TESTING

Performance Predictions

Published data on the creep strengths of Nickel 201 and Inconel 617 materials were used to predict the allowable pressure stresses in the channel and pin-fin heat exchanger configurations for the 1000-hr design life. The results of this evaluation indicated that Inconel 617 would have adequate creep life but Nickel 201 could be marginal under the operating conditions encountered in the panel. Consequently, a series of creep rupture tests were planned for Nickel 201 and Inconel 617 materials using internally pressurized 2 in. by 3 in. brazed panels. The design layouts of the creep-rupture test specimens were presented previously in figs. 13 through 16. Initially, Palniro 1 braze alloy was selected for both Nickel 201 and Inconel 617 panel assemblies. Limited tests were planned for Inconel 617 material to verify the initial evaluation and the strength of the braze joint.

A comparison of the pressures that were predicted to cause rupture in 1000 hrs in the critical areas of the panel test specimens is summarized in Table 18.

At operating conditions the most critical areas for the channel configuration is predicted to be the outer fiber. However, during the creep-rupture tests the specimens are in an isothermal environment and if the test temperature is set equal to the outer fiber temperature, then the braze joint becomes critical. To examine both critical areas and to verify the assumptions used in the analysis, two channel configurations were specified for the creep rupture tests:

(a) A channel specimen to be tested at the maximum operating temperature. The braze joint was predicted as the rupture point.

57

TABLE 18.–CRITICAL AREA COMPARISON FOR CHANNEL AND PIN-FIN SPECIMENS (100-HR STRESS RUPTURE)

Material	Configuration	Location	Test Temperature, °F	Pressure to cause rupture in 1000 hrs, psig
Nickel 201	Channel	Braze joint	1257*	1550
		Outer fiber	1452*	840
		Braze joint	1452	320
		Outer fiber	1257	4200
	Spaced channel	Braze joint	1257	6890
		Braze joint	1452	1450
		Outer fiber	1257	4200
		Outer fiber	1452	840
	Pin-Fin	Braze joint	1180*	1115
		Outer fiber	1390*	1328
		Braze joint	1390	205
		Outer fiber	1180	7197
Inconel 617	Channel	Braze joint	1205*	16000
		Outer fiber	1670*	7000
		Outer fiber	1205	44000
		Braze joint	1670	2600
	Spaced channel	Braze joint	1205	68000
		Braze joint	1670	11500
		Outer fiber	1205	44000
		Outer fiber	1670	7000
	Pin-Fin	Braze joint	1160*	6900
		Outer fiber	1580*	9430
		Braze joint	1580	1460
		Outer fiber	1160	44600

*Conditions during actual operation

(b) A spaced channel specimen to be tested at the maximum operating temperature. The braze joint area in this design (fig. 15) was increased to shift the critical area to the outer fibers. The arch was predicted as the rupture point.

The predicted behavior of the pin-fin specimens is also summarized in Table 18. In the case of the pin-fin specimen, the braze joint is the most critical area due in part to the improved heat transfer across the structure (lower outer fiber operating temperature). The plan, therefore, was to test the pin-fin specimens at the same temperature level as the channel specimens using the results of the spaced channel tests as a guide to verify that the pin-fin braze joint is more critical than the arch between pins.

Results of the initial tests at 1450°F on Nickel 201 channel and pin-fin panels indicated that the braze joint was excessively stressed. The test temperature was reduced to 1250°F to prevent overloading the braze joint. The revised test conditions are shown in Table 19. For the channel and pin-fin specimens for both Nickel 201 and Inconel 617 materials the test temperature was set at 1250°F, which is the maximum operating braze joint temperature of any configuration/material combination.

Pin-fin, channel, and spaced-channel specimens were fabricated. Fig. 32 shows the three face sheet designs used in the creep-rupture test specimen assemblies. Prior to the creep-rupture test, each panel was inspected as follows:

(a) X-ray examination to check for plugging and braze alloy coverage.

(b) Proof pressure test to verify basic structure integrity and no visible leakage.

(c) Holographic inspection to check for any small imperfections not detected by the proof pressure test.

Proof pressure levels are noted in Table 19. The specified value is at least 2000 psig except for the nickel pin-fin configuration, where it was necessary to limit the proof pressure to 800 psig, based on assumed properties at 80 percent of nominal and braze joint strength at 50 percent of parent metal.

Test Setup

A schematic of the creep-rupture test facility equipment setup is shown in fig. 33. Equipment installed in the facility is shown in fig. 34. The control panel is on the right, the furnace is in the center, and the temperature indicator is on the left.

The test setup permits testing of one to nine panel assemblies at temperatures to 1600°F and pressures to 6000 psig. Circuit isolation allows tests at the same temperatures to be conducted simultaneously at three pressure levels. Upon failure of an individual panel, valving will permit identification and isolation, with test interruption of that circuit only.

TABLE 19.—PANEL EVALUATION TESTS

Configuration	Material	Panel Configuration Dash Number	Proof Pressure At Room Temperature, psig	Test Temperature, °F	Applied Pressure, psig	Estimated Time-To-Rupture, Hrs
Channel	Inconel 617	-1	2000	1250	6000	1000 (Stop at 400 hrs)
Channel	Nickel 201	-2	2000	1250	3030 2480 2070	20 100 400
Spaced channel	Inconel 617	-3	2000	1560	6000	1000 (Stop at 400 hrs)
Spaced channel	Nickel 201	-4	2000	1400	3690	100
Pin fin	Inconel 617	-5	2000	1250	4000	1000 (Stop at 400 hrs)
Pin fin	Nickel 201	-6	800	1250	1260 1030 860	20 100 400

60

77549-5
F-34927
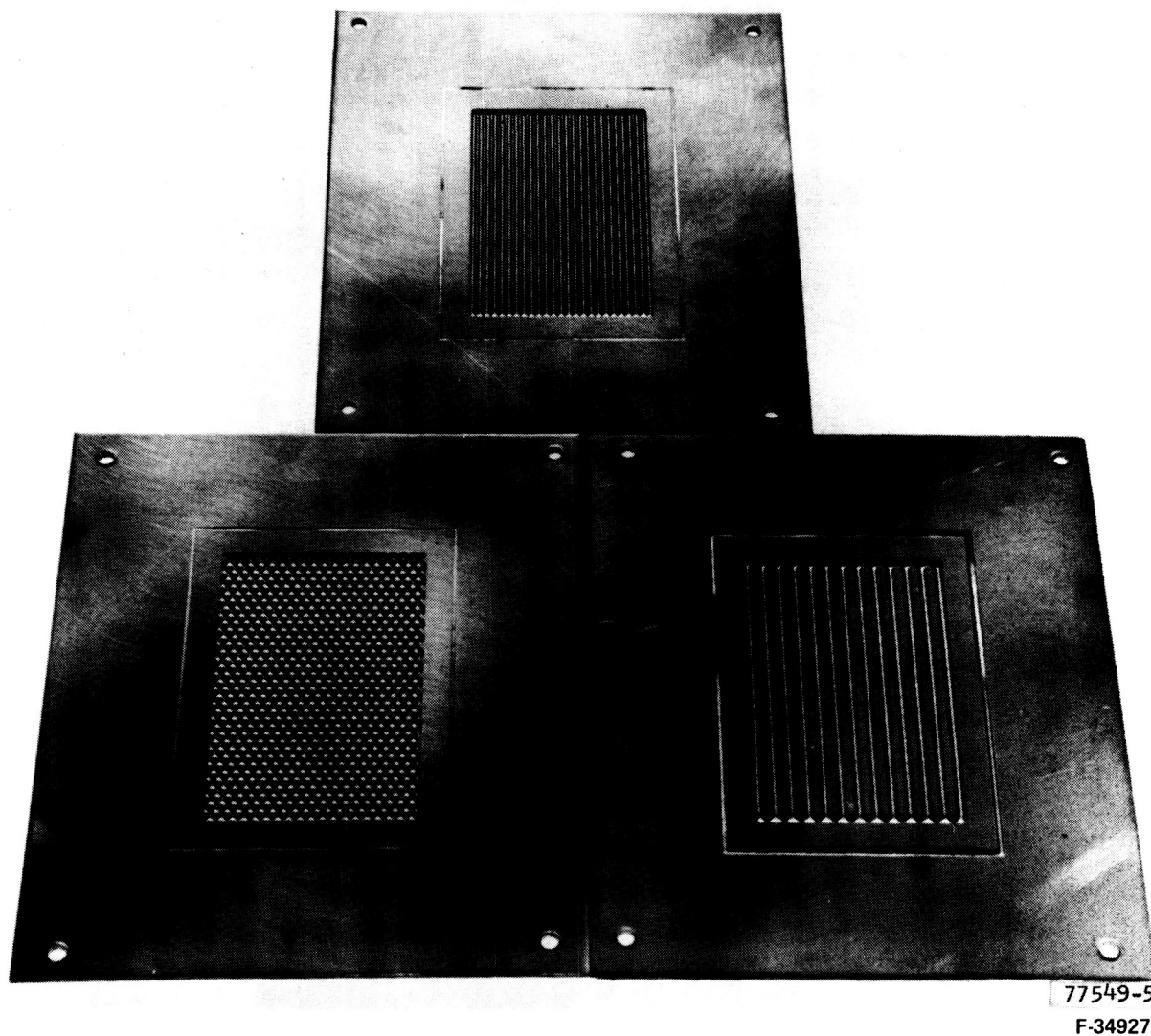
Figure 32.-Photochemical machined plates.

Nickel 201 Panel Test Results

The Nickel 201 creep-rupture test results are summarized in Table 20. The first pin-fin and channel specimens were tested at 1450°F and a pressure level calculated to produce rupture in 20 hrs. The test results, however, indicated that the panels were stronger than predicted. The joint efficiency factor in creep is apparently approaching 1.0 compared to an assumed factor of 0.50. The predicted creep-rupture life for the remaining panels was revised and is shown in Table 20.

Figure 33.—Creep-rupture test facility layout.

SYSTEM CAPABILITY

• OVEN TEMP AMBIENT TO 2000°F
• PRESSURES 0-6000 PSIG
• GASES N₂ TO 2000 PSI (LAB SUPPLY)
• "K" BOTTLES FOR 6000 PSI AND OTHER GASES
• ANY COMBINATION OF PRESSURES (MULTIPLES OF 3)
• 9 SAMPLES TOTAL

SYSTEM OPERATION

OVEN IS STABILIZED AT PROPER TEMPERATURE
SAMPLES ARE PRESSURIZED TO DESIRED PRESSURE.
SAMPLE MANIFOLD IS ISOLATED BY VALVE DOWN-
STREAM OF REGULATOR. FAILURE OF SAMPLE
CAUSES PRESSURE TO FALL ACTIVATING LOW PRES-
SWITCH. AUDIO ALARM IS SOUNDED (MANNED SHIFTS)
INDICATOR LIGHTS, ELAPSED TIME STOPS. FAILED
SAMPLE CAN BE ISOLATED AND TESTING CONTINUED.

62

F-34926

Figure 34.–Creep-rupture test facility equipment.

TABLE 20.—NICKEL 201 PANEL CREEP-RUPTURE TEST DATA

Configuration	SN	Ambient Temp, °F	Applied Pressure, psig	Time to Rupture, Hrs		LMP*	Location
				Predicted	Actual		
Nickel 201 Channel	1	1450	1040	20	152.8	42.37	Braze joint
	28	1250	3030	100	36.6	36.87	Parent metal
	29	1250	3030	100	0.9	34.12	Parent metal
	30	1400	1360	100	21.6	39.68	Parent metal
	31	1400	1360	100	76.4	40.70	Braze joint
	32	1400	1360	100	110.5	41.00	Braze joint
	33	1250	3030	100	0.4	33.52	Parent metal
	34	1250	2000	400	178.5	38.05	Braze joint
Nickel 201 Pin Fin	1	1450	405	20	104.4	42.06	–
	20	1250	1030	100	84.0	37.49	Parent metal
	21	1400	565	100	143.1	41.21	–
	22	1250	1030	100	21.1	36.46	Parent metal
	25	1250	860	400	242.3	38.28	–
	27	1400	560	100	77.9	40.72	Braze joint
Nickel 201 Spaced Channel	16	1400	3690	100	3.8	38.28	Braze joint
	18	1400	3690	100	0.8	37.02	Braze joint

*Larson-Miller parameter

The test data for the channel, pin-fin, and spaced-channel specimens were calculated using the Larson-Miller Parameter (LMP) and the results are shown in figs. 35 and 36, respectively. The test points are plotted on the curves together with the points corresponding to the design braze joint conditions of 1250°F for 1000-hrs at 750 psig for the channel design, 1200°F for 1000 hrs at 750 psig for the pin-fin design, and 1400°F for 1000 hrs at 750 psig for the spaced-channel design.

The data points, including those obtained at 1400 to 1450°F for channel and pin-fin specimens, all fall close to the predicted performance which is based on the creep-rupture strength of Nickel 201. This tends to substantiate that the braze point efficiency factor is approaching 1.0 for Nickel 201 panels.

Two Nickel 201 test panels before testing are shown on fig. 37; one is the SN 1 pin-fin specimen and the other is the SN 1 channel specimen. The back plates were Hastelloy X. These panels were tested at 1450°F. Panel appearance after testing is shown in fig. 38.

A typical cross section of the channel panel taken for metallographic examination is shown in fig. 39.

The contour of the flow passages is acceptable although the flow area is smaller than specified. The land thickness is within the specified tolerance. The land thickness is most critical in this panel design because this dimension controls the braze joint area, which is predicted to be critical. For this test, the face plate thickness was left greater than specified. Subsequent panel specimens used the design face plate thickness.

Panel brazing appears excellent with only small voids in the outer frame area. There appear to be some grain boundary separations, which start at several locations around the channel contours.

A cross section taken through the bulged area is shown on fig. 40. The separation occurred through the nickel-to-Hastelloy braze joint. The damage appears to have been caused when the panel bulge developed. The deformation shows ductile behavior. Separation probably initiated at the start of the channel land area where a stress concentration exists.

Sections from the SN 1 pin-fin panel tested at 1450°F are shown on fig. 41. The flow passage contour is smooth, and the flow area is as specified. The face plate thickness was again left greater than specified for this test. The face plate damage in the corner areas where it was still joined to the Hastelloy X support plate is believed to have occurred when the face plate suddenly separated.

Two types of separation are observed in fig. 41: in the braze joint and in the Nickel 201 parent metal. The necked-down appearance of the pin indicates that the parent metal separation was ductile. Only a minimum of alloying and penetration into the base metal is noted. The oxidation visible on the Nickel 201 pin surface is believed to have occurred between the time the panel ruptured, at 104.4 hrs, and when it was removed from the furnace, at 152.8 hrs (channel specimen rupture time).

65

Figure 35.-Creep rupture of Nickel 201 standard-channel and pin-fin panels.

A-30811

66
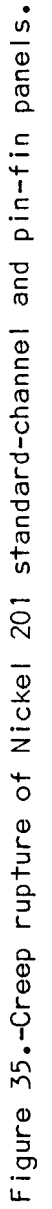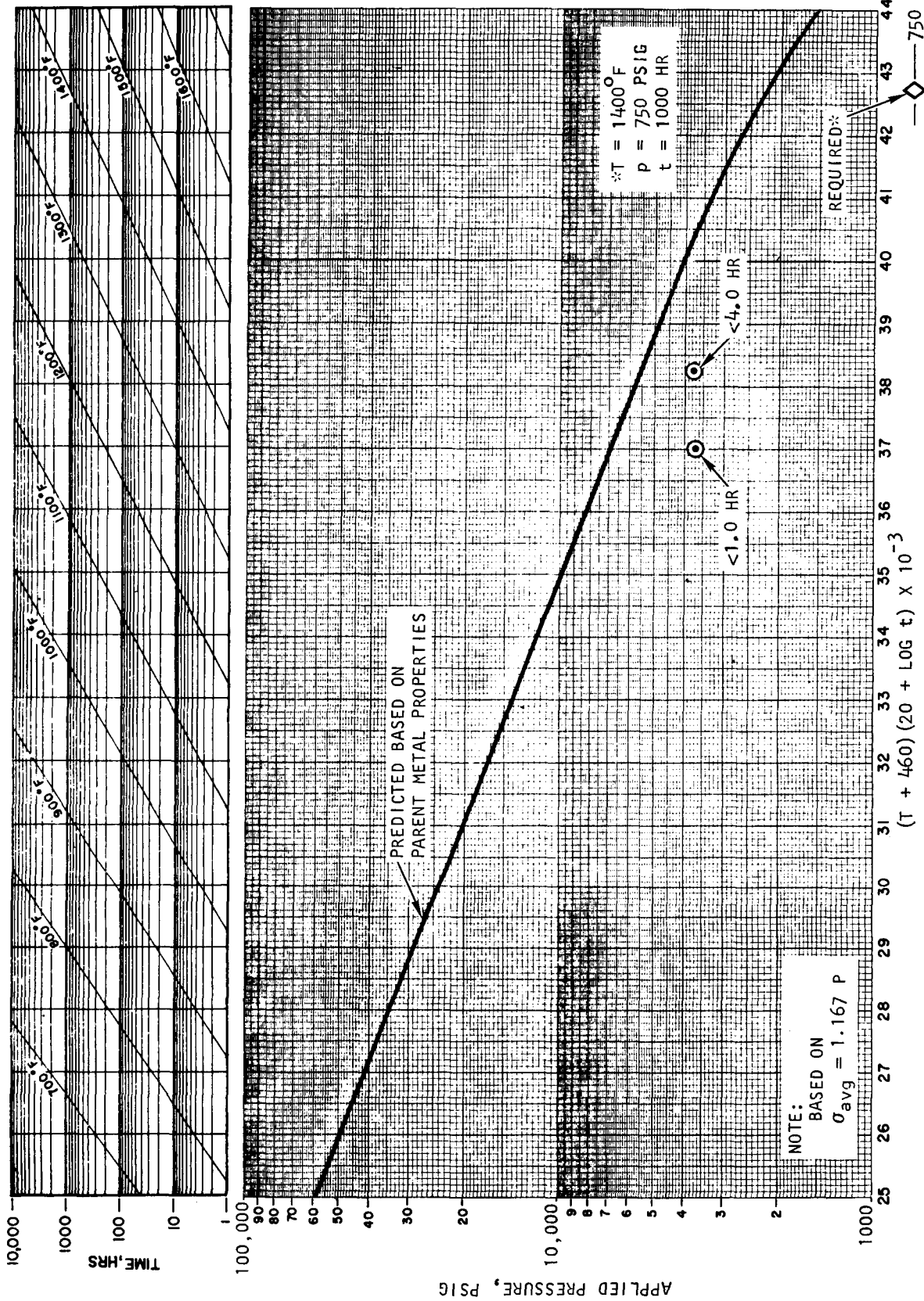
Figure 36.-Creep rupture of Nickel 201 spaced-channel panels.

67
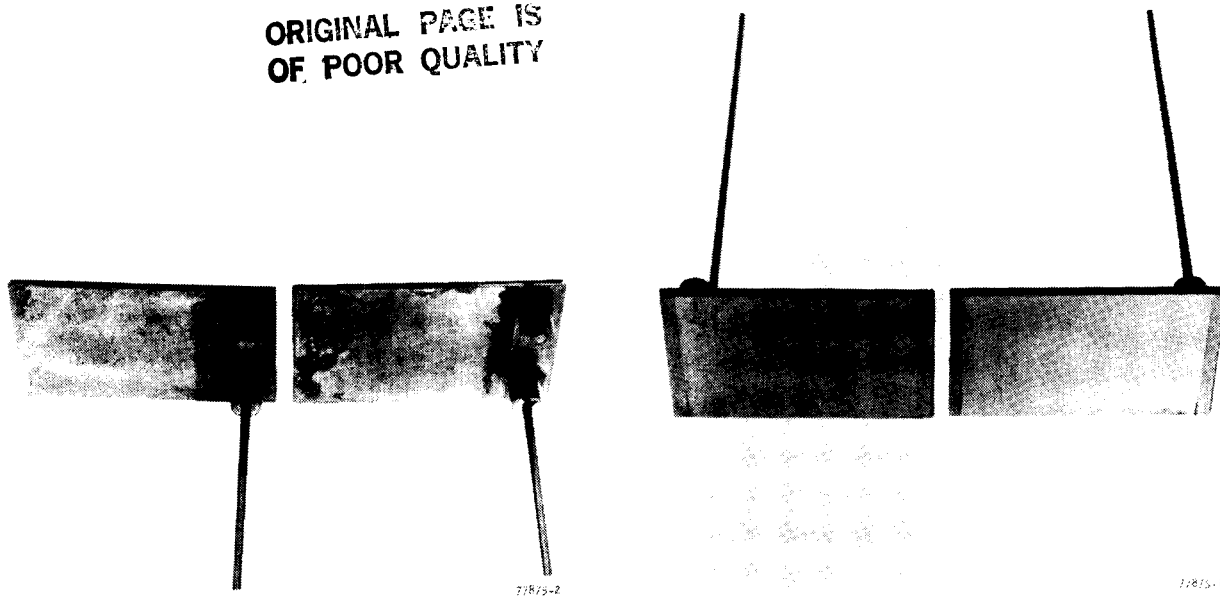
Figure 37.-SN 1 pin-fin and SN 1 channel
panels before creep-rupture testing.
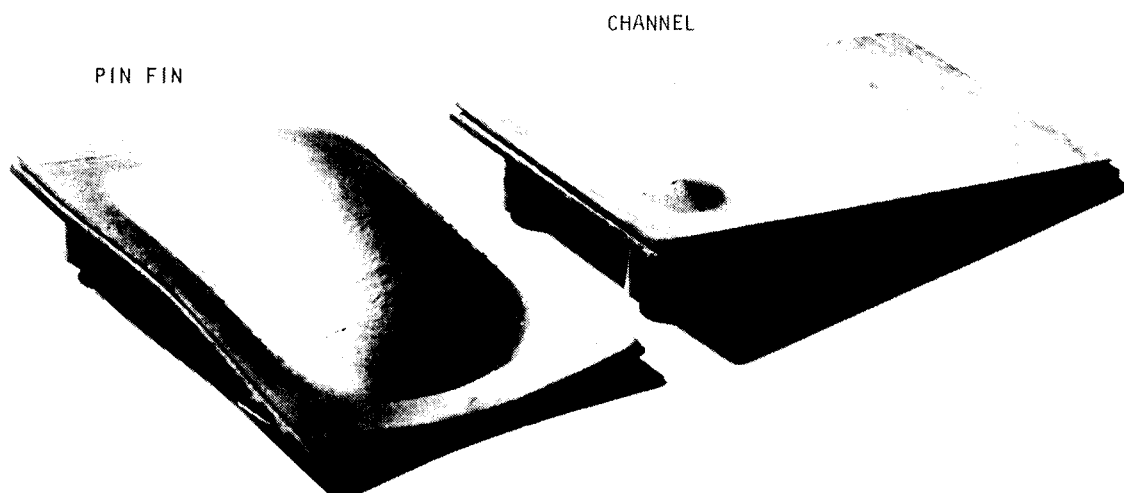
Figure 38.-SN 1 pin-fin and SN 1 channel
panels after creep-rupture testing.

F-48143
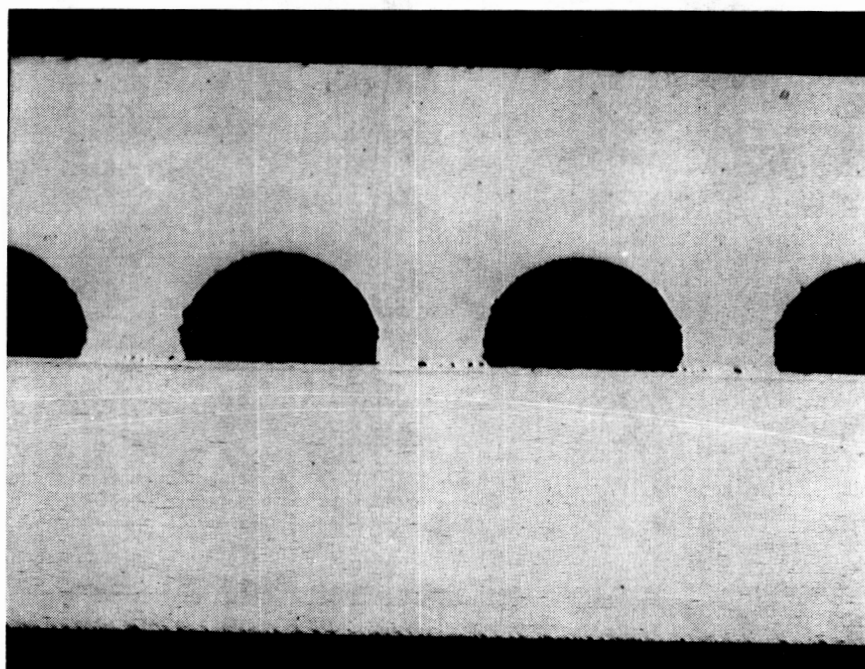
NICKEL 201
PCM FACE
PLATE

HASTELLOY X
BACK PLATE

Micro 8521   25X

F-34937

Figure 39.-Typical channel cross section (SN 1).
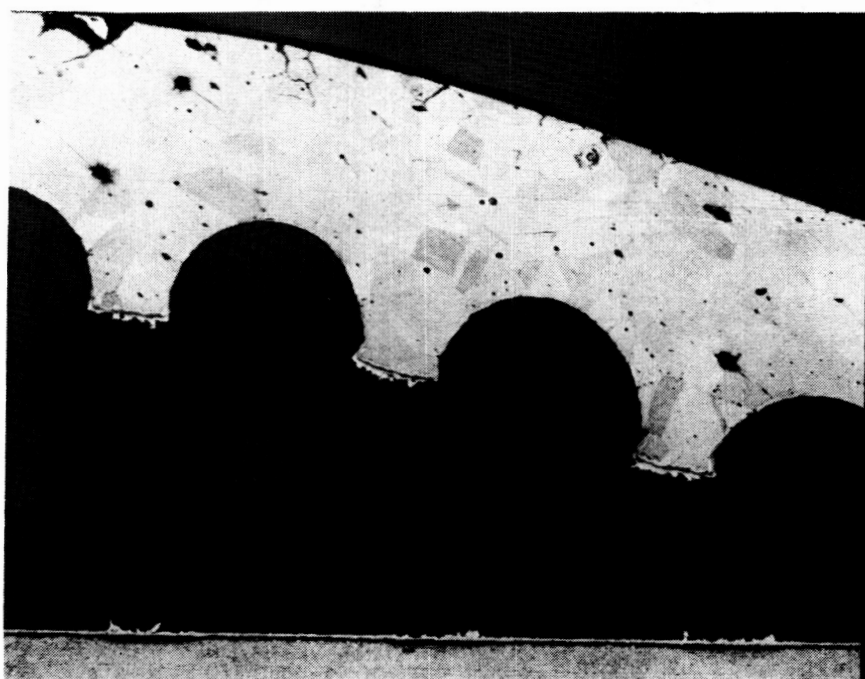
Micro 8521   25X

F-34938

Figure 40.-Braze joint separation (SN 1).
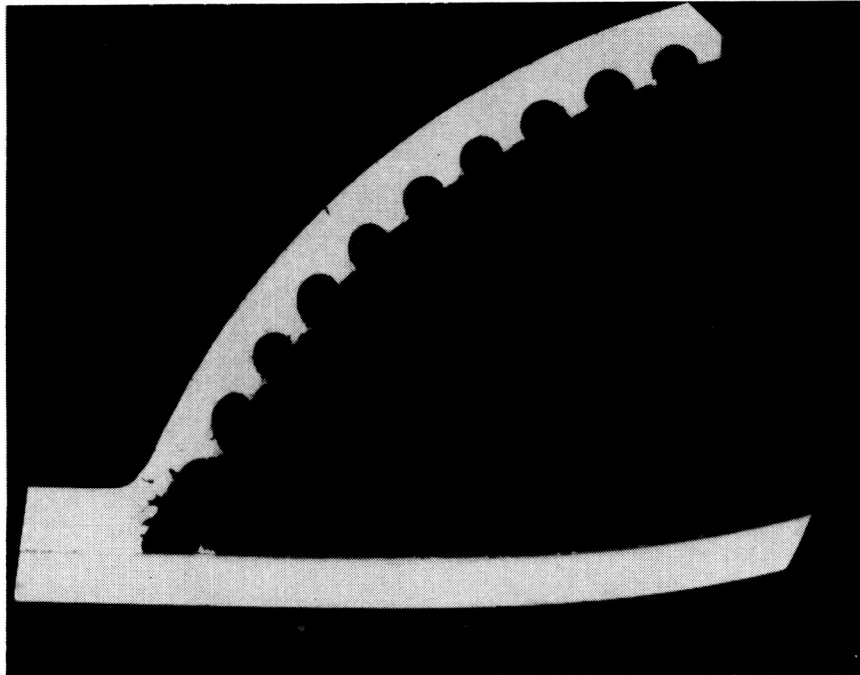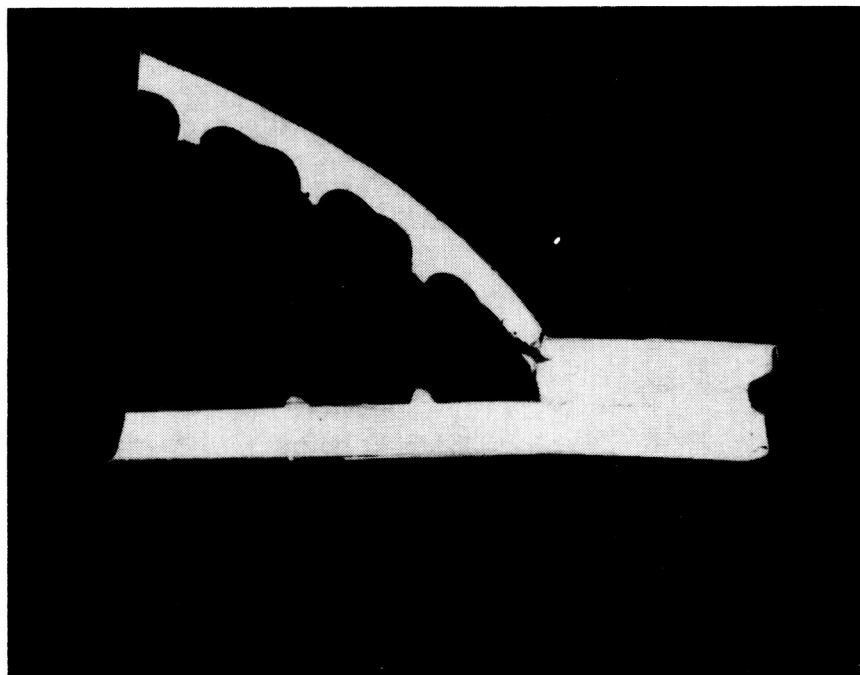
MICRO 8522   5X

MICRO 8523   5X

F-37234

Figure 41.-Sections taken from pin-fin specimen (SN 1).

Examination of the inside surface of the pin-fin face plate indicated that about one-half of the separations occurred through the parent metal and the other half through the pin braze joint.

Two of the channel specimens, SN 29 and SN 33, which were tested at 1250°F, ruptured prematurely. A metallographic section through the SN 29 panel is shown in fig. 42. The separation occurred through the parent metal and appeared to be ductile. The panel was well brazed and the passage geometry was close to nominal. The extent of matrix separation on the SN 33 panel was small; therefore, the panel was repaired and testing continued. The SN 33 panel again failed prematurely.


Mount 10707   22X

F-34957

Figure 42.-Section through separated panel (SN 29).

SN 28 and SN 34 channel specimens also demonstrated a time-to-rupture short of that predicted. However, the actual time-to-rupture is within the range of scatter for this type of test. SN 28 was repaired and testing was continued. The second failure of SN 28 was within the time range of scatter for this type of test.

Sections taken through the separated areas of SN 20 and SN 21 pin-fin panels following rupture indicated that on SN 20, which was run at 1250°F, the separation occurred through the parent metal; whereas SN 21, which was run at 1400°F, separated across the braze joint. Both specimens appeared to be well brazed.

Behavior of the pin-fin specimens is similar to that of the channel specimens. The metallurgical evaluation of the channel and pin-fin Nickel 201 creep-rupture test panels tend to confirm that at 1400°F the panel braze joint is the weak link. When the panels were tested at 1250°F, however, which is close to the actual joint operating temperature, the separation occurs within the parent metal.

The spaced channel specimens, SN 16 and SN 18, ruptured at the feeder channel after 15 to 30 sec at pressure and temperature. The panels were subsequently repaired (added doubler over feeder channel) and retested. In the second test series, both panels leaked in less than 4 hrs, short of the 100-hr predicted life.

The bulged area on the SN 18 panel was removed by electro-discharge machining and the panel was repaired. The removed segment was subjected to metallographic inspection and the results are presented in fig. 43. The separation occurred along the braze joint through a series of voids. The rupture in the channel is believed to be a secondary rupture.

The land area in these specimens was intentionally increased to force the critical area from the braze joint. This was to permit testing at the 1400°F operating condition that prevails in the arch without exceeding a critical creep-rupture stress in the braze joint at 1400°F. The test results, however, show that the separation still occurred in the braze joint after only a short period of time.

Visible deformation was observed in the spaced channel specimens after less than 1/2 hr exposure to 3960 psig at 1400°F. At these conditions, rupture was predicted to occur in the channel arch after 100 hrs of exposure. The finite element model used in data analysis of the arch construction is shown in fig. 44. The distorted geometry after application of a 2000-psig unit load is shown in figure 45.

For Nickel 201, the stress to cause 10 percent creep (readily visible) in 1/2 hr at 1400°F is approximately 5500 psi. As indicated in fig. 44, the combined stress (Von Mises) in the arch at 3960 psig internal pressure will be at this level and some creep distortion would be evident at times as short as 1/2 hr.

As the arch creeps it tends to form a cylindrical shape and the stresses relax. For a heavy cylinder the following formula are valid:

$$\sigma_{inner\ fiber} = 1.667P$$

$$\sigma_{outer\ fiber} = 0.667P$$

$$\sigma_{avg} = 1.167P$$
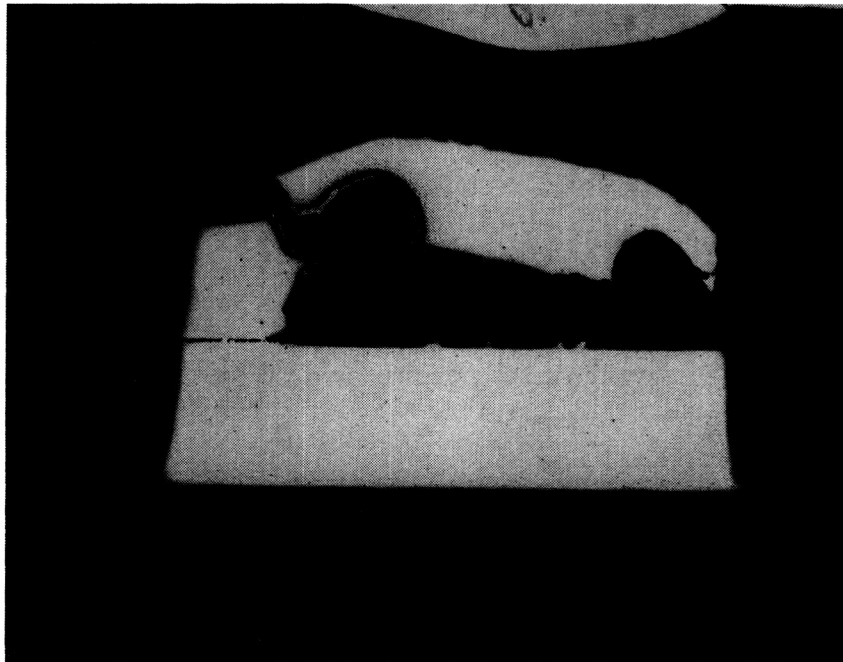
where: inner fiber radius = 0.020 in.
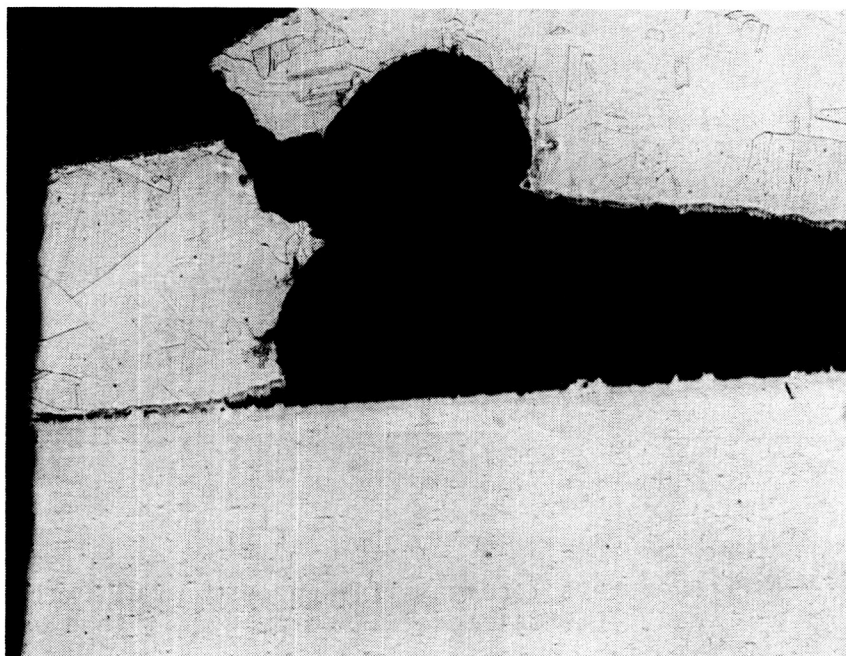
outer fiber radius = 0.040 in.

P = internal pressure

14X

Micro 10900   50X

F-34939

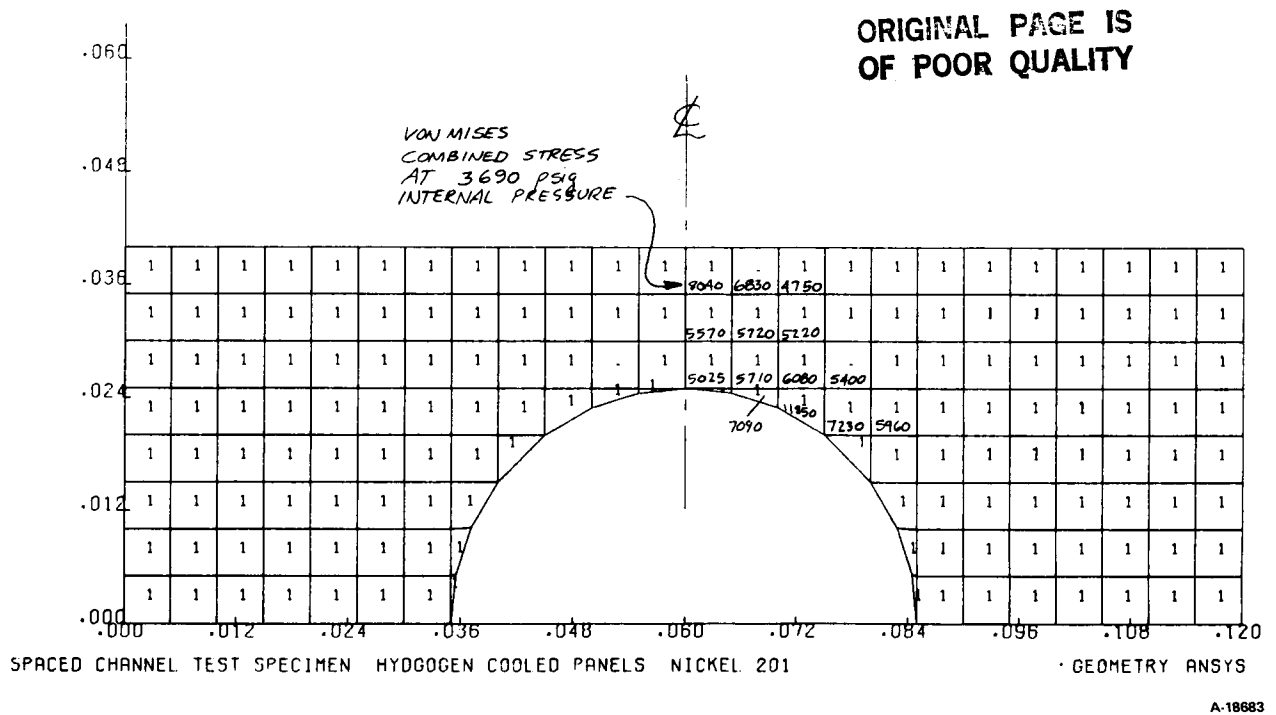Figure 43.-Section taken through separated area
on SN 18 spaced-channel specimen.
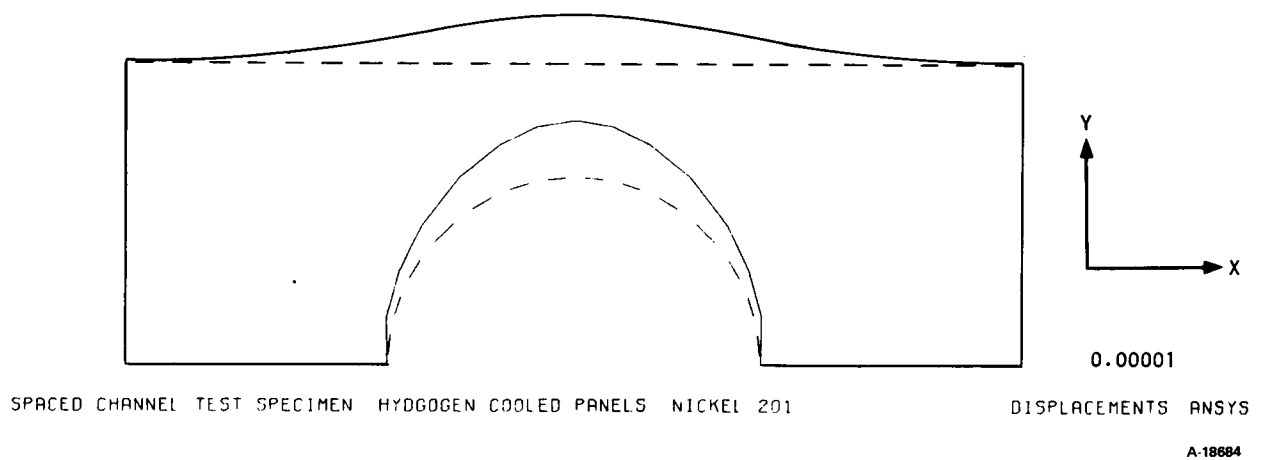
Figure 44.-Spaced-channel finite element model.

Figure 45.-Displacements in spaced-channel finite
element model (2000-psig unit load.)

74

Using the relationship for average fiber stress and the Nickel 201 creep properties the following revised rupture lives are predicted.

P, psig	Time to Rupture, hrs
3000	100
2228	400
1757	1000

The pressure to cause rupture is about 20 percent less than predicted by linear analysis.

Stress distribution in the Y direction is shown in fig. 46. A high stress will develop at the corner and act as a tearing load on the braze joint. For an internal pressure of 3690 psig, the peak corner stress is 9570 psi (stress concentration factor, SCF = 1.0), which is about twice as high as predicted using a linear analysis.
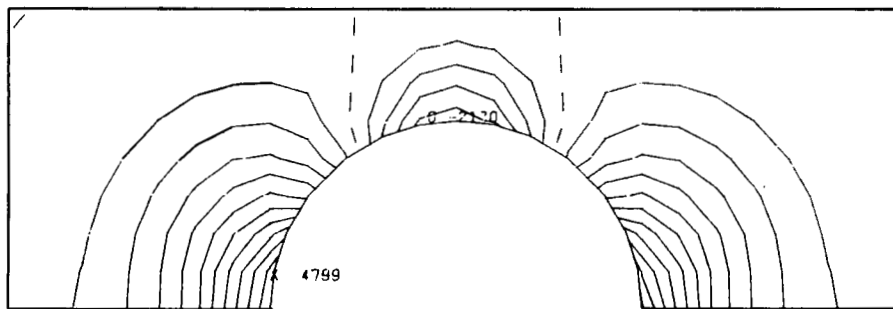
SPACED CHANNEL TEST SPECIMEN   HYDGOGEN COOLED PANELS   NICKEL 201   Y STRESS   ANSYS

Figure 46.-Stresses in Y direction (2000 psig internal pressure).

The model was rerun with only every other node fixed in the braze region. This simulates the condition of approximately 50 percent braze voids. In this case the peak corner stress increases to 14,980 psi, with the SCF = 1.0, and 29,940 psi with the SCF = 2.0. Thus, it is possible to exceed the joint short term ultimate tensile strength if the braze coverage is poor. In this case the panel would separate along the braze joint rather than in the channel arch. Even with complete brazing however, the corner area within the channel is more highly stressed than the arch. The most critical area within the channel specimen is the 1250°F braze joint rather than at the 1400°F arch.

Inconel 617 Panel Test Results

Three Inconel 617 pin-fin creep-rupture test panels were fabricated using boronized nickel chrome braze alloy. Creep-rupture tests were conducted in accordance with the test matrix presented below. A face plate thickness of 0.004 in. was used for the estimate of SN 40 specimen life.

SN	Face Plate Configuration	Applied Pressure, psig	Test Temperature, °F	Predicted Creep-Rupture Life, Hrs
40	Pin-fin	2890	1250	85
41	Pin-fin	2890	1250	1175
42	Pin-fin	3500	1250	111

For this series of tests, the ratio of joint strength to parent metal strength was assumed to be 50 percent as compared to 35 percent obtained from prior testing.

The test conditions were maintained for 1707 hrs for the SN 41 panel and for 1375 hrs for the SN 40 and SN 42 specimens with no evidence of imminent rupture. The test pressure was raised sequentially to 5500 psig as follows: 3500 psig for one hour, 4000 psig for one hour, 4500 psig for one hour, 5000 psig for one hour, and finally 5500 psig.

The estimated life at the 5500 psig pressure and 1250°F test temperature, using parent metal properties is 111, 1539 and 524 hrs for specimens SN 40, SN 41, and SN 42, respectively, assuming no damage from previous testing at lower pressures. With 675 additional hrs accumulated at the new conditions, there was no evidence of impending rupture. It was concluded that the boronized nickel chrome braze joint is equal in creep-rupture strength to the Inconel 617 base material at the 1250°F test temperature. Furthermore, it was surmised that the thickness of the face sheet on SN 40 panel must be greater than the estimated value of 0.004 in.

The SN 40 specimen was subjected to a burst pressure test at room temperature. At approximately 20,000 psig (rupture occurred as pressure was being increased) failure occurred by fracturing one pin. The sudden release of support caused the pin to tear a round hole in the surface of the panel as shown in fig. 47. The panel was sectioned for metallurgical examination. Results are presented in figs. 48 and 49. Separation has occured in the parent metal. Fig. 50 presents a section taken through a round pin and shows the thin face sheet. The face sheet thickness was measured and found to be 0.0065 to 0.008 inch. The diamond shaped marks on fig. 50 were made during a hardness traverse. The Rockwell C readings obtained from this traverse are shown on the figure and are summarized in Table 21. Results indicate that the Inconel 617 base material is hardened. Some hardening of the base metal is expected due to formation of borides when boronized nickel-chrome filler alloy is used.
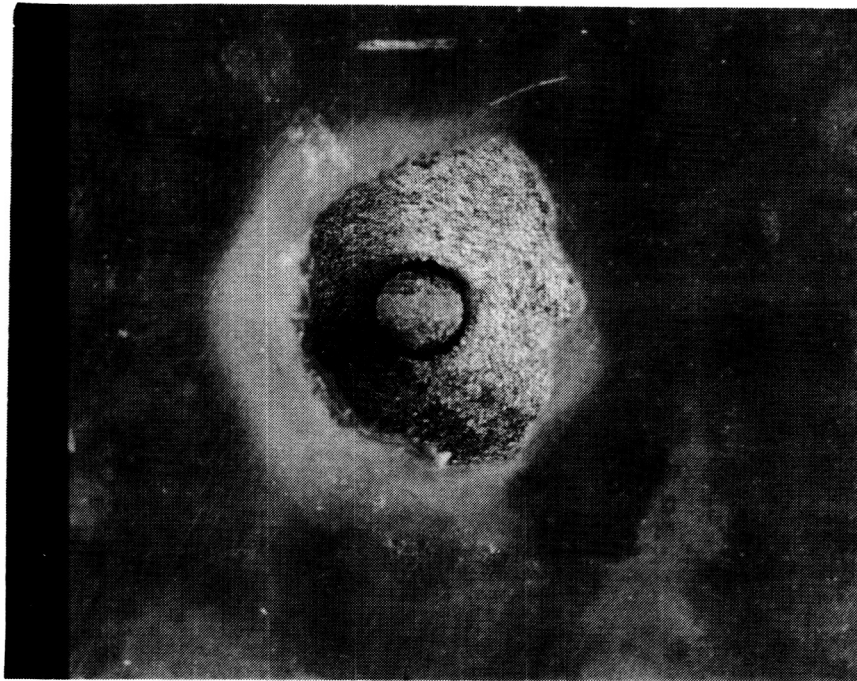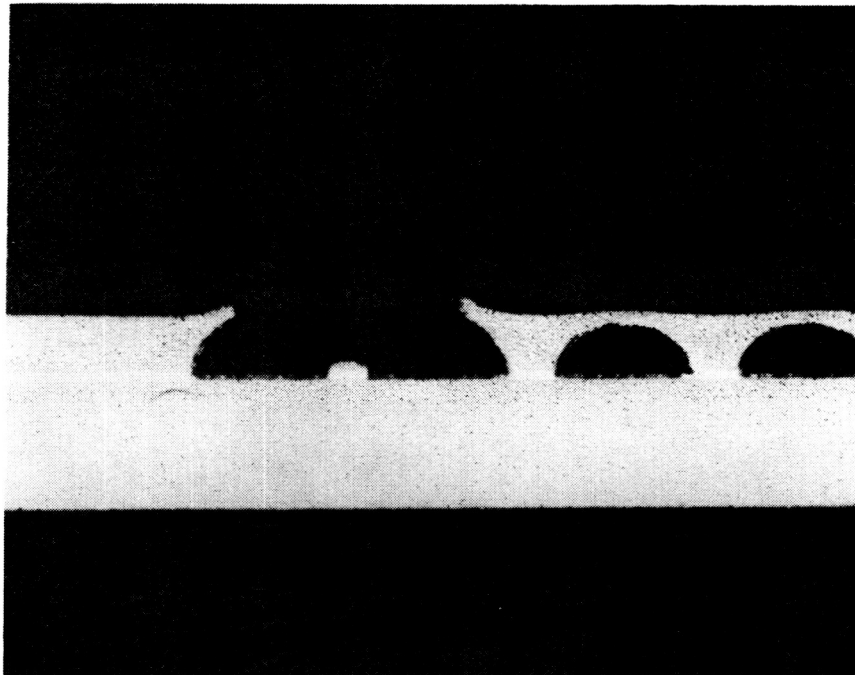
Figure 47.-Pin fracture hole in SN 40 pin-fin panel
following burst pressure test.

F-34920

Figure 48.-Section taken through pin fracture area of SN 40
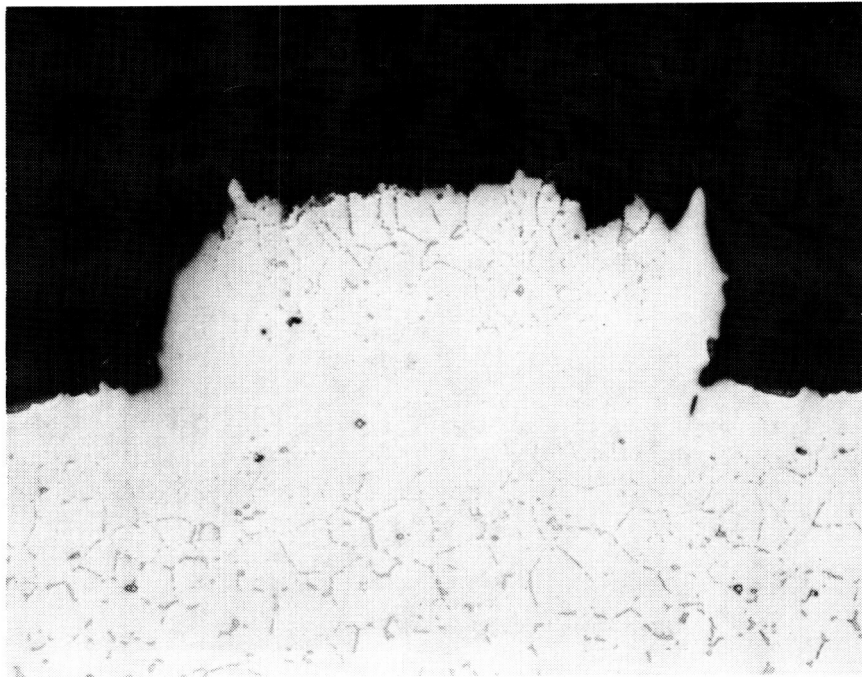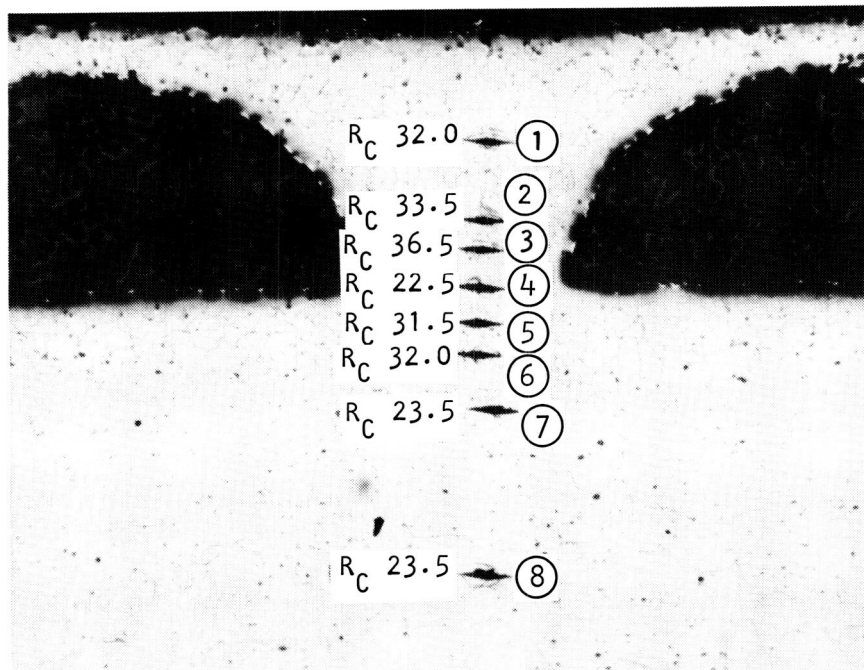pin-fin panel (low magnification).

Figure 49.-Section taken through pin fracture area of
SN 40 pin-fin panel (high magnification).

F-34924

Figure 50.-Section taken through unfractured pin
of SN 40 pin-fin panel.

Comparison with the hardness readings obtained for the brazing development test specimen (see fig. 28), however, indicates that the extent of hardening for the SN 40 test panel is substantially greater.

Based on these hardness readings, the corresponding approximate ultimate strengths were estimated using data for steels (ref. 14) and are also presented in Table 21. Supplier data for Inconel 617 (refer to Table 7) lists a typical room temperature ultimate strength of 106,600 psi for hot rolled rod and 110,000 psi for cold-rolled sheet. On the SN 40 test panel, the estimated average room temperature ultimate strength of the SN 40 test panel of Inconel 617 material around the fracture region is in excess of these values.

TABLE 21.-ULTIMATE STRENGTH ESTIMATES

Location*	Hardness Reading HRC	Approximate Ultimate Strength, psi
1	32.0	145,000
2	33.5	151,000
3	36.5	165,000
4	22.5	115,500
5	31.5	143,500
6	32.0	145,000
7	23.5	118,500
8	23.5	118,500

*Starting with the location closest to the top of the face sheet.

Published data (ref. 15), supplier data, and tensile tests conducted on Inconel 617 in this program (Table 7) indicate room temperature strength increases as a result of aging. For comparison with SN 40 room temperature results, room temperature data reflecting effect of aging on ultimate and yield strengths of Inconel 617 (ref. 15) is depicted in fig. 51. The estimated average room temperature ultimate strength for Inconel 617 material from SN 40 creep-rupture test panel hardness readings, the supplier data, and tensile test data from this program for aged Inconel 617 are also shown in fig. 51.

The strengthening effect is most pronounced at the panel creep-rupture test temperature of 1250°F. The limited test data from this program (room temperature burst pressure test of SN 40 panel exposed to 1250°F for 2386 hrs, and tensile test results) tend to substantiate the Inconel 617 strength increase pattern illustrated in fig 51.
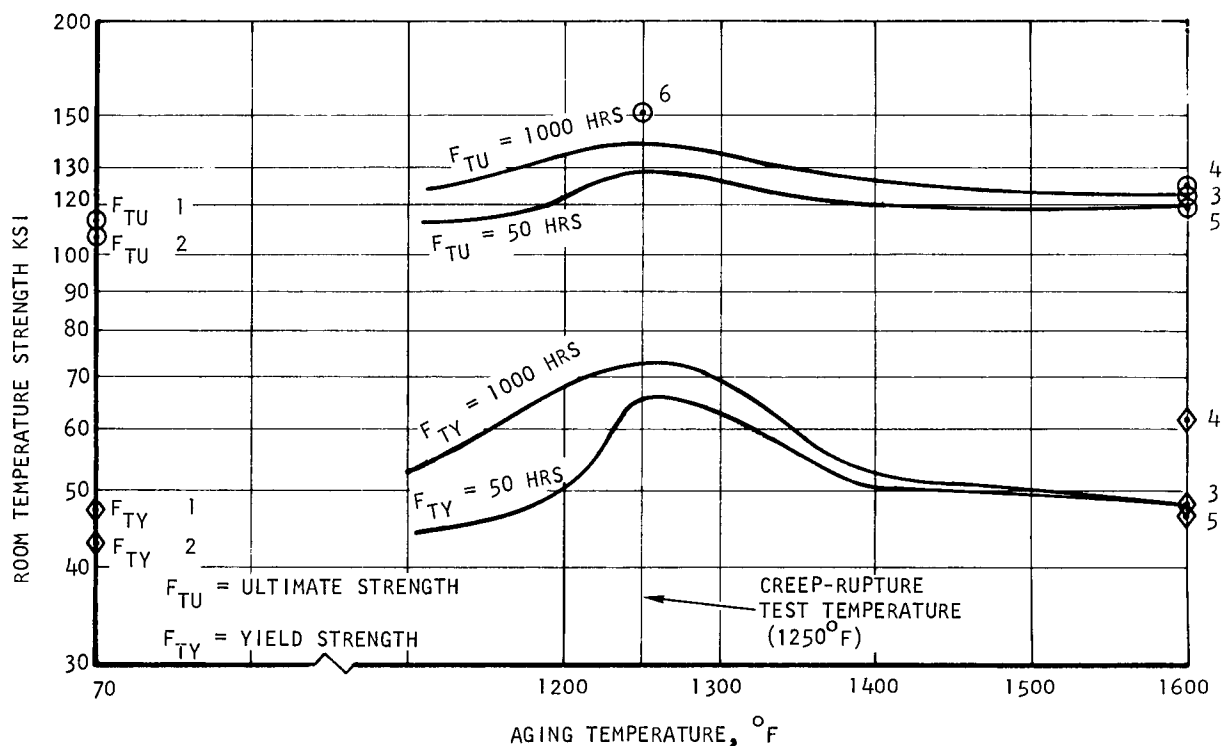
1. Supplier data for solution treated, cold rolled sheet. Huntington Alloys, "Inconel Alloy 617" 20M9-72T-46, 1972.

2. Supplier data for solution treated, hot rolled rod. Data Sheet, International Nickel Company.

3. Supplier data for hot rolled rod, aged 1000 hours at $1600°$ F. Data Sheet, International Nickel Company.

4. Tensile test data from this program. A 0.015-in. thick test section, brazed with Palnino 1 and exposed 1000 hrs at $1600°$ F in air (Table 7, data item 2).

5. Tensile test data from this program. A 0.44-in. diameter test section, pseudo brazed and aged 1000 hrs at $1600°$ F in air (Table 7, data item 2).

6. Estimated average room temperature ultimate strength of SN 40 creep-rupture test panel Inconel 617 base material aged for 2386 hrs at $1250°$ F. (Based on hardness readings for locations 1, 2 and 3 of Figure 50).

Figure 51.-Effects of aging on room temperature tensile properties of Inconel 617 hot-rolled rod.

No conclusive data for the effect of aging on the elevated temperature strength of Inconel 617 was obtained. An increase in elevated temperature strength with aging is, however, an expected characteristic on the basis of data for similar Inconel alloys such as Inconel 625 (ref. 16). This hardening effect would occur in engine panels during operation. Elevated temperature tensile testing of aged specimens is required to determine the effects of aging on elevated temperature strength of Inconel 617.

Conclusion and Recommendations

Results of creep-rupture tests indicate that, for Nickel 201 panels, the strength of the Palniro 1 braze joint approaches that of the parent metal at operating conditions. The photochemically milled channel configuration appears to have an adequate margin at the design condition of 1250°F for 1000 hrs at 750 psig. The pin-fin design is marginal for the design condition of 1200°F for 1000 hrs at 750 psig. An increase in the pin diameter would be desirable to provide a greater creep-rupture strength margin. However, the effect on the thermal performance of the panel would have to be investigated.

The Inconel 617 panels brazed with Palniro 1 braze alloy exhibited an adequate creep-rupture design margin, in spite of the presence of multiregional braze joint structures (see Fabrication Process Development, Inconel 617 Panels). Creep-rupture testing of the pin-fin Inconel 617 panels brazed with the boronized nickel chrome filler alloy indicate a joint creep-rupture strength equal to that of the parent metal at operating conditions.

PANEL REVERSE BENDING FATIGUE TESTING

During the initial phase of the program, panel design, materials, and fabrication processes were selected. Panels composed of Nickel 201 face plates and Hastelloy X back plates and panels fabricated entirely of Inconel 617 were identified as the most promising candidates for meeting the overall program goals.

Performance Predictions

Early predictions, based on published data, indicated that Nickel 201 would meet the 10,000-cycle design goal but would have marginal creep life. Inconel 617 would not meet the cycle life goal but represented an improvement over the Hastelloy X panels and would have adequate creep life. Results of tensile tests indicated that the ductility of both Nickel 201 and Inconel 617 is appreciably reduced by brazing and aging, suggesting a reduction in the fatigue life. A fatigue test plan was, therefore, established to obtain experimental data to support the preliminary fatigue life predictions and materials selection.

81

Test Setup

The test apparatus shown in fig. 52 was used to apply a known alternating strain by bending the specimen around the opposed curved mandrel surfaces. A hydraulic ram moved the mandrels through the required stroke (fig. 53a) while the ends of the specimen were restrained from moving in the direction of ram travel (fig. 53b). Ram force levels were monitored by an integral load cell. Stroke reversal was controlled by a four-way solenoid valve and limit switches. Adjustable contacts permitted control of stroke length which was required due to variations in specimen deflection with mandrel radius. Stroke speed was controlled by throttling the flow of hydraulic fluid to the apparatus. A timer-controlled hold was imposed at the peak of the ram travel in each direction for the 2 minute hold-time test. Elevated temperature tests were conducted by installing an electric furnace over the specimen holding section and heating to the specified temperature. The control system included switches connected in series with the pump which automatically terminated testing when the specimen cavity pressure decayed below a preset value.

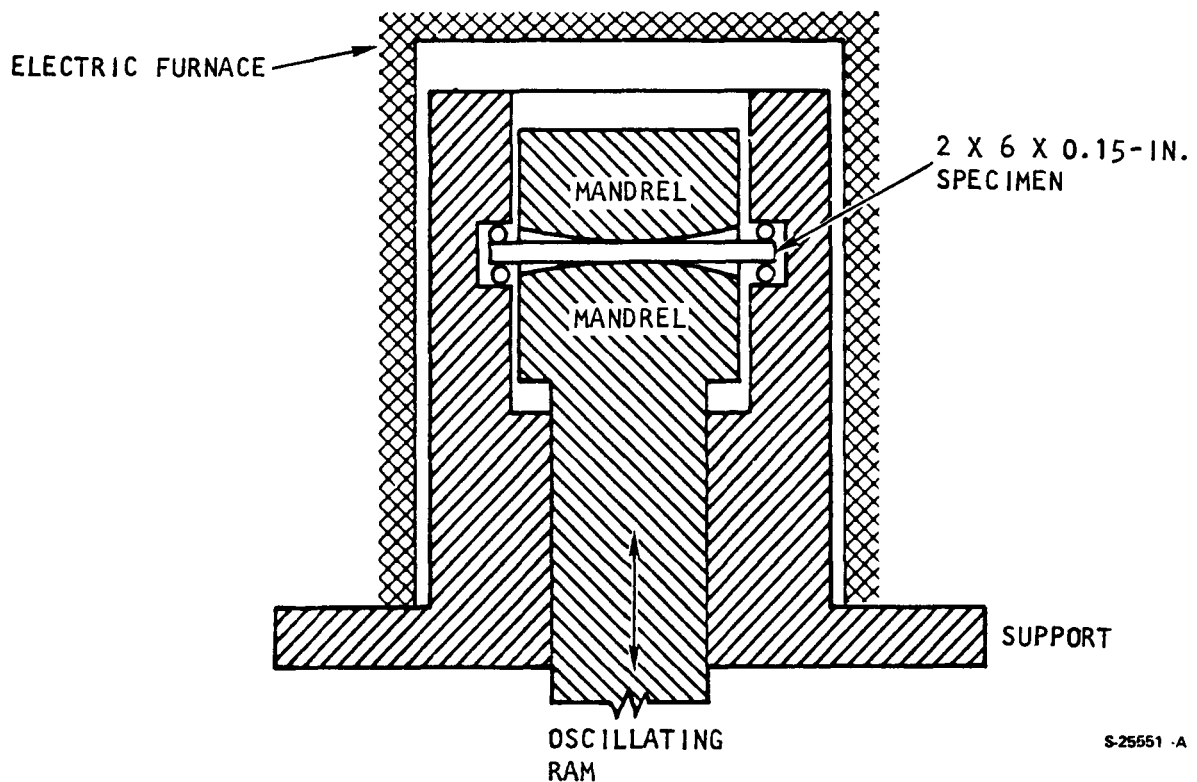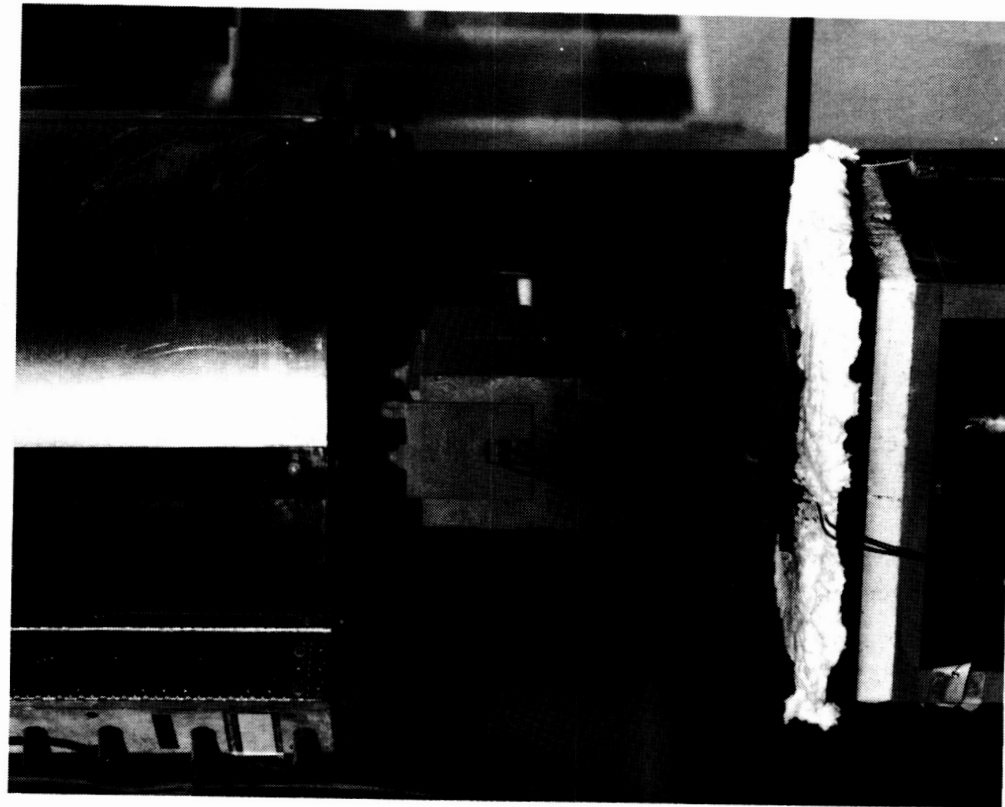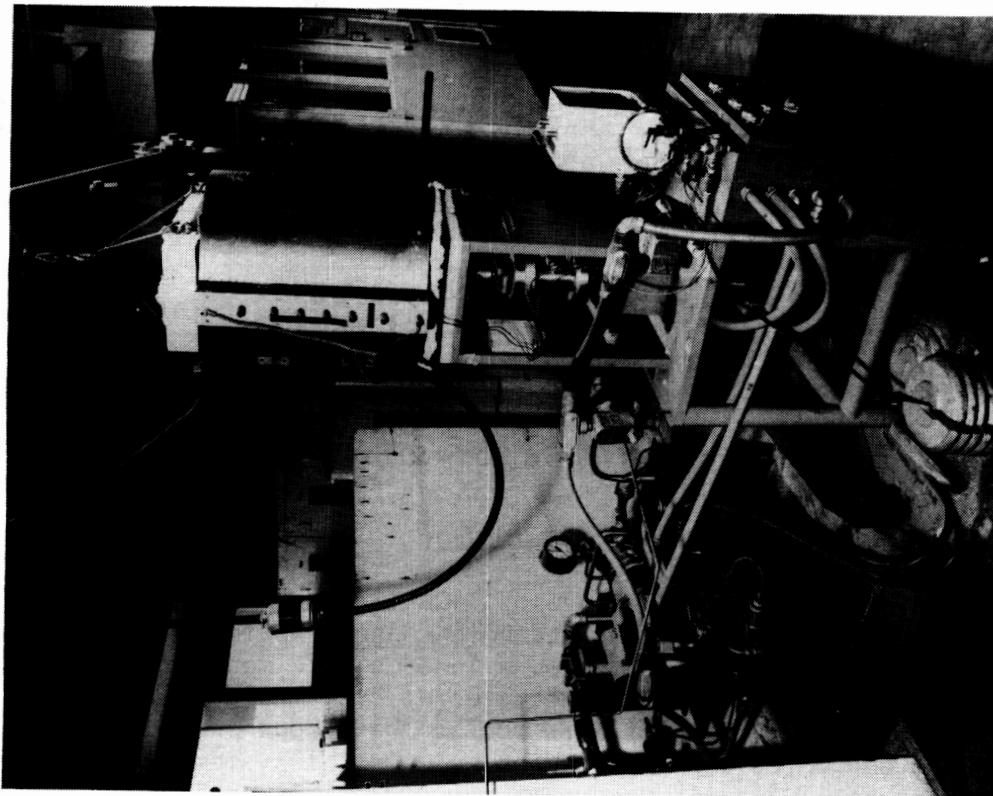Figure 52.-Test apparatus for low cycle fatigue tests.

F-37046

b. Stationary housing containing test specimen and mandrels

a. Hydraulic ram and electric furnace installed over the specimen holding section.

Figure 53.-Reverse bending fatigue test setup.

Specimen Design

The detailed design of the fatigue test specimens is presented in figs. 54 through 57). The photo-chemically machined face plates were brazed on both sides of the 0.060-in-thick support plate. Two tubes provide for separate pressurization of the upper and lower cavities. The channel specimens for the initial tests incorporated two channel patterns, one oriented longitudinally and one laterally. Fig. 58 shows a Nickel 201 channel specimen prior to assembly for braze and following braze. Nickel 201 specimens were brazed using Palniro 1 filler alloy, 0.001 in. thick. The braze surfaces were gold plated to enhance alloy flow and wetting. Inconel 617 test panels were brazed using 0.001-in. thick boronized nickel chrome foil.
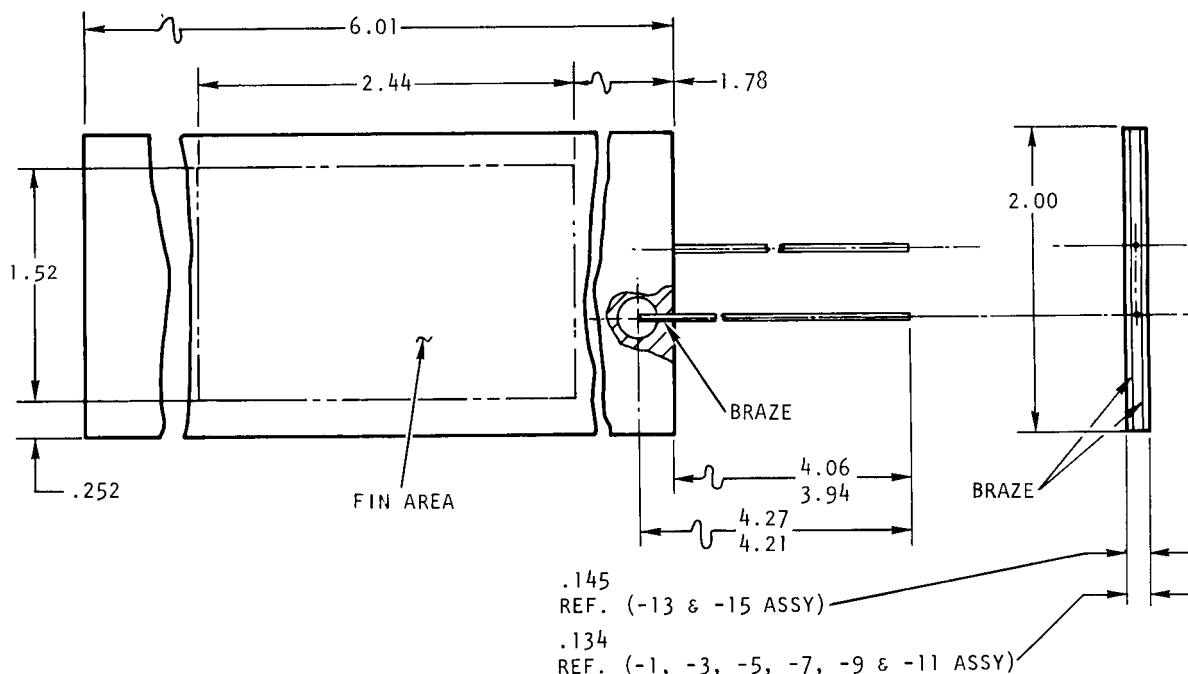
Figure 54.-Test specimen panel assembly.

Following braze, the specimens were subjected to a 1000-hr argon aging cycle at 1450°F in preparation to initiation of fatigue tests.

Test Plan

Testing was conducted in two phases. During the first phase, channel specimens of both material systems and both channel pattern orientations (lateral and longitudinal) were tested with each specimen incorporating the two channel patterns. The better material system and the more critical channel orientation were identified. During the second phase, the balance of testing was conducted using the selected material system for all specimens (pin-fin and channel) and the more critical channel orientation for all channel specimens.

84
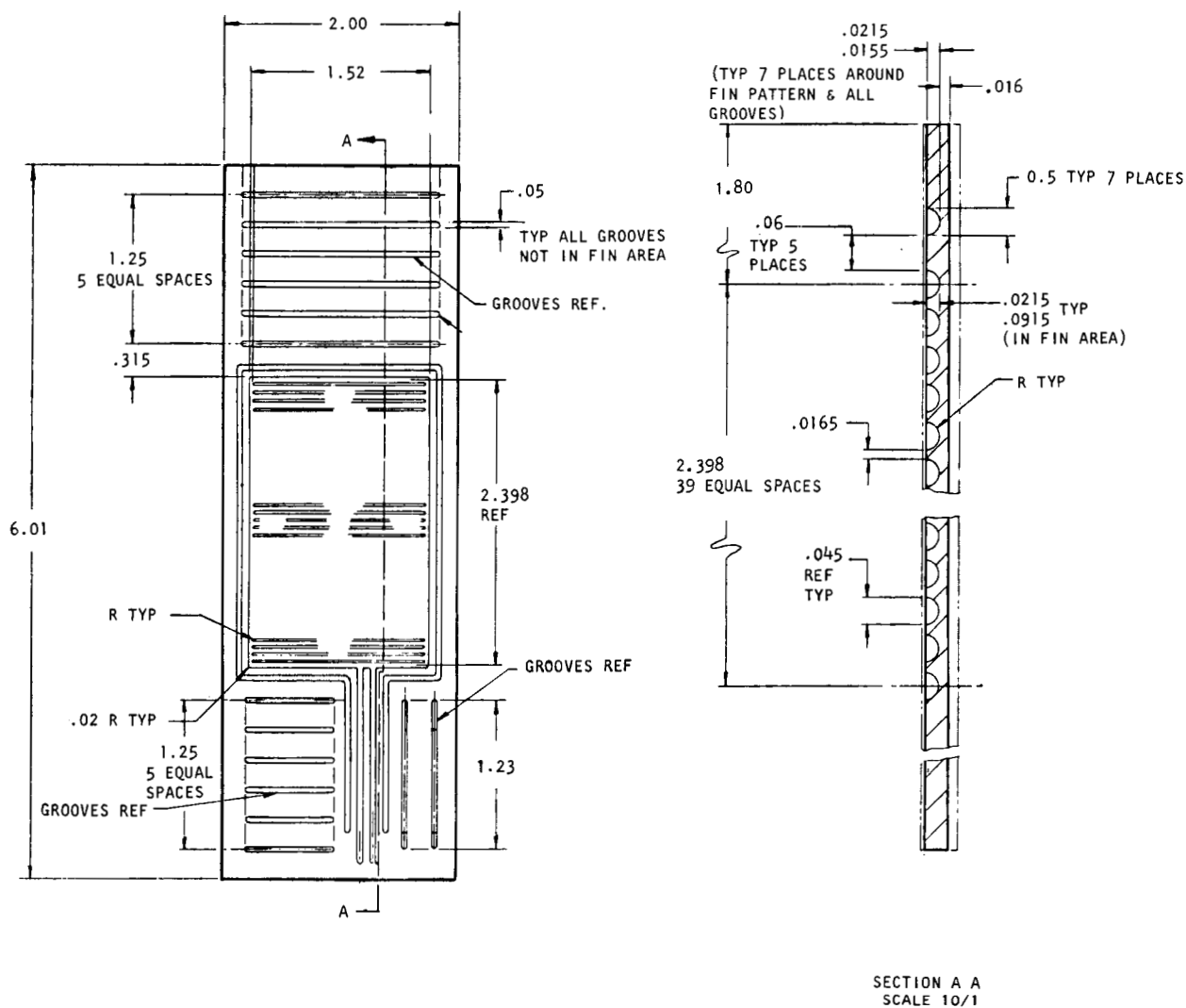
Figure 55.-Lateral fin face plate.

After fabrication, all the specimens were subjected to a room temperature proof test at 1000 psig to verify pressure containment capability and were then aged in argon for 1000 hrs at 1450°F. Proof pressure tests were repeated following the aging cycle.
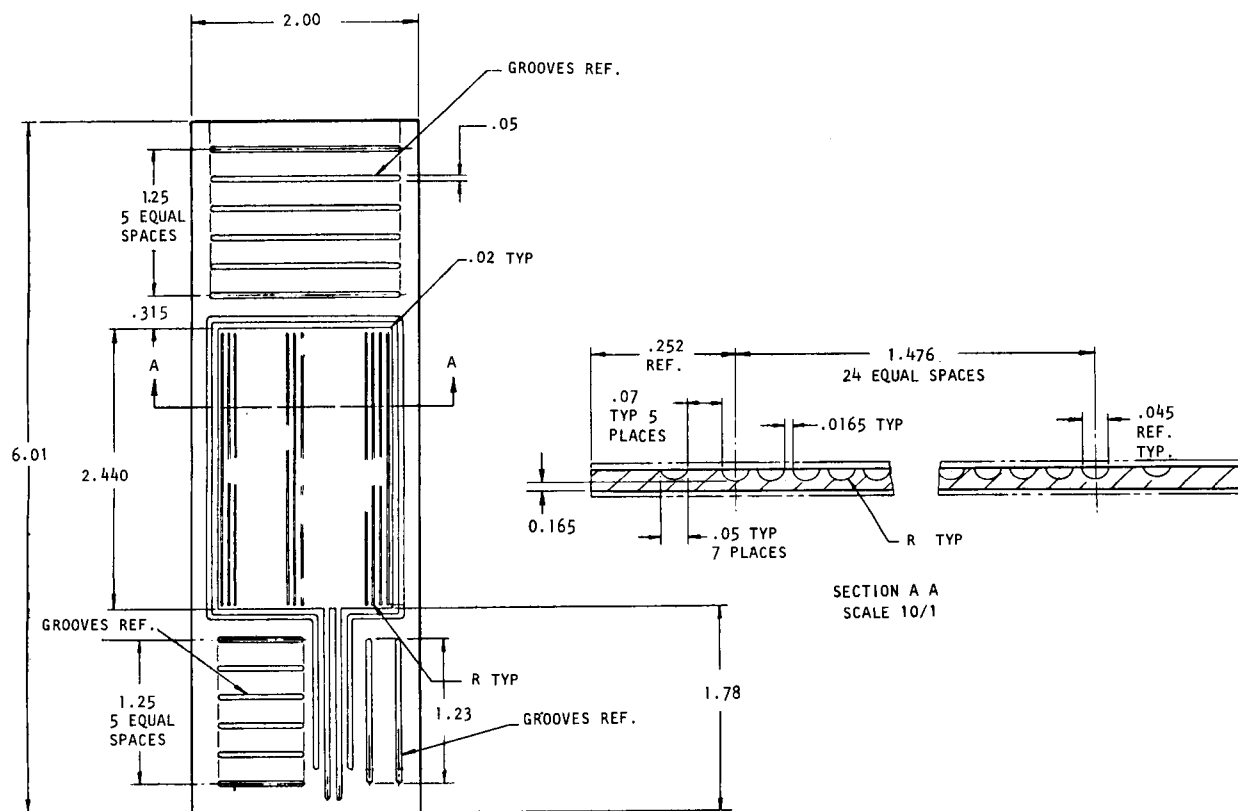
Figure 56.-Longitudinal fin face plate.

The selected test temperatures were 1400°F for the Nickel 201 panels and 1600°F for Inconel 617 channel specimens. These temperatures represent the anticipated maximum face sheet temperatures at the design heat flux.

The reverse bending fatigue tests were conducted with and without hold times to impose plastic-creep (P-C) and plastic-plastic (P-P) type cycles, respectively. A P-C type of cycle is obtained by loading the specimen and then allowing the stress to relax while maintaining a constant strain. The P-P and P-C type loadings are diagrammed in fig. 59 and 60, respectively. A hold time of 3 minutes was initially specified to allow specimens to incur creep damage. Subsequent hold time tests with both Nickel 201 and Inconel 617, however, indicated that after two minutes the load had stabilized and was
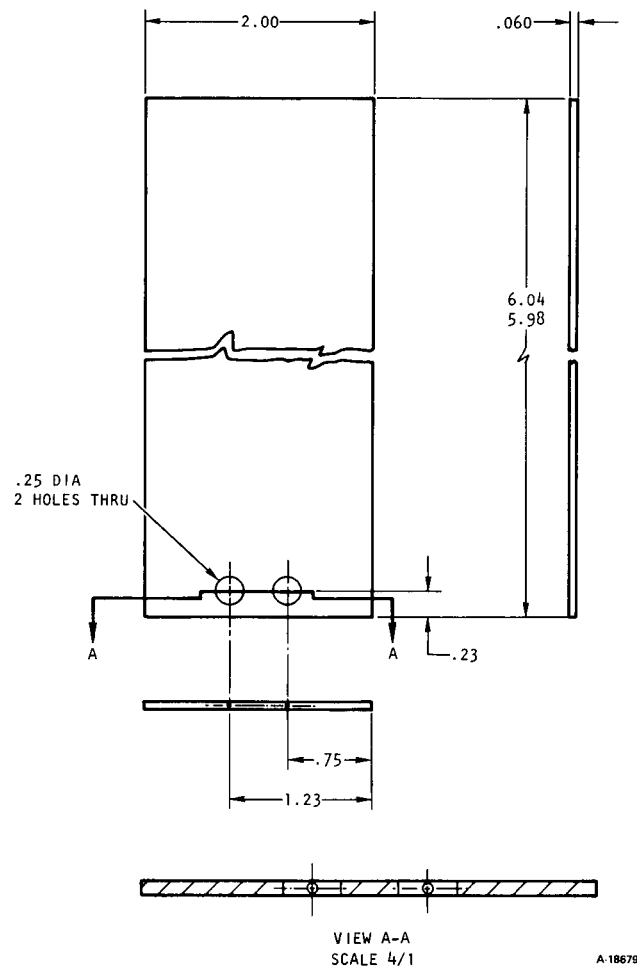
Figure 57.-Support plate.

essentially constant during the final minute of the dwell period. Rapid load relaxation was recorded in the first minute followed by a gradual decrease during the second minute leading to a constant load level for the remainder of the hold-time. A typical 3 minute hold curve is presented in fig. 61. Consequently, a two minute hold time was specified for all subsequent P-C type tests.

The mandrel radii selection for the reverse bending fatigue tests was made from existing test fixture mandrels with the goal of providing a good spread of data. Mandrel radii of 9, 16, and 32-in. were selected. The test matrix is presented in Table 22.

C-2
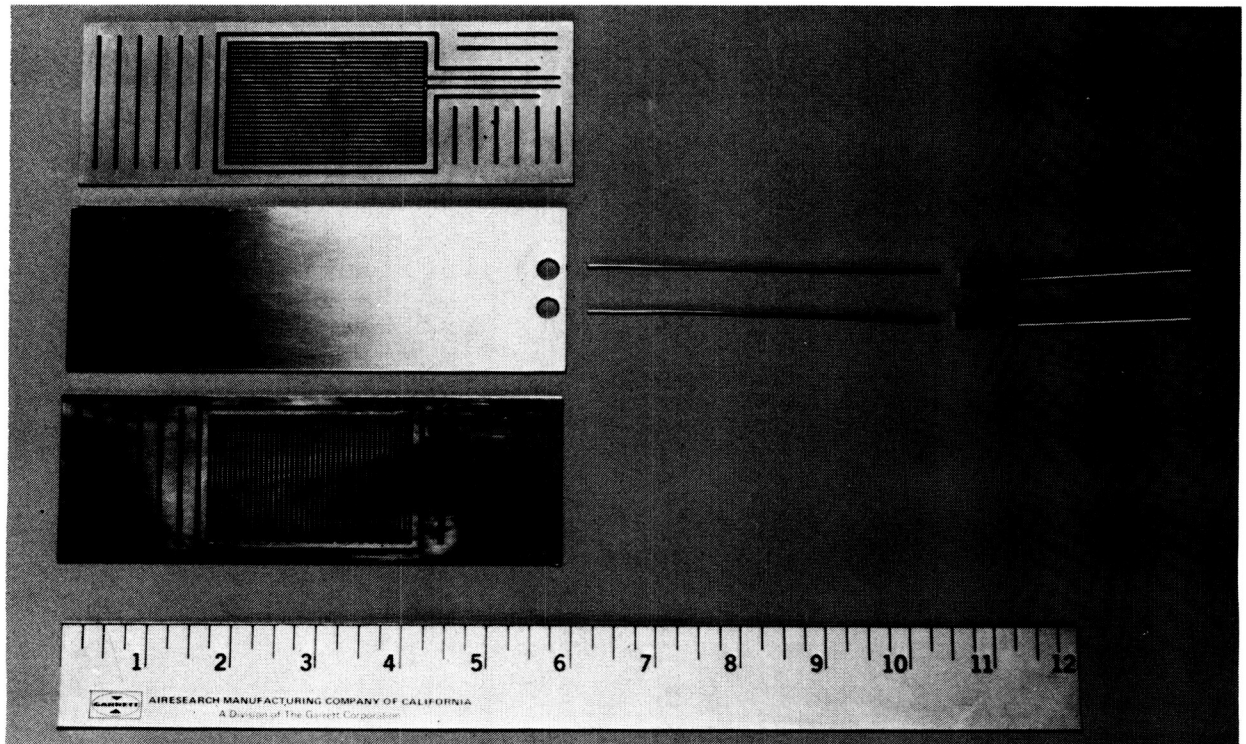
A. NICKEL 201/HASTELLOY X DETAIL PARTS PRIOR TO ASSEMBLY
FOR BRAZE
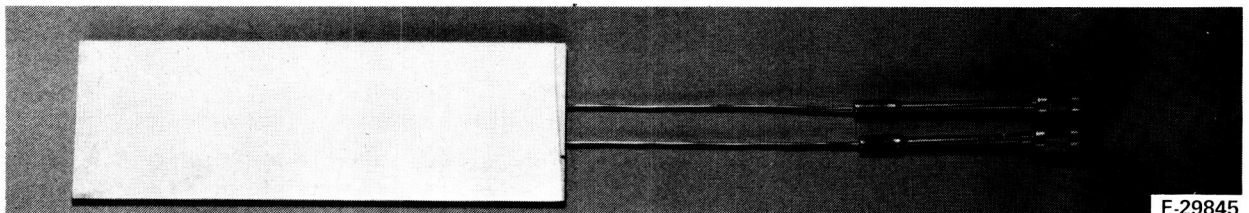
F-29845

B. NICKEL 201/HASTELLOY X ASSEMBLY FOLLOWING BRAZE

F-29846

Figure 58.-Nickel 201 reverse bending fatigue test specimen.

STRAIN

TENSION

0

TIME

COMPRESSION

← APPROXIMATELY 2 SEC →
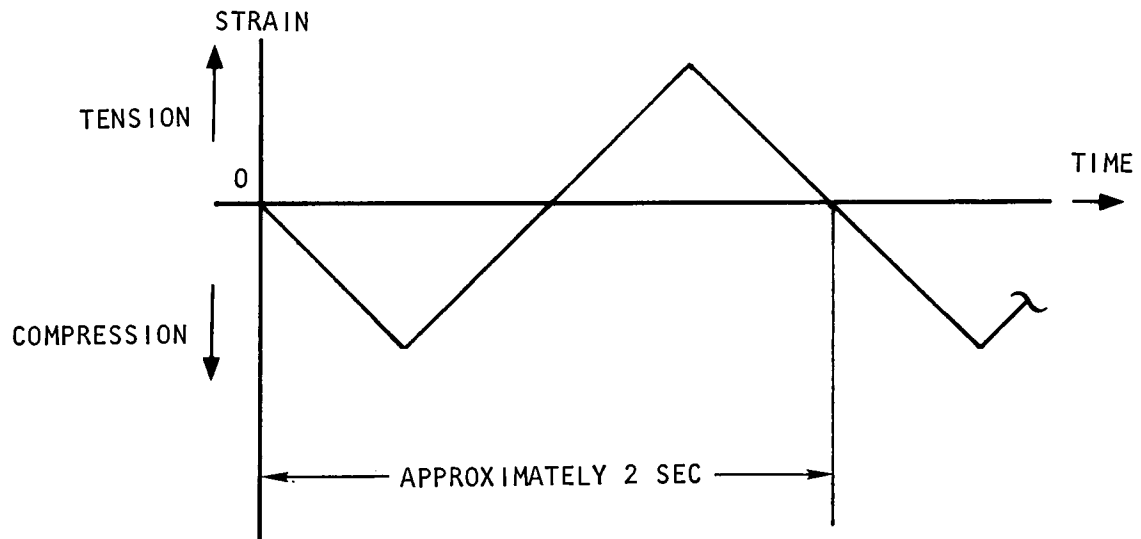
S-25531 -A

Figure 59.-P-P cycle.

STRAIN

TENSION

← 3 MIN →

0

TIME

COMPRESSION

← 3 MIN →

← APPROXIMATELY 6 MIN. 2 SEC. →
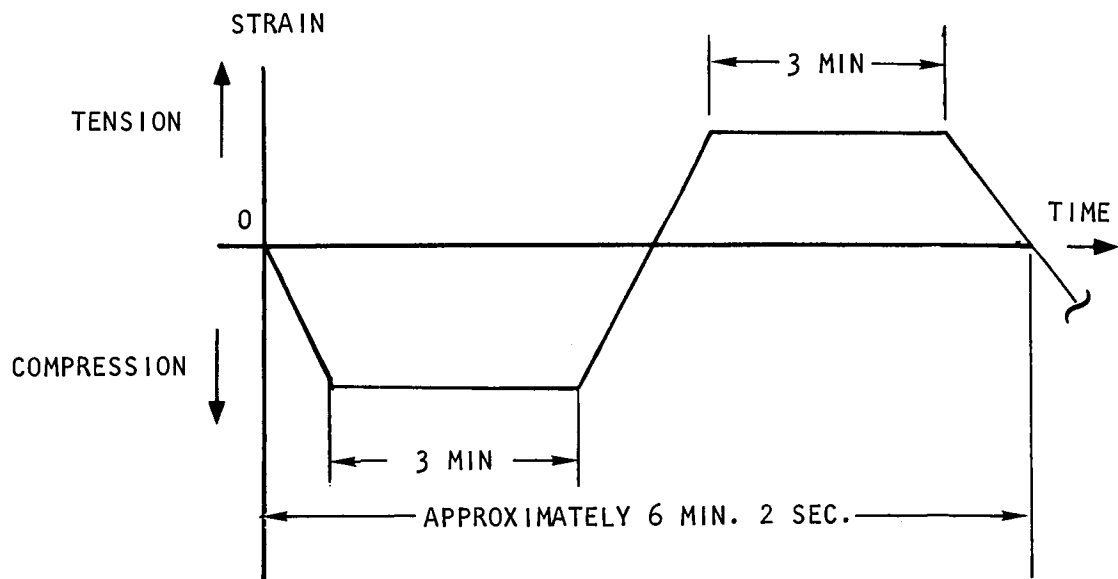
S-25532 -A

Figure 60.-P-C cycle.

89
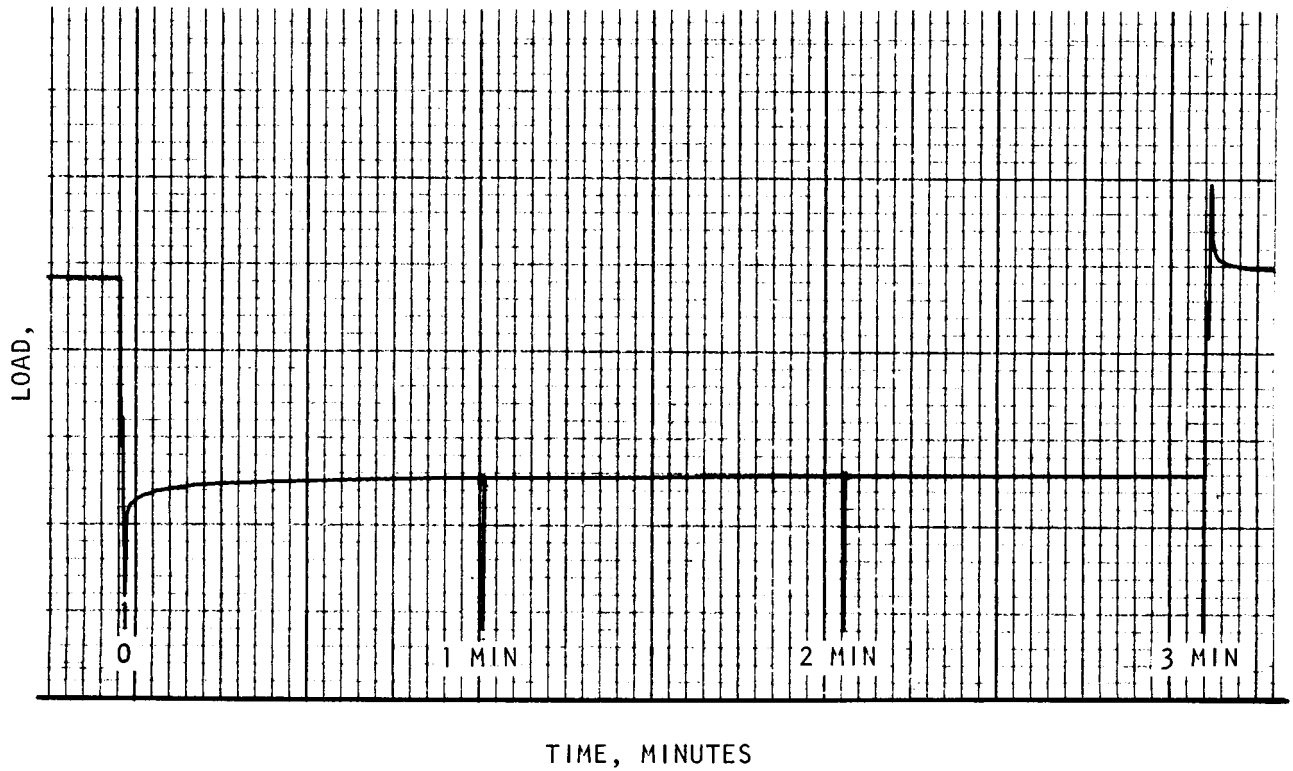
TIME, MINUTES

A-18676

Figure 61.-Load vs. time--2 minute hold time test.

TABLE 22.-REVERSE BENDING TEST SPECIMEN MATRIX
(2 Face Plates Per Specimen)

	Face Plate Material	Test Temperature, °F	Hold Time, min	Number of Face Plates								
				Pin-Fin			Lateral Channel			Longitudinal Channel		
				Mandrel Radius, in.								
				9	16	32	9	16	32	9	16	32
Initial Phase	Nickel 201	1400	0	0	0	0	3	1	0	3	1	0
			2	0	0	0	0	1	0	0	1	0
	Inconel 617	1600	0	0	0	0	3	4	0	2	3	0
			2	0	0	0	0	2	0	0	2	0
Final Phase	Nickel 201	1400	0	3	8	4	0	3	4	0	0	0
			2	5	6	4	4	3	4	0	0	0

Test Procedure

The basic test procedure was as follows:

(1) Adjust the ram travel to produce the desired amount of contact between the specimen and the mandrels at test temperature. The central region of the test specimen must conform to the mandrel radius to give the known alternating strain. A limited acceptable deflection range exists since insufficient deflection will yield reduced strain levels, and excessive deflections will produce unacceptable strains at the transition from a pressurization cavity to solid metal.

(2) Install specimen in test machine and connect pressurization lines.

(3) Heat the specimen to the required test temperature.

(4) Pressurize both panel cavities to 40 ±5 psig with nitrogen and rig the machine to shut down the test when the pressure drops to 20 ±5 psig.

(5) Fatigue cycle the test specimens at 0.4 to 0.5 Hz. For the tests with hold time, a 2-minute hold time was imposed at the end of each stroke in each direction.

(6) Cycle to failure one side of the specimen as indicated by pressure drop. Record cycles and continue testing until the second side fails. Record cycles.

(7) Examine the failed specimens to find the location of the fracture. Specimens that failed in an unusual pattern or that failed in an unexpectedly small number of cycles were examined to determine the cause of the unusual behavior.

To set the proper stroke, a calculation was made to determine the required ram travel at room temperature to produce the end deflection necessary to wrap a 1.5-in. central region of the specimen around each of the 9, 16, and 32-in. radius mandrels. Calibration tests were conducted and the relative thermal growths of the stationary housing and the ram/mandrels were measured. The thermal growth of the stationary housing exceeded the ram/mandrel growth by 0.012-in. at the test temperatures of 1400° to 1600°F. The thermal growth measurements permitted offsetting the calculated stroke at room temperature to assure that the specimen was centered between the mandrels and with respect to the stationary housing at the test temperature.

The procedure of setting the ram travel to produce the calculated 1.5-in. contact area between the test specimen and the mandrel at each end of the stroke (wrap) and biasing the room-temperature midpoint setting was used in the initial tests with 9-in. and 16-in. radius mandrels and both Nickel 201 and Inconel 617 specimens.

During the final tests, it was noted that the calculated ram travel setting for a nominal 1.5-in. wrap, produced excessive deflections in the first few specimens tested, resulting in premature fracture of the face plates. To eliminate the possibility of the unpredictable end effects influencing the test results, and since even a 0.200-in. contact area is sufficient to induce the

desired face plate strains, the ram travel for all subsequent tests was reduced to produce approximately 0.50-in. wrap of the central region of the specimen around the mandrel. Load-deflection curves were generated for all the initial and final phase tests to provide supplementary data.

Test Results--Initial Phase

The initial phase reverse bending fatigue tests were conducted on channel specimens of both Nickel 201 and Inconel 617 material systems. Each specimen contained a lateral channel and a longitudinal channel face plate. The test results are summarized in Tables 23, 24 and 25 and shown in figs. 62 and 63. The pressurization tubes to the longitudinal passages of SN 2 and SN 8 Inconel 617 test specimens were plugged or broke off before the face sheets could be fatigue fractured. Consequently, no data is presented for these channels.

For the Nickel 201 test specimens using 9-in. and 16-in. radii mandrels, the test life and the applied strain result in a calculated reduction in area of 51 percent by the strain range partitioning method. This value was used to update predicted test lives, as presented in Tables 23 and 24.

For Inconel 617, the calculated reduction in area of 37.6 percent resulted in a predicted LCF life which agreed with actual test data for the lateral channel. It overestimated the LCF life for longitudinal channels by a factor of approximately 2.5. An average reduction in area of 30 percent was selected and used to update predicted test lives for Inconel 617 specimens, with and without hold-time, as presented in Table 23 and 24.

The averages in Table 24 indicate that the LCF prediction technique is conservative for the laterally oriented channels and optimistic for the longitudinally oriented channels for tests without hold-time, when the above reduction-in-area values are used. The reduction in the LCF life caused by introduction of hold time between cycle reversals was greater than expected. The effect of hold time was greatest for the longitudinal channel orientation.

The reverse bending fatigue test results further indicate that the lateral channel pattern is the more critical of the two orientations. The laterally oriented channels had the lowest LCF life in all tests for all materials.

Because of the different thermal conductivities of Nickel 201 and Inconel 617, different temperatures and temperature gradients will exist with the same imposed heat flux. The corresponding temperature differentials at the design heat flux of 500 Btu/sec-ft^2 are shown in Figure 64, along with the nominal surface temperatures used in the analysis and a basis for establishing test conditions.

Based on the respective ΔT's, the design strain levels were calculated for both Nickel 201 and Inconel 617 channel specimens and are shown in figs. 62 and 63. The resulting LCF life predictions for both materials at the design conditions are summarized in Table 25 and indicate that with either channel orientation, the predicted LCF life for the Nickel 201/Hastelloy X materials combination is superior to Inconel 617.

Consequently, for final phase testing, Nickel 201 was selected for further evaluation in tests using both pin-fin and lateral channel face plates.

TABLE 23.-INITIAL TESTS
REVERSE BENDING FATIGUE-TEST RESULTS
NICKEL 201 AND INCONEL 617 CHANNEL SPECIMENS

SN	Hold Time min.	Test Temp. °F	Face Plate Material	Mandrel Radius in.	*Predicted Cycles to Fracture		Actual Cycles to Fracture	
					Lateral Channels	Longitudinal Channels	Lateral Channels	Longitudinal Channels
2	0			9	147	362	209	370
6	0			9	147	362	127	304
8	0	1400	Nickel	9	147	362	139	380
5	0		201	16	388	971	454	911
3	2			16	379	936	219	348
1	0			9	74	220	157	170
4	0			9	74	220	114	127
8	0			9	74	220	84	(1)
2	0	1600	Inconel	16	241	889	387	(1)
6	0		617	16	241	889	341	480
9	0			16	241	889	360	521
11	0			16	241	889	451	591
3	2			16	174	421	117	145
5	2			16	174	421	112	143

*Predictions are based on reduction in area of 51 percent for Nickel 201/
Hastelloy X specimens and a reduction in area of 30 percent for Inconel 617
specimens, as calculated from the test results for actual cycles to fracture.

(1) No data point is presented because the pressurization tubing to these
passages was plugged or broken.

Test Results-Final Phase

Testing was in accordance with the test matrix presented in Table 22. The
test results are summarized in Table 26 and in fig. 65 and 66. The predicted
cycles to failure on Table 26 were based on the data from the initial-phase
tests, Tables 23 and 24, adjusted for minor differences in specimen thickness
dimensions. The adjusted data from these tables are included in figs. 65 and 66.
The equations used for these prior predictions and the final recommended
equations, as noted in fig. 65 and 66, are discussed below.

Side 2 of SN 2 and side 1 of SN 7 lateral channel specimens and the sides
1 of the SN 13 and SN 17 pin-fin specimens exhibited premature leaks in an area
outside of the flexure zone. The strain level in this area is lower than that
induced within the contact area by the mandrels. This suggests defective face
plate materials. Data for these sides were, therefore, eliminated from
subsequent evaluations.

Material	Test Temp. °F	Mandrel Radius in.	Hold Time min.	Channel Orientation	*Predicted Cycles to Fracture	Actual Cycle to Fracture (Average)
Nickel 201	1400	9	0	Lateral Longitudinal	147 362	158[1] 351[1]
		16	0	Lateral Longitudinal	388 971	454[2] 911[2]
		16	2	Lateral Longitudinal	379 936	219[2] 348[2]
Inconel 617	1600	9	0	Lateral Longitudinal	74 220	118[1] 148[3]
		16	0	Lateral Longitudinal	241 889	384[4] 531[1]
		16	2	Lateral Longitudinal	174 421	115[3] 144[3]

*Predictions are based on reduction in area of 51 percent for Nickel 201/ Hastelloy X specimens and a reduction in area of 30 percent for Inconel 617 specimens, as calculated from the test results for actual cycles to fracture.

(1) Average of three specimens.

(2) One specimen tested.

(3) Average of two specimens.

(4) Average of four specimens.

Combined Results of Initial and Final Phases

The combined initial and final phase reverse bending fatique test results for Nickel 201 lateral channel and pin-fin specimens are presented in figs. 65 and 66 respectively.

TABLE 25.—COMPARISON OF PREDICTED LIFE AT DESIGN HEAT FLUX

Material Combination	Predicted Life At Design Heat Flux, Cycles To Failure				Design Goal Cycles
	Lateral Channels		Longitudinal Channels		
	Hold Time	No Hold	Hold Time	No Hold	
Nickel 201/Hastelloy X	5400	10,000	8,200	>10,000	10,000
Inconel 617	650	2,000	900	3,500	
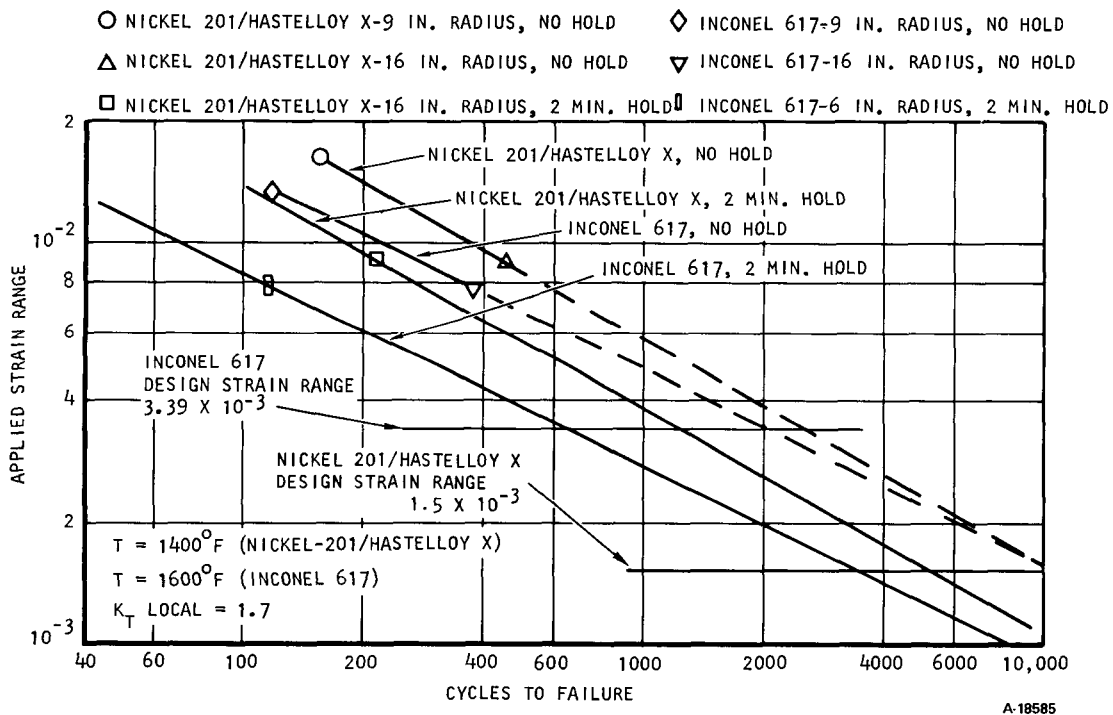
Figure 62.—Reverse bending tests of lateral channels with and without hold time, Nickel 201 and Inconel 617.

Figure 63.-Reverse bending tests of longitudinal channels with and
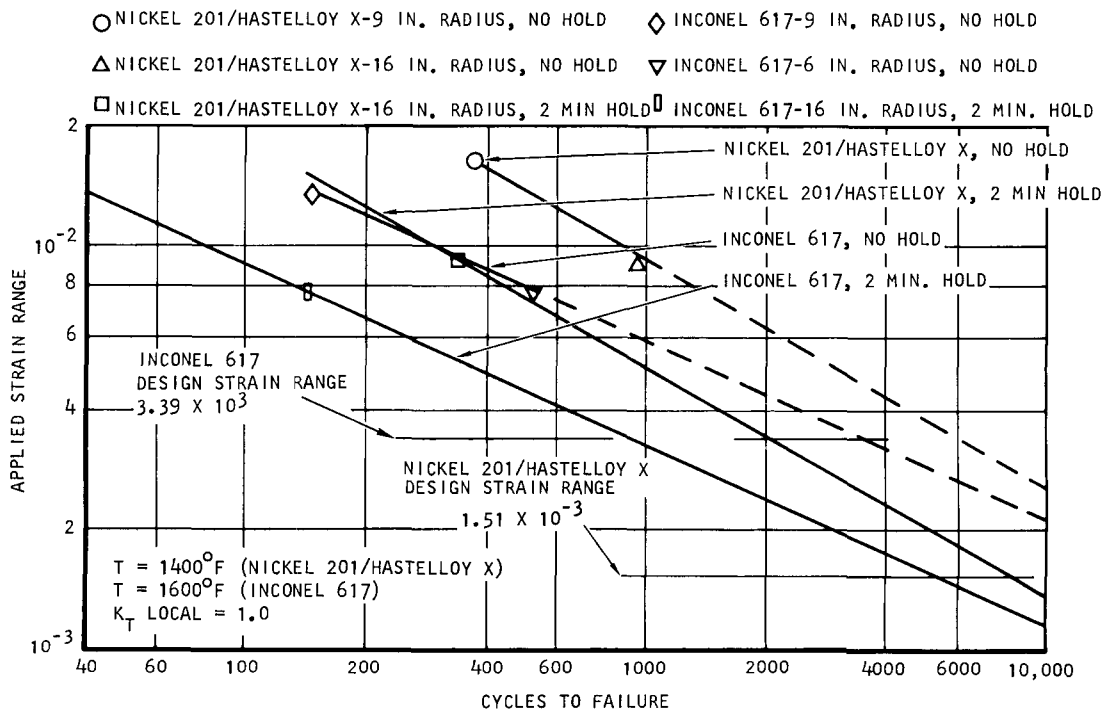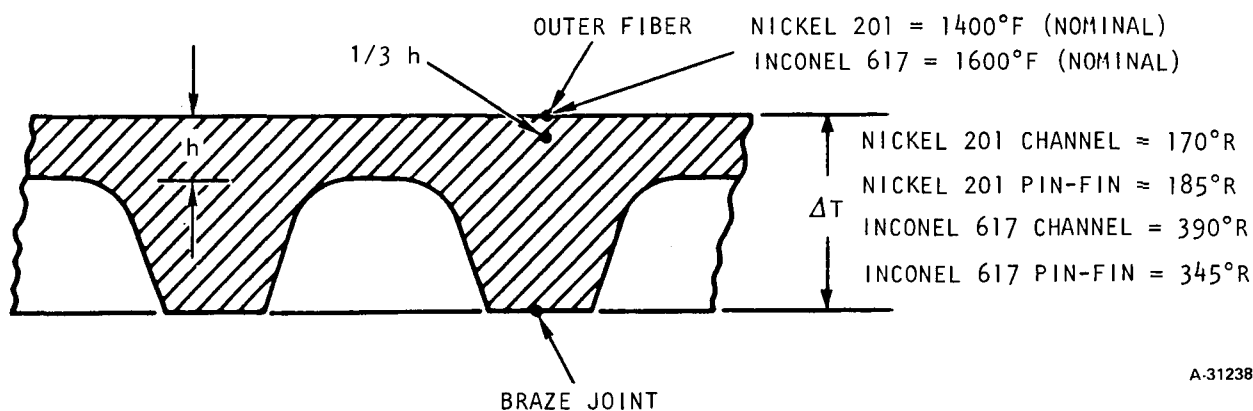without hold time, Nickel 201 and Inconel 617.

Figure 64.-Cooling jacket in-depth temperature
gradients at the design heat flux.
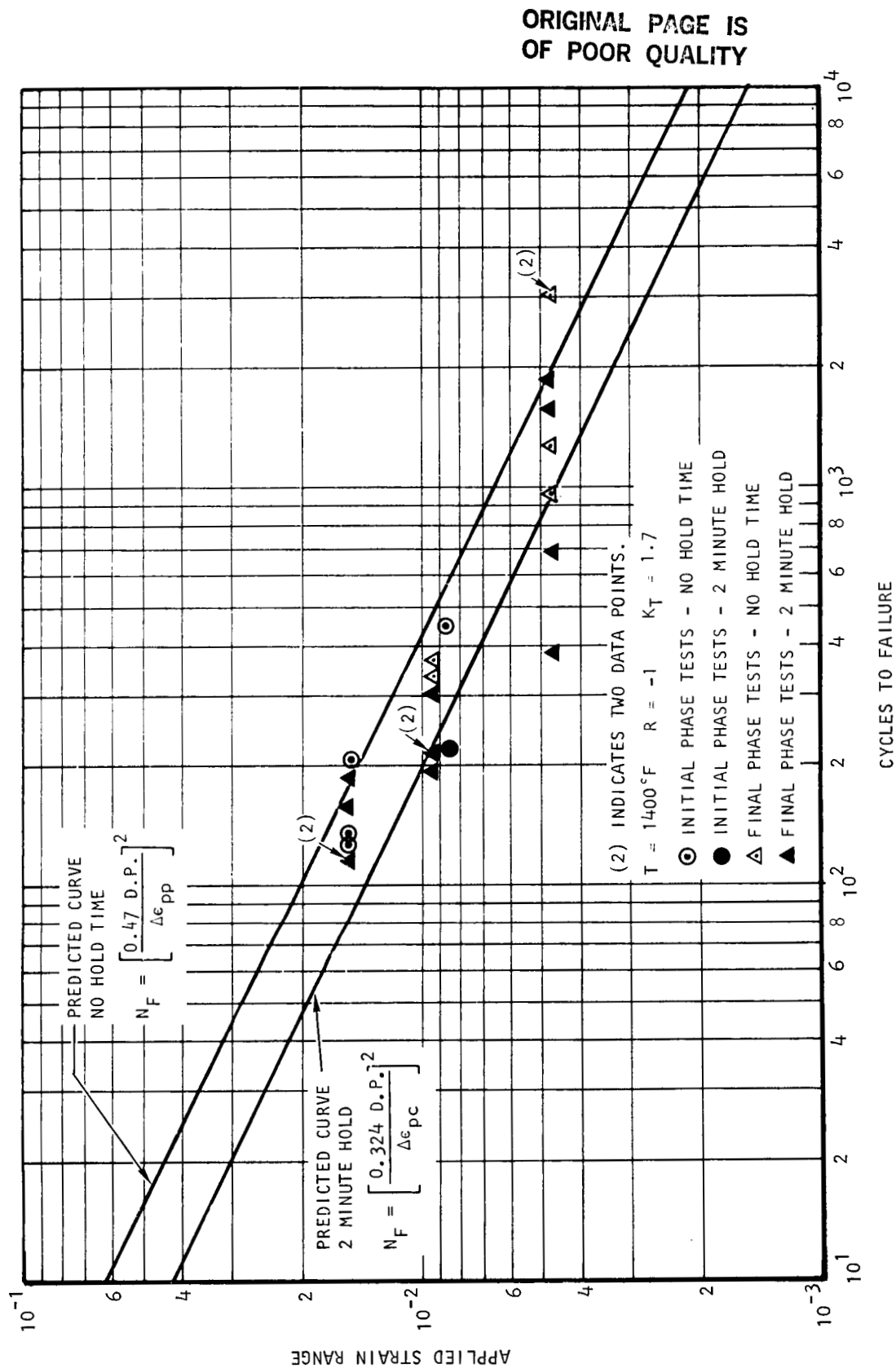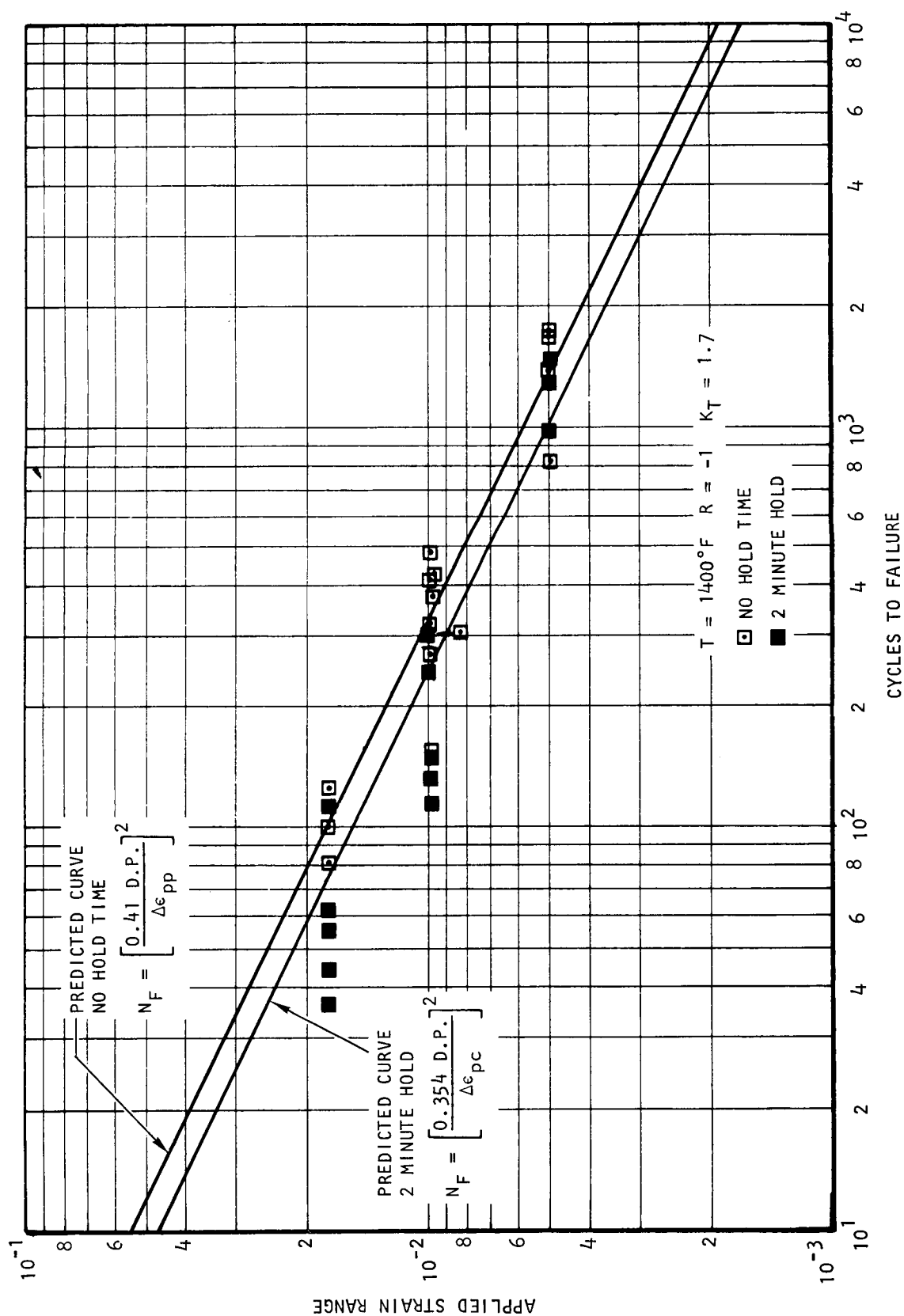
Figure 65.—Comparison of test results with predictions, Nickel 201/
Hastelloy X lateral channels, all tests.

97

Figure 66.—Comparison of test results with predictions, Nickel 201/ Hastelloy X pin-fin panels—final phase of tests.

TABLE 26.-FINAL PHASE REVERSE BENDING FATIGUE TEST RESULTS

SN	Hold Time, min.	Test Temp. °F	Cooling Jacket Config.	Mandrel Raduis, in.	Predicted Cycles to Fracture	Actual Cycles to Fracture		Remarks
						Side 1	Side 2	
13	0			9	128	--	100	(1)
14	0			9	128	124	82	
4	2			9	52	46	34	
17	2			9	52	--	60	(1)
18	2			9	52	111	54	
2	0	1400	Pin-Fin	16	339	152	301	
3	0			16	339	319	413	
15	0			16	339	274	485	
16	0			16	339	427	370	
1	2			16	136	150	130	
5	2			16	136	112	291	
6	2			16	136	246	307	
9	0			32	1119	1409	1776	
10	0			32	1119	826	1702	
7	2			32	450	1468	1302	
8	2			32	450	1428	990	
15	2			9	57	187	118	
16	2			9	57	157	122	
7	0			16	375	--	363	(1)
14	0	1400	Lateral Channel	16	375	211	330	
1	2			16	151	193	306	
2	2			16	151	216	--	(1)
11	0			32	1238	3030	977	
12	0			32	1238	1283	3046	
3	2			32	498	388	1860	
4	2			32	498	685	1558	

(1) Defective face plate material on side with no entry.

A basic relationship from the strain range partitioning method of analysis (ref. 17) was used to calculate the predicted and test LCF lives. The basic equation is as follows,

$$N_F = \left[\frac{C\ D.P}{\varepsilon_{pp}} \right]^n$$

where: N_F = cycles to failure

C = intercept constant

99

$$D.P. = \ln \frac{100}{100-RA} = \text{ductility}$$

n = slope exponent

RA = percent reduction in area

$\Delta\varepsilon_{pp}$ = plastic strain range

$\Delta\varepsilon_{pc}$ = strain range with creep

The parameters C and n are selected by trial to provide agreement with the test data.

Initial phase fatigue test results indicated that a reduction in area (RA) of 51 percent represented a typical measure of the ductility of the brazed and aged Nickel 201 material at 1400°F.

An RA of 51 percent was used in subsequent calculations to determine the D.P. = 0.713 factor.

Calculation of the plastic strain range, $\Delta\varepsilon_{pp}$, included a strain concentration factor of 1.7, which was found to be a typical value by an ANSYS finite element computer model analysis. This factor was used for pin fins and lateral channels. The peak strain range was calculated by considering the "wrap" of a specimen of thickness h on the mandrel of radius R.

$$\Delta\varepsilon_{peak} = \frac{1.7h}{R+\frac{h}{2}}$$

The plastic strain was obtained by subtracting the elastic strain range, as determined on the basis of yield stress, σ_{ys}, and tensile modulus, E, at the test temperature.

$$\Delta\varepsilon_{pp} = \Delta\varepsilon_{peak} - \frac{2\sigma_{ys}}{E}$$

The initial phase reverse bending tests were limited to mandrel radii of 9 and 16 inches. The data indicated that the LCF life of the pin-fin and lateral channel configurations with no-hold time can be represented by the relation

$$N_F = \left[\frac{0.595 \; D.P.}{\Delta\varepsilon_{pp}}\right]^{1.6}$$

and with 2 min. hold time, the relation

$$N_F = \left[\frac{0.435 \ D.P}{\Delta \epsilon_{pp}} \right]^{1.67}$$

Results of the final phase LCF tests indicate that the fatigue life predictions can be better approximated by the following modified equations:

$$N_F = \left[\frac{0.41 \ D.P}{\Delta \epsilon_{pp}} \right]^{2} \quad \text{pin-fins, no hold time}$$

$$N_F = \left[\frac{0.354 \ D.P.}{\Delta \epsilon_{pc}} \right]^{2} \quad \text{pin fins, 2.0-minute hold time}$$

$$N_F = \left[\frac{0.47 \ D.P.}{\Delta \epsilon_{pp}} \right]^{2} \quad \text{lateral channels, no hold time}$$

$$N_F = \left[\frac{0.324 \ D.P.}{\Delta \epsilon_{pc}} \right]^{2} \quad \text{lateral channels, 2.0-minute hold time}$$

These equations are plotted in figs. 65 and 66 and demonstrate the relationship between the predicted and actual LCF test lives.

In an actual engine panel the thermal protection system (TPS) surface is subjected to biaxial compression on heat-up and to bi-axial tension on cooldown due to the restraining effect of the support plate. In a biaxial stress field where tensile and compressive stresses exist simultaneously in both axes, the effective strain applied to an element will be less than that which would exist if the same stress level was applied uniaxially.

The reverse bending tests conducted on the channel specimens simulate uniaxial loading. As a result, the LCF life predictions of an engine panel based on the low cycle fatigue life of lateral channels would be conservative; comparisons made on the basis of the LCF life predictions of longitudinal channels would be optimistic. For a given strain (and hence a corresponding equivalent panel ΔT), the average of the LCF lives for lateral and longitudinal channels is a better measure of the life expectancy for the biaxial stress condition in an engine panel. The LCF life predictions for the channel

configuration presented in fig. 67 are adjusted to simulate a biaxial stress condition by multiplying the test life of the lateral channels by the following ratio:

$$\frac{N_{\text{lateral channels}} + N_{\text{longitudinal channels}}}{N_{\text{lateral channels}}}$$

where

N = Test LCF life

LCF curves presented in fig. 67 assume that in actual application, 80 percent of engine operation will be over 2 minutes in duration and 20 percent will be less than 2 minutes in duration. The following relationship was used to calculate the final value of the predicted LCF life.

Life = (Life with hold time x 0.80) + (Life without hold time x 0.20)

Conclusions and Recommendations

The goal of this series of tests was to assess the life of the thermal protection surface, using the selected materials and passage configurations, with a goal of 10,000-cycle life at the design heat flux.

Initial phase reverse bending fatigue tests were conducted on channel specimens of the selected materials, Nickel 201 and Inconel 617, and on lateral and longitudinal channel pattern orientations. Results indicated that the lateral channel pattern was the more critical of the two orientations. With either channel orientation, the predicted LCF life for Nickel 201/Hastelloy X materials combination was superior to Inconel 617.

Nickel 201 was selected for further evaluation in tests using both pin-fin and lateral channel plates in the final phase testing. Test results indicate that with Nickel 201 in both pin-fin and channel coolant passage configurations, the design goal of a 10,000-cycle life can be achieved.

The data obtained from the panel reverse bending fatigue tests exhibit a maximum scatter factor of about 5. Most of the results are within a factor of 2 on cycle life. This is a very satisfactory grouping for fatigue data and leads to confidence in the test method and reproducibility of results.

The test method itself is based on simulation of thermally induced strains by the imposing of mechanical strains at isothermal conditions. Evaluation of fatigue performance under thermal conditions that simulate actual engine operation is desirable for verification of structural life. The temperature gradients that exist under operating conditions preclude simultaneous simulation of strains in all parts of the structure using isothermal test conditions. Sub-element tests can be designed to subject the cooled structure to thermally
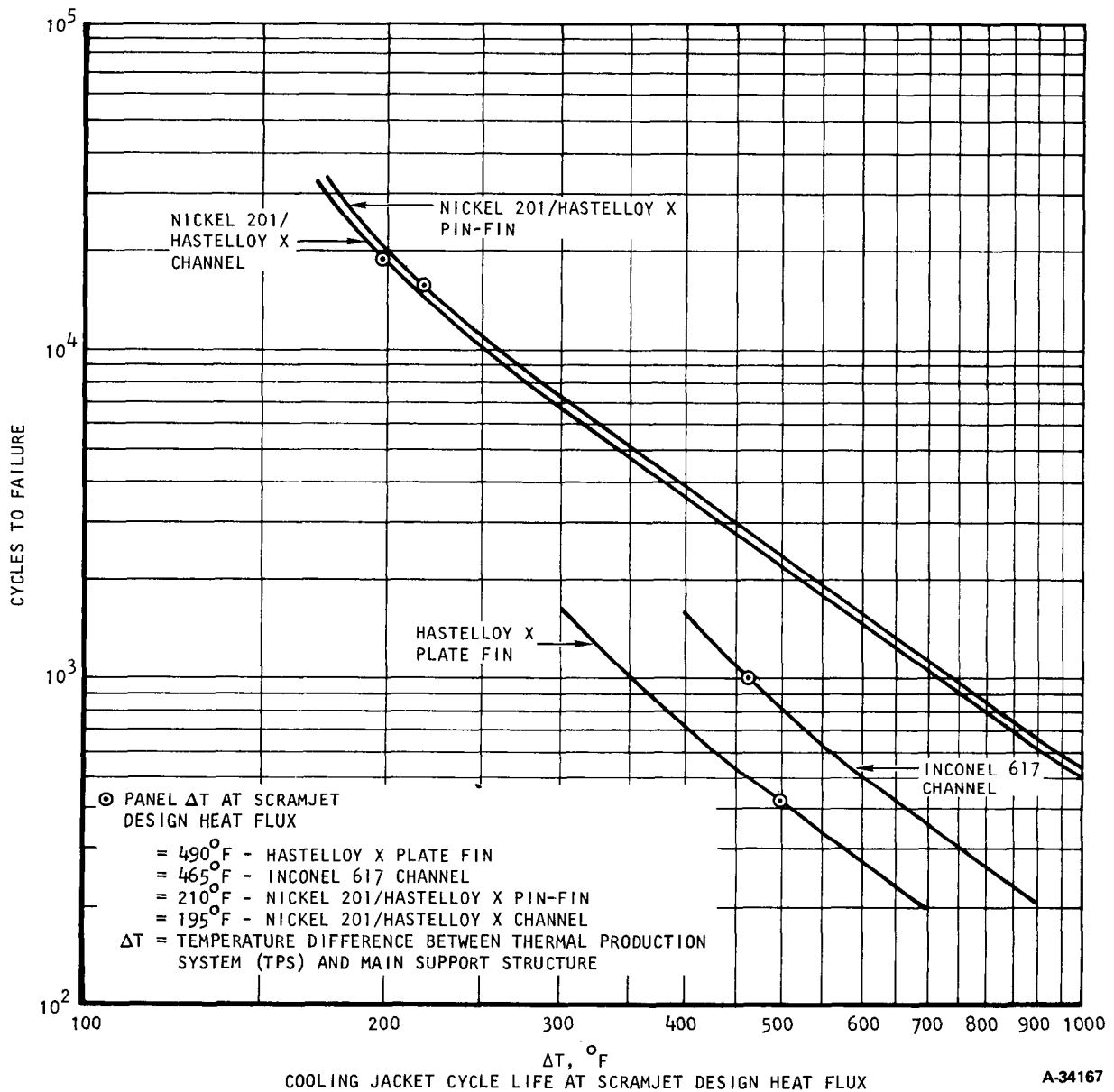
102

Figure 67.-Predicted cycle life vs. ΔT between thermal protection
system (TPS) face sheet and main support structure

induced strains using either static loading (electrical heating) or dynamic loading (wind tunnels). The high flux loadings of interest in this application generally favor testing in high temperature, high Mach number tunnels for realistic simulation.

PANEL FLUIDIZED BED TESTING

The fuel injection struts designed for the scramjet consist of a pin-fin Nickel 201 cooling system brazed to an Inconel 718 support structure. These two materials differ in thermal expansion coefficients. Testing in a fluidized bed was selected to evaluate the low cycle fatigue life of this material system. This was done to provide a more representative thermal environment than available with reverse bending tests.

Specimen Design

The design of the fluidized bed test specimen is shown in figs. 68 and 69. The specimen consists of an Inconel 718 sheet with a Nickel 201 face sheet brazed to each side. Each face sheet contains a pin-fin matrix which is identical to that of the reverse bending pin-fin test specimen. The overall size of the fluidized bed test specimen, was minimized to reduce thermal lag of the heavier edge section and ensure failure in the matrix area. Two face sheets are incorporated to provide for symmerical heating of the specimen, thereby precluding bowing of the specimen during heating and cooling. The face plates incorporate provisions for pressurizing each cooling passage independently.

Palniro 1 filler alloy, 0.001-in. thick was used in brazing the Nickel 201 pin-fin face sheets to the Inconel 718 support plate. Tests with braze evaluation specimens indicated no difference in braze joint quality between gold coated, nickel coated, and uncoated braze surfaces. All specimens showed excellent wetting and filleting. For added assurance of braze joint quality, however, all test specimens were plated with a flash coating of 0.00005 to 0.0001-in. thick nickel on the braze surfaces.

Following braze, the specimens were pressure tested and holographically examined. Fig. 70 is typical result of the holographic inspection performed on the fluidized bed test specimens. This panel shows unbrazed pins on one side. Unbrazed pins occurred along the edges of some of the other panels. Such voids would result in reduced face sheet life. The panels were, nevertheless, tested as is, to avoid imposition of effects from additional braze cycles.

Prior to testing, the test specimens were aged in argon at 1450°F for 1000 hrs.

Test Setup and Procedure

The test setup for the fluidized bed tests is shown in fig. 71. An adapter plate, fig. 72 was used for mounting the calibration and the test specimens on the plunger arm for sequential immersion into the hot and cold beds. Fig. 72 presents a photograph of the calibration test specimen installed on the

Figure 68.-Pin-fin face plate.

105
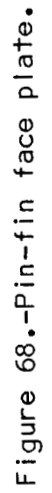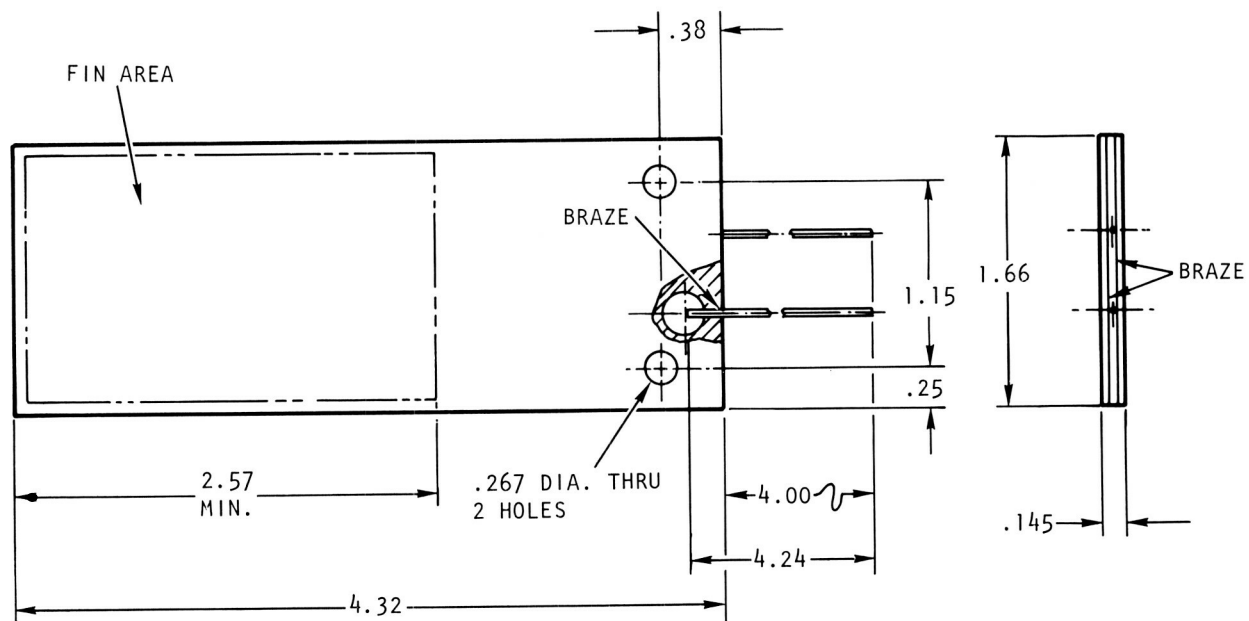
Figure 69.-Test specimen panel assembly

Figure 70.-Fluidized bed fatigue test specimen
holographic inspection SN 1 at 1000 psig.

a. FLUIDIZED BED TEST RIG

b. TEMPERATURE RECORDING EQUIPMENT

F-34958

Figure 71.-Fluidized bed test setup.

F-34930

Figure 72.-Calibration test specimen installation
for fluidized bed tests.

adapter plate and the plunger arm. One to three dummy plates were installed
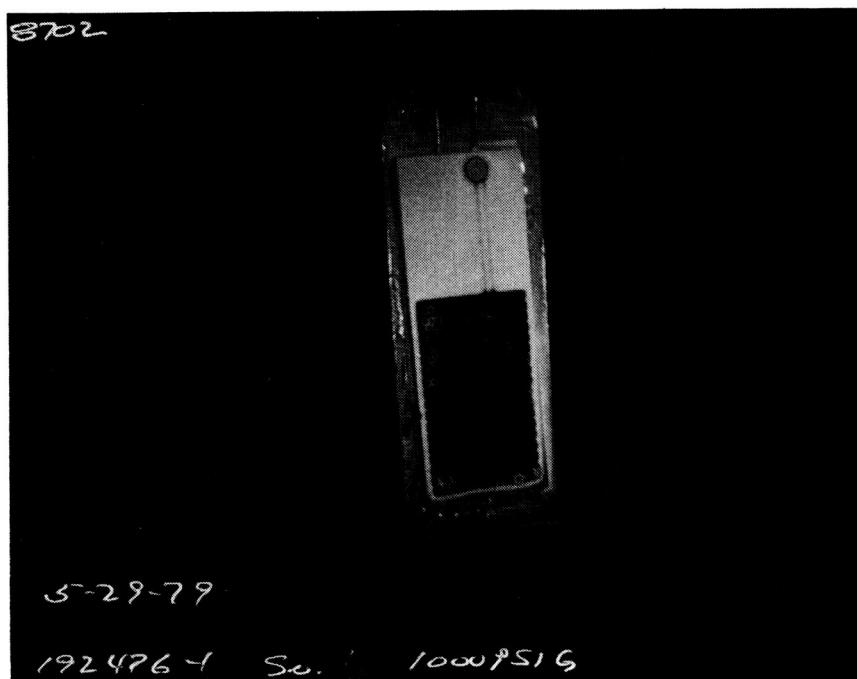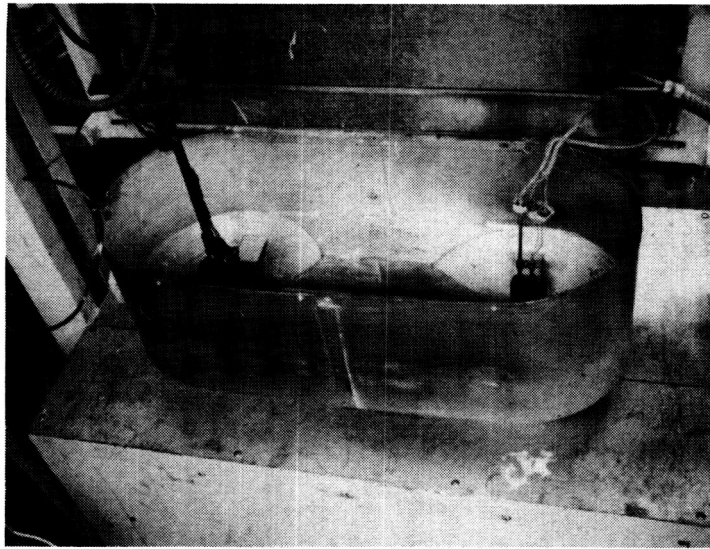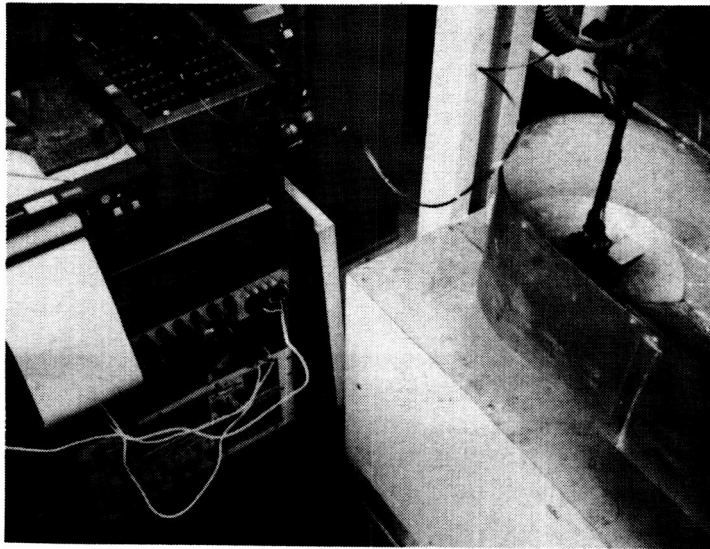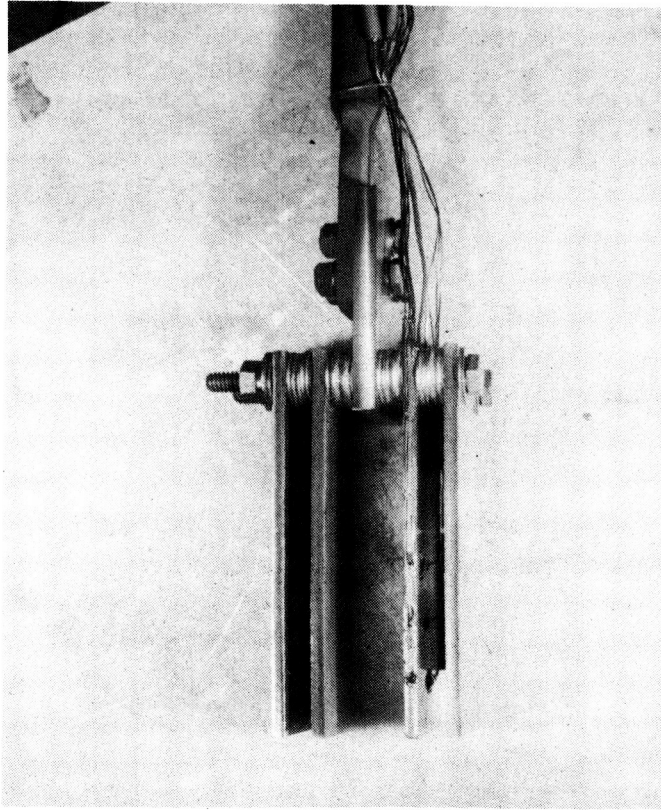during fatigue and calibration tests, respectively, to achieve a consistent
heating rate for all the specimens.

The setup permits testing of one to four panel assemblies at temperatures
to 1800°F and pressures to 1000 psig. Upon failure of an individual panel,
valving will permit identification and isolation with test interruption to
that circuit only. A timer in the test machine control apparatus allowed for
the automatic cycling of the specimen between the hot and cold beds.

Test Results

The test results indicated that the design temperature differential between
the Nickel 201 face sheet and the Inconel 718 support plate cannot be obtained
when the face sheet is at the 1390°F operating temperature. Consequently,
induced stresses and strains in the face sheet are not as severe as those antic-
ipated in an operating panel. To cause a face sheet failure in less than 1000
cycles, a ΔT of 340°F is required when the face sheet is at 1390°F. The largest
ΔT obtained during test was 113°F at a face sheet temperature of 521°F. The
corresponding life is over 19,000 cycles.

Limited verification of the ability of the Palniro 1 braze joint, however, was obtained during the fluidized bed tests. The calculated combined pressure and thermal stress in the braze joint with the joint and face sheet at 1180°F (8,400 psi) is comparable to the calculated stress at the design condition with a 1390°F face sheet and a 1180°F braze joint (7,930 psi). Tests at a constant specimen temperature of 1180°F indicated that, after approximately 100 cycles, areas with sound braze as determined by pre-test holographic examination, remained intact. Metallurgical evaluation of these joints showed no distressed areas.

Conclusions and Recommendations

The low-cycle fatigue life capability of the Nickel 201/Inconel 718 material system was not demonstrated during the fluidized bed tests because the required test conditions could not be achieved. A limited verification of the ability of the Palniero 1 braze joint to accommodate the coefficient of expansion mismatch between the materials was obtained. Further testing, with revised test specimen and sound braze joints, is recommended to evaluate the full thermal life capability of the Nickel 201/Inconel 718 material combination.

CONCLUDING REMARKS

Results of the study indicate that the basic goal of increasing the life of hydrogen cooled structures two orders of magnitude relative to that of the Hypersonic Research Engine can be reached using available materials, fabrication technologies, and joining methods. (The Hypersonic Research Engine, which used brazed Hastelloy X plate-fin coolant passages, had a design life of 100 thermal cycles and 10 hours.) However, the study, which consisted of preliminary screening of concepts, materials, and fabrication techniques plus analysis and testing(including tensile, creep rupture, and fatigue tests), also indicated that the increase in life was not as great as anticipated based on published material properties.

The cooling jacket concepts that evolved from the initial screening and were the subject of the detailed analysis and testing consisted of either rectangular grooves or pin-fins photo-chemically machined into either Nickel 201 or Inconel 617 skins that were brazed to a backing plate to form the coolant flow channels. This approach positions the relatively weaker braze joint material at the back of the passage where the temperatures are lowest. The initial screening indicated that the rectangular channels had the longest life potential; however, the pin-fin passages were also retained because they provided higher heat transfer capability, albeit at the expense of higher pressure drop, suitable for regions of very high heat flux. Similarly, Nickel 201 offered the potential of longer life but the creep rupture performance appeared questionable; therefore, Inconel 617 was also retained because it appeared to have adequate creep life. Palniro 1 was selected as the primary filler alloy used for brazing both materials.

Tensile tests of specimens subjected to pseudo-braze and age cycles indicated that the ductility of both Nickel 201 and Inconel 617 was substantially reduced by the combined effects of brazing and aging. These findings were substantiated by low cycle fatigue tests of hollow bar Inconel 617 specimens which indicated significant reductions in fatigue life. The reductions in life were commensurate with the loss in ductility and could be predicted analytically if the appropriate reduction in area was used in the fatigue calculations. Tensile tests of specimens aged in argon (to separate the effects of braze cycle and aging from those of oxidation) produced marked improvements in reduction in area relative to results obtained with specimens aged in air; however, measured reductions in area were well below values listed in the literature even for the argon-aged specimens. Since in the intended engine application the cooled structure will be operating in an oxygen deficient environment, the argon atmosphere was deemed to be more representative than air and was used for aging all subsequent test specimens.

Creep rupture tests of fabricated coolant passage specimens produced results that agreed closely with predicted lives indicating that creep-rupture strength is not appreciably reduced by brazing and aging. Both Nickel 201 and Inconel 617 specimens brazed with Palniro I met (Inconel 617 exceeded) the *design life goal* of 1000 hrs. However, for Inconel 617 the braze joint was found to be the weak link and even longer creep-rupture life, approaching that of the parent metal, was obtained using boronized nickel chrome as the brazing alloy.

Results of isothermal reversed bending fatigue tests indicated that the advanced fabrication techniques of this study have significantly increased the fatigue life of the coolant passages relative to the brazed plate-fin Hastelloy X passage technology of the Hypersonic Research Engine. For conditions corresponding to the design heat flux, the estimated life (based on results of tests of specimens that had been pre-aged for 1000 hrs at 1450°F) is 19,000 cycles for the Nickel 201 channel configuration and 16,000 cycles for the pin-fin configuration. For the Inconel channel configuration, the estimated life is 1000 cycles, whereas for the earlier brazed plate-fin Hastelloy X configuration the estimated life is only 430 cycles. Attempts to determine the effects of differences in the coefficient of thermal expansion on fatigue life of a configuration composed of Nickel 201 coolant passages brazed to an Inconel 718 support structure using a fluidized bed test technique were unsuccessful because of an inability to establish the required temperature difference between the hot surface and the support structure.

Additional research is required to establish the fatigue characteristics of the dissimilar metal coolant passages (Nickel 201/Inconel 718), which is the configuration presently envisioned for the scramjet fuel strut; and to investigate the embrittling effects of the hydrogen coolant on the coolant passage which is a potential problem that was not investigated in the present study.

REFERENCES

1   Hypersonic Research Engine Project--Phase II, Structures and Cooling
    Development, Final Technical Data Report. Data Item No. 55-7.18,
    NASA CR-112087, May 18, 1972.

2   Killackey, J.J.; Katinszky E.A.; Tepper, S.; Vuigner, A.A.; Wright, C.C.;
    and Stockwell, G.G.: Thermal-Structural Design Study of an Airframe-
    Integrated Scramjet. Prepared under Contract No. NAS1-13984 by AiResearch
    Manufacturing Company, The Garrett Corporation. NASA CR-159039, May 1980.

3   Wieting, Allan R.; and Guy, Robert W.: Thermal-Structural Design/Analysis
    of an Airframe-Integrated Hydrogen-Cooled Scramjet. J. of Aircraft, Vol.
    13, No. 3, March 1976, pp. 192 to 197.

4   Kelly, H. Neale; Gellersen, E.W.; and Richard, C.E.: Development of Fabri-
    cation Techniques and Performance Tests of Hydrogen-Cooled Structural
    Panels. Presented at the Aerospace Structures Design Conference, The
    Pacific Science Center, Seattle, WA, August 4-5, 1969.

5   Richard, C.E.; Duncan, J.D.; Demogenes, C.; and Flieder, W.G.: Low-Cycle
    Fatigue Evaluation for Regeneratively Cooled Panels. Prepared under
    Contract No. NAS1-5002 by AiResearch Manufacturing Company, The Garrett
    Corporation. NASA CR-1884, October 1971.

6   Wieting, Allan R.: Empirical Correlations for Heat Transfer and Flow
    Friction Characteristic of Rectangular Offset-Fin Plate-Fin Heat Exchangers,
    Transactions of the ASME Series C, Volume 97, Journal of Heat Transfer,
    August 1975, pp. 4 to 8 to 490.

7   Gray, Hugh, R.: Embrittlement of Nickel-, Cobalt-, and Iron-Base Super-
    alloys by Exposure to Hydrogen. NASA TDN-7805, Lewis Research Center,
    January 1975.

8   Harris, J.A., Jr.: Properties of Materials in High Pressure Hydrogen at
    Cryogenic, Room, and Elevated Temperatures. NASA CR-124394, July 31, 1973.

9   Girard, E.H., et. al.: Study of Ductile Coatings for the Oxidation
    Protection of Columbium and Molybdenum Alloys. Report No. AD 634 402,
    U.S. Navy, May 1966.

10 Fueki, K.; and Wagner, J.B.: "Studies of the Oxidation of Nickel in the
    Temperature Range of 900° to 1400°C". Electrochem, Soc., 112, No. 4
    April 1965, p. 385.

11 Liebert, C.H., and Stecura, S.: Ceramic Thermal Protective Coating
    Withstands Hostile Environment of Rotating Turbine Blades. NASA
    Tech. Brief B75-10290, December 1975.

12   "Fatigue-Testing of Nickel -200 Panels." Hypersonic Research Engine Project-
      Phase IIA, NASA CR-66842, January 10, 1969.

13   Brinkman, C.R.; Rittenhouse, P.C.; Corwin, W.R.; Strizak, J.P.; Lystrup, A.;
      and DiStefono, J.R.: Application of Hastelloy X in Gas-Cooled Reactor
      Systems. ORNL/TM-5405. Oakridge National Laboratory, October 1976.

14   SAE Handbook. SAE J417b, P. 4.07, 1982.

15   Microstructure and Phase Stability of Inconel Alloy 617. Mankind, W.L.;
      Hosier, J.C.; Basseford, T.H.; Metallurgical Transactions, Volume 5,
      December 1974.

16   Aerospace Structures Metal Handbook. Code 4117, P. 14 and 15.   June 1976.

17   Manson, S.S.: "The Challenge to Unify Treatment of High Temperature
      Fatigue--A Partisan Proposal Based on Strainrange Partitioning." Fatigue
      at Elevated Temperatures, ASTM STP 520, American Society for Testing and
      Materials, 1973, pp. 744-782.

1. Report No. NASA CR-3949	2. Government Accession No.	3. Recipient's Catalog No.
4. Title and Subtitle Advanced Fabrication Techniques for Hydrogen-Cooled Engine Structures		5. Report Date November 1985
		6. Performing Organization Code
7. Author(s) O.A. Buchmann, V.V. Arefian, H.A. Warren, A.A. Vuigner and M.J. Pohlman		8. Performing Organization Report No. 81-17928
9. Performing Organization Name and Address AiResearch Manufacturing Company 2525 W. 190th Street Torrance, Ca. 90509		10. Work Unit No.
		11. Contract or Grant No. NAS1-14180
12. Sponsoring Agency Name and Address National Aeronautics and Space Administration Washington, DC 20546		13. Type of Report and Period Covered CONTRACTOR REPORT OCTOBER 1975 TO JUNE 1982
		14. Sponsoring Agency Code 505-33-53-14

15. Supplementary Notes

Langley Technical Monitor: H.N. Kelly
Final Report

16. Abstract

This report documents a program for development of coolant passage geometries, material systems, and joining processes that will produce long-life hydrogen-cooled structures for application to scramjet. Tests were performed to establish basic material properties, and samples constructed and evaluated to substantiate fabrication processes and inspection techniques.

Results of the study indicate that the basic goal of increasing the life of hydrogen-cooled structures two orders of magnitude relative to that of the Hypersonic Research Engine can be reached with available means. Estimated life is 19 000 cycles for the channels and 16 000 cycles for pin-fin coolant passage configurations using Nickel 201. Additional research is required to establish the fatigue characteristics of dissimilar-metal coolant passages (Nickel 201/Inconel 718) and to investigate the embrittling effects of the hydrogen coolant.

17. Key Words (Suggested by Author(s)) Regeneratively cooled structure Scramjet Thermal protection system Fuel injection strut	18. Distribution Statement ▆▆▆▆▆▆▆▆▆▆▆▆▆▆▆▆▆▆▆ Until November 1987 Subject Category 39
19. Security Classif. (of this report) Unclassified	20. Security Classif. (of this page) Unclassified

19. Security Classif. (of this report) Unclassified	20. Security Classif. (of this page) Unclassified	21. No. of Pages 124	22. Price